

Theory of organic stereoisomerism in harmony with molecular symmetry

Shinsaku Fujita

Received: 12 May 2009 / Accepted: 13 September 2010 / Published online: 30 September 2010
© Springer Science+Business Media, LLC 2010

Abstract A new theory of stereoisomerism in harmony with molecular symmetry has been developed by starting from *RS*-stereoisomeric groups correlated to stereoisograms and their correlation diagrams. The substitution positions of a stereoskeleton are permuted by a set of epimerizations at the *RS*-stereogenic centers of the stereoskeleton. The product of epimerizations and the mirror-image transformation of the skeleton characterize the total feature of isomerization, which is based on the axiom of organic stereoisomerism. Then, stereoisomeric groups are formulated to develop the theory of stereoisomerism after several related groups are defined, e.g., stereoisogram groups, epimerization groups, local symmetry groups, epimeric stereoisogram groups, epimeric *RS*-stereoisomeric groups, and multiple epimerization groups. On the basis of the stereoisomeric groups, stereoisomeric representations are derived and employed to discuss correlation diagrams of stereoisograms. On the other hand, molecular-symmetry representations are derived from the stereoisomeric groups and employed to discuss molecular symmetries. Typical topics of stereochemistry, e.g., the CIP system for giving *RS*-stereodescriptors and the Fischer-Rosanoff convention for naming DL-series of sugars, are discussed on the basis of the present theory.

Keywords Stereoisomerism · Stereochemistry · Enantiomerism · *RS*-diastereomerics · *RS*-stereoisomeric · Stereoisogram · Correlation diagram · *RS*-stereodescriptors · Molecular symmetry · Cyclobutane

S. Fujita (✉)

Shonan Institute of Chemoinformatics and Mathematical Chemistry,
Kaneko 479-7, Ooimachi, Ashigara-Kami-Gun, Kanagawa-Ken 258-0019, Japan
e-mail: shinsaku_fujita@nifty.com

1 Introduction

Since the beginning of organic stereochemistry founded by van't Hoff [1] and Le Bel [2], stereoisomerism and molecular symmetry (molecular chirality) have been discussed in a combined fashion, because they are partly related to each other in spite of conceptual distinction between them. For example, a pair of a molecule and its mirror-image molecule is discussed by using the term “chirality” from a viewpoint of molecular symmetry, where the term “achirality” is pairwise used. On the other hand, the same pair is alternatively discussed by using the term “enantiomerism” (or “enantiomeric relationship”) from a viewpoint of stereoisomerism, where the term “diastereoisomerism” (or “diastereomeric relationship”) is used as a counterpart. Chirality and enantiomerism have close relationship because enantiomerism is based on the relationship between two chiral molecules of opposite chirality senses. In contrast, diastereoisomerism has nothing to do with chirality, because pseudoasymmetric cases investigated by Fischer provide examples of achiral and diastereomeric compounds [3,4]. More strictly speaking, the relationship between diastereoisomerism and chirality is indirect (via enantiomerism), because diastereoisomerism is defined as “stereoisomerism other than enantiomerism” in the IUPAC 1996 Recommendations [5].

The comments in the preceding paragraph can be summarized into the following two schemes: “stereoisomerism = enantiomerism + diastereoisomerism” and “enantiomerism \leftrightarrow chirality (molecular symmetry)”, which show entangled features of the combined situation between stereoisomerism and molecular symmetry. The entangled features had long been unnoticed, as exemplified by the title “Specification of Molecular Chirality” of the original version of the Cahn-Ingold-Prelog (CIP) system [6]. So long as we judge from the title, *RS*-stereodescriptors of the CIP system were apparently claimed to specify chirality, which is a kind of properties concerned with molecular symmetry. Even the original version of the CIP system, however, aimed at the assignment of *RS*-stereodescriptors to pseudoasymmetric cases [7], although chirality does not directly participate in these cases because these are achiral and diastereomeric to each other.

Later, the revised version of the CIP system [8] changed its basis from chirality to stereogenicity. Although stereogenicity seemingly referred to stereoisomerism to be treated by the CIP system, the differentiation between chirality and stereogenicity was still insufficient, so that the stereogenicity was found to be a simple combination of enantiomerism and diastereoisomerism. Although there appeared convincing comments on the differentiation between chirality and stereogenicity by Mislow and Siegel [9] and on the consistency of *RS*-stereodescriptors to molecular symmetry by Helmchen [10], the concept of stereogenicity has not been directly defined as a basis of specifying *RS*-stereodescriptors in the IUPAC 1996 Recommendations [5] and even in the IUPAC 2004 Provisional Recommendations [11, P-91.1.1.1]. Instead, the term “stereogenic units” has been defined as a remedy for the absence of such a direct definition. This remedy, however, has concealed the fact the differentiation between chirality and stereogenicity has not been fully demonstrated. Moreover, there remains a critical drawback: the concept of stereogenicity has no pairwise nature (especially diastereoisomerism, except enantiomerism), even though *R* and

S-stereodescriptors due to stereogenicity should be pairwise given to diastereomers as well as to enantiomers.

For the purpose of avoiding the drawback, Fujita's USCI (unit-subduced-cycle-index) approach for investigating pairwise nature due to chirality in molecular symmetry [12, 13] and in enumeration of stereoisomers [14, 15] has been extended so as to be capable of investigating pairwise nature in stereoisomerism. Thereby, the concept of *RS-stereogenicity* has been developed by Fujita [16, 17], where the CIP system was clarified to be based on the pairwise nature due to *RS-stereogenicity*. Then the pairwise nature due to *RS-stereogenicity* was related to *RS*-diastereomeric relationships for specifying *R* and *S*-stereodescriptors, just as the pairwise nature due to chirality was related to enantiomeric relationships [12, 13]. These two types of relationships have been integrated to *RS*-stereoisomeric relationships by developing stereoisograms, which turned out to contain holantimeric relationships as an additional type of relationships [16]. Such stereoisograms have been categorized into five types (Types I–V), which indicate that *RS-stereogenicity* is inherent in Types I, III, and V, while chirality is inherent in Types I, II, and III [16, 18].

The investigations described in the preceding paragraph have been mainly concerned with cases having a single *RS-stereogenic* center. Recently, an extension to treat multiple *RS-stereogenic* centers has been discussed by Fujita in this journal [19], where the concept of *correlation diagrams of stereoisograms* was developed to characterize a set of stereoisograms generated at the respective *RS-stereogenic* centers. However, the previous investigation [19] was restricted to special cases such as di- or trisubstituted cyclobutanes, so that the generality of correlation diagrams has not been fully demonstrated. In particular, it has been still unsolved how stereoisograms generally behave in such a correlation diagram.

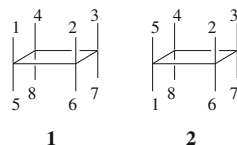
The present paper is devoted to develop a new theory of stereoisomerism, which aims at clarifying the generality of correlation diagrams and at untangling the combined situation between stereoisomerism and molecular symmetry. The task of achieving the aims requires several new concepts for clarifying the behavior of stereoisograms in a correlation diagram, e.g., epimerization groups, local symmetry groups, epimeric stereoisogram groups, epimeric *RS-stereoisomeric* groups, multiple epimerization groups, stereoisomeric groups, stereoisomeric representations, and molecular-symmetry representations. Thereby, the theory of stereoisomerism to be developed is in harmony with molecular symmetry, so that it will serve as a new approach to a logical and mathematical foundation which has been long-awaited over 130 years from the beginning of organic stereochemistry.

2 Stereoskeletons and stereoisomers

2.1 Locant numbering of stereoskeletons

A molecule (or a promolecule in a more abstract fashion) is regarded as a derivative of a stereoskeleton with a set (Ω) of n substitution positions. The stereoskeleton is a three-dimensional object which belongs to a molecular-symmetric group $\mathbf{G}_{C\sigma}^*$, where its substitution positions accommodate a set of (pro)ligands to produce such

Fig. 1 Modes of locant numbering of a cyclobutane stereoskeleton



a (pro)molecule. For the formulation of promolecules and proligands, see [20]. The molecular-symmetric group $\mathbf{G}_{C\sigma}^*$ is usually selected as a point group or a related group (e.g., a wreath product):

$$\mathbf{G}_{C\sigma}^* = \mathbf{G}_C + \sigma^* \mathbf{G}_C, \quad (1)$$

where \mathbf{G}_C contains proper rotations, while the coset $\sigma^* \mathbf{G}_C$ contains improper rotations. Such substitution positions are sequentially numbered as follows:

$$\Omega = \{\Omega_1, \Omega_2, \dots, \Omega_n\}. \quad (2)$$

The group $\mathbf{G}_{C\sigma}^*$ governs the stereoskeleton in the form of a coset representation:

$$\mathbf{G}_{C\sigma} = \mathbf{G}_C + \sigma \mathbf{G}_C, \quad (3)$$

where symbols without an asterisk represent such coset representations (as permutations), so that \mathbf{G}_C contains permutations corresponding to proper rotations, while the coset $\sigma \mathbf{G}_C$ contains permutations corresponding to improper rotations.

Each permutation contained in Eq. 3 depends on an initial mode of locant numbering. For example, let us consider a cyclobutane stereoskeleton shown in Fig. 1, which belongs to a point group \mathbf{D}_{4h} . The eight substitution positions construct a set Ω , which is an orbit governed by a coset representation $\mathbf{D}_{4h}/(C_5)$ [13]. When we select the numbering of **1** as an initial mode of locant numbering, a rotation C_4^* ($\in \mathbf{G}_C$) is represented by the following permutation:

$$C_4^* \sim C_4 = \begin{pmatrix} 1 & 2 & 3 & 4 & 5 & 6 & 7 & 8 \\ 2 & 3 & 4 & 1 & 6 & 7 & 8 & 5 \end{pmatrix} = (1\ 2\ 3\ 4)(5\ 6\ 7\ 8), \quad (4)$$

where each locant number ($i = 1, 2, \dots, 8$) appearing as the subscript of Ω_i is adopted to denote the permutation for the sake of simplicity. Note that the operation C_4^* represents a rotation by 90° around the four-fold axis perpendicular to the cyclobutane plane at its center. On the other hand, when we select another numbering of **2** as an initial mode of locant numbering, the rotation C_4^* ($\in \mathbf{G}_C$) is represented by another permutation:

$$C_4^* \sim C_4' = \begin{pmatrix} 1 & 2 & 3 & 4 & 5 & 6 & 7 & 8 \\ 6 & 3 & 4 & 5 & 2 & 7 & 8 & 1 \end{pmatrix} = (1\ 6\ 7\ 8)(2\ 3\ 4\ 5). \quad (5)$$

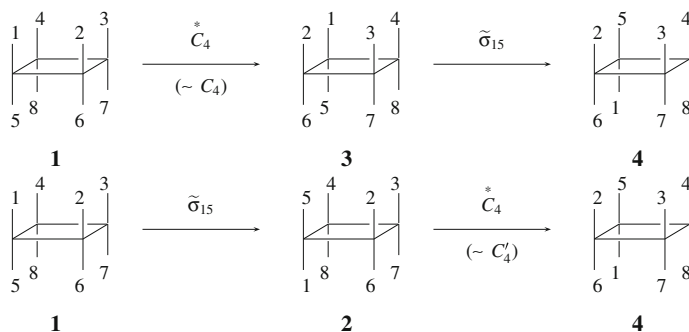


Fig. 2 Molecular symmetry and isomerization process of a cyclobutane stereoskeleton

In order to discuss the isomerization of cyclopropane derivatives, we should take account of two aspects: i.e., the conversion of such locant numbering (e.g., $\tilde{\sigma}_{15}$ for the conversion **1** \rightarrow **2**) as well as a rotation (e.g., C_4^*) of the molecular-symmetry group (e.g., D_{4h}). Although $\tilde{\sigma}_{15}$ ($= (1\ 5)(2)(3)(4)(6)(7)(8)$) and C_4^* (Eq. 4 or Eq. 5) are represented by permutations on Ω , they belong to distinct categories of operations. Hence, we are allowed to postulate that they are commutable as exemplified by Fig. 2.

The conversion shown in the first row of Fig. 2, i.e., **1** \rightarrow **3** \rightarrow **4**, corresponds to the product $\tilde{\sigma}_{15} \times C_4^*$, where the permutation C_4 (Eq. 4) is used as the concrete form of C_4^* . The symbol \times is used to indicate that the first operation C_4^* and the second operation $\tilde{\sigma}_{15}$ belong to distinct categories of operations. On the other hand, the second conversion shown in Fig. 2, i.e., **1** \rightarrow **2** \rightarrow **4**, corresponds to the product $C_4' \times \tilde{\sigma}_{15}$, where the permutation C_4' (Eq. 5) is used as the concrete form of C_4^* . As found by Fig. 2, we obtain the following equation:

$$\tilde{\sigma}_{15} \times C_4^* = C_4' \times \tilde{\sigma}_{15}, \tag{6}$$

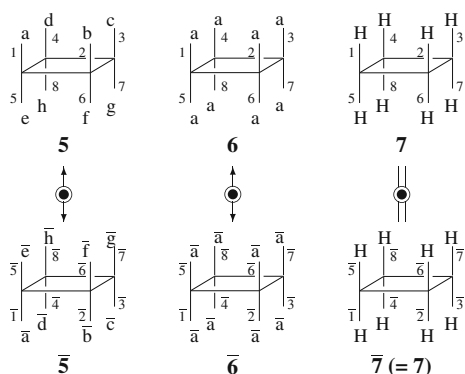
where C_4^* in the left-hand side corresponds to the permutation C_4 (Eq. 5), while C_4' in the right-hand side corresponds to the permutation C_4' (Eq. 5). Obviously, we obtain $\tilde{\sigma}_{15} C_4' \tilde{\sigma}_{15}^{-1} = C_4^*$ as a product of permutations.

The discussion described above can be generalized to give:

$$\tilde{\sigma}_i \times \mathbf{G}_C = \mathbf{G}_C \times \tilde{\sigma}_i, \tag{7}$$

where a permutation representation corresponding to the group \mathbf{G}_C in the left-hand side is selected to be \mathbf{G}_C while a permutation representation corresponding to the group \mathbf{G}_C in the right-hand side is selected to be $\tilde{\sigma}_i \mathbf{G}_C \tilde{\sigma}_i^{-1}$. Note that the equation $\tilde{\sigma}_i \mathbf{G}_C = \mathbf{G}_C \tilde{\sigma}_i$ does not always hold true, but there are cases of $\tilde{\sigma}_i \mathbf{G}_C \neq \mathbf{G}_C \tilde{\sigma}_i$ as products of permutations.

Fig. 3 Promolecules derived by applying functions to a cyclobutane stereoskeleton. The symbols a/\bar{a} etc. denote pairs of enantiomeric proligands



2.2 Functions for determining stereoisomers

In the present approach, a promolecule (or more concretely, a molecule) is considered to be generated by putting proligands (or more concretely, ligands) on the substitution positions of a stereoskeleton. For the concepts of promolecules and proligands, see [20]. When a cyclobutane stereoskeleton (e.g., **1**) is adopted as an example, the process of the substitution is controlled by a function f exemplified by

$$\begin{aligned} f(1) &= a, f(2) = b, f(3) = c, f(4) = d, \\ f(5) &= e, f(6) = f, f(7) = g, f(8) = h, \end{aligned} \quad (8)$$

where the symbols $f(1) = a$, etc. represent the substitution of a proligand 'a' for the position 1, and so on. When the proligands, a, b, ..., and h, are chiral, the positions denoted by a locant number with a bar accommodate the corresponding enantiomeric proligands as follows:

$$\begin{aligned} f(\bar{1}) &= \bar{a}, f(\bar{2}) = \bar{b}, f(\bar{3}) = \bar{c}, f(\bar{4}) = \bar{d}, \\ f(\bar{5}) &= \bar{e}, f(\bar{6}) = \bar{f}, f(\bar{7}) = \bar{g}, f(\bar{8}) = \bar{h}, \end{aligned} \quad (9)$$

where the symbol ' \bar{a} ' etc. denote the enantiomeric proligand of 'a' etc.

The resulting promolecules **5** and $\bar{5}$ shown in Fig. 3 belong to C_1 , where these promolecules construct an enantiomeric pair belonging to C_s , which is a subgroup of the D_{4h} -group of the stereoskeleton. The promolecule **5** (or $\bar{5}$) is converted its homomer under the action of the D_4 -group (the maximum chiral subgroup of D_{4h}). For example, the skeleton **3** generated by C'_4 (Eq. 5) gives an homomer of **5** by applying the function represented by Eq. 8. So long as we investigate stereoisomerism, such a set of homomers generated by the elements of D_4 can be considered to be a single molecular entity.

As an extreme case, let us consider the following function:

$$\begin{aligned} f(1) &= f(2) = f(3) = f(4) = f(5) = f(6) = f(7) = f(8) = a, \\ f(\bar{1}) &= f(\bar{2}) = f(\bar{3}) = f(\bar{4}) = f(\bar{5}) = f(\bar{6}) = f(\bar{7}) = f(\bar{8}) = \bar{a}. \end{aligned} \quad (10)$$

The resulting promolecules **6** and $\bar{6}$ shown in Fig. 3 belong to \mathbf{D}_4 , which is a subgroup of the \mathbf{D}_{4h} -group of the stereoskeleton. In this case, the elements of \mathbf{D}_4 generate a set of identical promolecules, which is also regarded as a set of homomers as an extreme case. Obviously, such an extreme set can be also considered to be a single molecular entity, so long as we investigate stereoisomerism.

A more extreme case is cyclobutane itself, where the corresponding function is represented as follows:

$$\begin{aligned} f(1) = f(2) = f(3) = f(4) = f(5) = f(6) = f(7) = f(8) = \text{H}, \\ f(\bar{1}) = f(\bar{2}) = f(\bar{3}) = f(\bar{4}) = f(\bar{5}) = f(\bar{6}) = f(\bar{7}) = f(\bar{8}) = \text{H}, \end{aligned} \quad (11)$$

where no stereoisomers appear. The resulting promolecule **7** ($= \bar{7}$) shown in Fig. 3 belongs to \mathbf{D}_{4h} , which is identical with the \mathbf{D}_{4h} -group of the stereoskeleton. As a matter of course, the elements of \mathbf{D}_4 generate a set of identical promolecules, which is a set of homomers as a more extreme case. Hence, the set can be also considered to be a single molecular entity, so long as we investigate stereoisomerism.

Suppose that each pair of enantiomers is considered to be a single entity. Thereby, such a pair of enantiomers and an achiral molecule (promolecule) can be treated in a common theoretical framework. For example, the pair $5/\bar{5}$ (chiral promolecules) is an entity belonging to \mathbf{C}_s . Even if each molecule of the pair is chiral (e.g., \mathbf{C}_1 for **5** or $\bar{5}$), the pair (e.g., \mathbf{C}_s for the pair $5/\bar{5}$) can be treated as a single entity under \mathbf{D}_{4h} . Note that one set of homomers belonging to \mathbf{C}_1 can be equalized to give a single entity under \mathbf{D}_4 , the other set of homomers belonging to \mathbf{C}_1 (of opposite chirality sense) can be equalized to give a single entity under \mathbf{D}_4 , and these two sets in an enantiomeric relationship construct an achiral single entity under \mathbf{D}_{4h} . On a similar line, the pair $6/\bar{6}$ (chiral promolecules) is an entity belonging to \mathbf{D}_{4h} and the molecule **7** (an achiral promolecules) is self-enantiomeric (achiral) so as to be regarded as an entity belonging to \mathbf{D}_{4h} .

In general, $\mathbf{G}_{C\sigma}^*$ (Eq. 3) for specifying the molecular symmetry of a stereoskeleton is used to treat (self-)enantiomeric pairs of promolecules derived from the stereoskeletons. Even if the molecular symmetries of such (self-)enantiomeric pairs are reduced to subgroups of $\mathbf{G}_{C\sigma}^*$, they can be discussed by using $\mathbf{G}_{C\sigma}^*$ in place of such reduced subgroups, once we adopt the concept of *homomers*, which are equalized to generate a single entity under the action of \mathbf{G}_C^* .

3 RS-stereoisomeric groups and stereoisomeric groups

3.1 RS-stereoisomeric groups

By starting from the coset representation $\mathbf{G}_{C\sigma}$ (Eq. 3) of the molecular-symmetric group $\mathbf{G}_{C\sigma}^*$ (Eq. 1), an RS-Stereoisomeric group $\mathbf{G}_{C\sigma\hat{\sigma}\hat{\tau}}$ is defined according to a previous paper [18]. The representative σ appearing in $\mathbf{G}_{C\sigma}$ (Eq. 3) is a reflection which changes the stereoskeleton into a mirror-image, where the configuration of each ligand, at the same time, is converted into the opposite configuration to produce

the corresponding enantiomeric ligand in isolation. Let the symbol $\tilde{\sigma}$ represent a permutation which has the same cycle structure as σ but causes no alternation of ligand configurations. Let the symbol \hat{I} be a permutation which causes no change of the stereoskeleton of the molecule but alters ligand configurations. Then the following two groups are obtained:

$$\mathbf{G}_{C\tilde{\sigma}} = \mathbf{G}_C + \tilde{\sigma}\mathbf{G}_C \quad (12)$$

$$\mathbf{G}_{C\hat{I}} = \mathbf{G}_C + \hat{I}\mathbf{G}_C. \quad (13)$$

Definition 1 (*RS-Stereoisomeric group*) The collection of the cosets appearing in Eqs. 3, 12, and 13 generates the *RS-Stereoisomeric group* $\mathbf{G}_{C\sigma\tilde{\sigma}\hat{I}}$ as follows:

$$\mathbf{G}_{C\sigma\tilde{\sigma}\hat{I}} = \mathbf{G}_C + \sigma\mathbf{G}_C + \tilde{\sigma}\mathbf{G}_C + \hat{I}\mathbf{G}_C, \quad (14)$$

which contains $\mathbf{G}_{C\sigma}$ (Eq. 3), $\mathbf{G}_{C\tilde{\sigma}}$ (Eq. 12), and $\mathbf{G}_{C\hat{I}}$ (Eq. 13) as subgroups of index 2.

Obviously, Eqs. 3, 12, and 13 show that $\sigma^2 \in \mathbf{G}_C$, $\tilde{\sigma}^2 \in \mathbf{G}_C$, and $\hat{I}^2 \in \mathbf{G}_C$. However, it is not always true that $\sigma^2 = I$ or $\tilde{\sigma}^2 = I$, whereas we may postulate $\hat{I}^2 = I$. As shown later, we can presume $\sigma^2 = I$ and $\tilde{\sigma}^2 = I$ if σ and $\tilde{\sigma}$ are appropriately selected for the purpose of investigating organic stereoisomerism.

Because the subgroup \mathbf{G}_C is a normal subgroup of $\mathbf{G}_{C\sigma\tilde{\sigma}\hat{I}}$, the coset decomposition represented by Eq. 14 generates the following factor group of order 4:

$$\dot{\mathbf{G}}_{C\sigma\tilde{\sigma}\hat{I}} = \mathbf{G}_{C\sigma\tilde{\sigma}\hat{I}}/\mathbf{G}_C = \{\mathbf{G}_C, \sigma\mathbf{G}_C, \tilde{\sigma}\mathbf{G}_C, \hat{I}\mathbf{G}_C\}. \quad (15)$$

The elements of the coset $I\mathbf{G}_C$ ($= \mathbf{G}_C$) change an original molecule into its homomers, which are regarded as being identical with the original molecule. The coset $\sigma\mathbf{G}_C$ corresponds to molecules which are homomeric to each other and are regarded as being enantiomeric to the original molecule. The coset $\tilde{\sigma}\mathbf{G}_C$ corresponds to molecules which are homomeric to each other and are regarded as being *RS*-diastereomeric to the original molecule. The coset $\hat{I}\mathbf{G}_C$ corresponds to molecules which are homomeric to each other and are regarded as being holantimeric to the original molecule. The three relationships (i.e., enantiomeric, *RS*-diastereomeric, and holantimeric relationships) are illustrated by a stereoisogram [16]. A quadruplet of molecules (*RS*-stereoisomers) contained in such a stereoisogram is regarded as an equivalence class (an orbit), which is in turn manipulated as a single entity so as to develop a new scheme for investigating geometric and stereoisomeric features in stereochemistry [21].

3.2 Axiom of organic stereoisomerism

Suppose that the stereoskeleton governed by the *RS*-Stereoisomeric group $\mathbf{G}_{C\sigma\tilde{\sigma}\hat{I}}$ (Eq. 14) has n *RS*-stereocenters (*RS*-stereogenic centers), where an epimerization at the i -th *RS*-stereocenter is represented by the symbol $\tilde{\sigma}_i$ ($i = 1, 2, \dots, n$). Then the total epimerization $\tilde{\sigma}$ is defined as follows:

Definition 2 (*Product of epimerizations*) The permutation $\tilde{\sigma}$ is defined by the product of epimerization operations at every *RS*-stereocenters:

$$\tilde{\sigma} = \tilde{\sigma}_1 \tilde{\sigma}_2 \dots \tilde{\sigma}_i \dots \tilde{\sigma}_n = \prod_{i=1}^n \tilde{\sigma}_i, \quad (16)$$

where every epimerizations at the right-hand side are commutable.

Because of $\tilde{\sigma}_i^2 = I$, Eq. 16 shows that $\tilde{\sigma}^2 = I$. Although the scope of the present approach is restricted to cases satisfying Eq. 16, this restricted scope is sufficient to cover organic stereoisomerism by considering the following axiom:

Definition 3 (*Axiom of organic stereoisomerism*) The reflection operation σ is represented by the following equation:

$$\sigma = \tilde{\sigma} \hat{I} = \hat{I} \tilde{\sigma}. \quad (17)$$

This is called *an axiom of organic stereoisomerism*, from which we start the present approach to the theory of organic stereoisomerism.

It should be noted that, in some discussions on stereoisomerism, an appropriate set of *RS*-stereogenic centers is adopted in place of the whole set of *n RS*-stereogenic centers. Even in these cases, the adopted set of epimerizations is considered to satisfy Eqs. 16 and 17.

Because $\tilde{\sigma}_i$ and \hat{I} are commutable, $\tilde{\sigma}$ and \hat{I} are also commutable so that the reflection operation $\sigma (= \tilde{\sigma} \hat{I})$ incorporated in processes of stereoisomerism satisfies $\sigma^2 = (\tilde{\sigma} \hat{I})^2 = \tilde{\sigma}^2 \hat{I}^2 = I$. Hence, we are able to generate basic groups for discussing stereoisomerism:

$$\mathbf{H}_{\hat{I}} = \{I, \hat{I}\} \quad (18)$$

$$\mathbf{H}_{\tilde{\sigma}} = \{I, \tilde{\sigma}\} \quad (19)$$

$$\mathbf{H}_{\sigma} = \{I, \tilde{\sigma} \hat{I}\} = \{I, \sigma\}, \quad (20)$$

which correspond to $\mathbf{G}_{C\hat{I}}$ (Eq. 13), $\mathbf{G}_{C\tilde{\sigma}}$ (Eq. 12), and $\mathbf{G}_{C\sigma}$ (Eq. 3). By starting from Eqs. 18–20, we define a stereoisogram group \mathbf{H}_s as follows:

Definition 4 (*Stereoisogram group*) The stereoisogram group \mathbf{H}_s contains the transversal corresponding to Eq. 14, i.e.,

$$\mathbf{H}_s = \{I, \sigma, \tilde{\sigma}, \hat{I}\} = \{I, \tilde{\sigma} \hat{I}, \tilde{\sigma}, \hat{I}\}, \quad (21)$$

is a group under presumption of Eqs. 16 and 17.

Note that such relationships as $\sigma \tilde{\sigma} = \tilde{\sigma} \hat{I} \tilde{\sigma} = \hat{I} \in \mathbf{H}_s$ show that the set \mathbf{H}_s is closed under multiplication operations. Because \mathbf{H}_s specifies a stereoisogram, it is called *a*

stereoisogram group.¹ Because the stereoisogram group \mathbf{H}_s (Eq. 21) is concerned with the global symmetry of the stereoskeleton at issue, it is more specifically called a *main stereoisogram group* if necessary.

The *RS*-stereoisomeric group $\mathbf{G}_{C\sigma\tilde{\sigma}\hat{I}}$ (Eq. 14) is rewritten to the direct product of \mathbf{H}_s (Eq. 21) and \mathbf{G}_C , i.e.,

$$\mathbf{G}_{C\sigma\tilde{\sigma}\hat{I}} = \mathbf{H}_s \times \mathbf{G}_C \quad (22)$$

$$= \mathbf{H}_{\tilde{\sigma}} \times \mathbf{H}_{\hat{I}} \times \mathbf{G}_C = \mathbf{H}_{\tilde{\sigma}} \times \mathbf{H}_{\sigma} \times \mathbf{G}_C = \mathbf{H}_{\sigma} \times \mathbf{H}_{\hat{I}} \times \mathbf{G}_C \quad (23)$$

Accordingly, the coset decomposition represented by Eq. 14 is formally represented by the following equation:

$$\mathbf{G}_{C\sigma\tilde{\sigma}\hat{I}} = (I + \sigma + \tilde{\sigma} + \hat{I}) \overset{\times}{\mathbf{G}}_C = (I + \tilde{\sigma}\hat{I} + \tilde{\sigma} + \hat{I}) \overset{\times}{\mathbf{G}}_C \quad (24)$$

$$= (I + \tilde{\sigma})(I + \hat{I}) \overset{\times}{\mathbf{G}}_C = (I + \tilde{\sigma})(I + \sigma) \overset{\times}{\mathbf{G}}_C = (I + \sigma)(I + \hat{I}) \overset{\times}{\mathbf{G}}_C, \quad (25)$$

because we are able to put $\overset{\times}{\mathbf{G}}_C = \{I\} \times \mathbf{G}_C$ for Eq. 22 and $\overset{\times}{\mathbf{G}}_C = \{I\} \times \{I\} \times \mathbf{G}_C$ for each direct product of Eq. 23. For the sake of simplicity, such symbols as $\overset{\times}{\mathbf{G}}_C$ are used in the present article in order to show coset decompositions of direct-product groups, where the part $\{I\} \times \{I\} \times \cdots \times \{I\}$ is appropriately interpreted without losing generality.

For example, let us consider a cyclopropane stereoskeleton **1** (Fig. 4a), where a point group \mathbf{D}_{4h} is selected as the corresponding molecular-symmetry group ($\overset{*}{\mathbf{G}}_{C\sigma}$) and its coset representation $\mathbf{D}_{4h}/(\mathbf{C}_s)$ is regarded as $\mathbf{G}_{C\sigma}$ (Eq. 3). For the sake of simplicity, the coset representation $\mathbf{D}_{4h}/(\mathbf{C}_s)$ is equalized to \mathbf{D}_{4h} , where \mathbf{D}_{4h} corresponds to $\mathbf{G}_{C\sigma}$ and \mathbf{D}_4 corresponds to \mathbf{G}_C .

When we select arbitrarily the original numbering shown by the structure **1** (Fig. 4), we obtain following permutations:

$$I = \begin{pmatrix} 1 & 2 & 3 & 4 & 5 & 6 & 7 & 8 \\ 1 & 2 & 3 & 4 & 5 & 6 & 7 & 8 \end{pmatrix} = (1)(2)(3)(4)(5)(6)(7)(8) \quad (26)$$

$$\sigma_h = \begin{pmatrix} 1 & 2 & 3 & 4 & 5 & 6 & 7 & 8 \\ \bar{5} & \bar{6} & \bar{7} & \bar{8} & \bar{1} & \bar{2} & \bar{3} & \bar{4} \end{pmatrix} = \overline{(1\ 5)(2\ 6)(3\ 7)(4\ 8)}, \quad (27)$$

where the reflection satisfies $\sigma_h^2 = I$. They are used to generate the following coset representation:

$$\mathbf{D}_{4h} = \mathbf{D}_4 + \sigma_h \mathbf{D}_4. \quad (28)$$

¹ An *RS*-stereoisomeric group generated from the point group \mathbf{S}_4 may be $\mathbf{S}_{4\sigma\tilde{\sigma}\hat{I}} = \mathbf{C}_2 + \mathbf{S}_4\mathbf{C}_2 + \tilde{\mathbf{S}}_4\mathbf{C}_2 + \hat{\mathbf{I}}\mathbf{C}_2$. Although the corresponding factor group $\mathbf{S}_{4\sigma\tilde{\sigma}\hat{I}}/\mathbf{C}_2$ can be constructed according to Eq. 15, the transversal $\{I, \mathbf{S}_4, \tilde{\mathbf{S}}_4, \hat{\mathbf{I}}\}$ is not a group. So long as we consider an epimerization $\tilde{\sigma}$ at each pair of two positions belonging to the coset representation $\mathbf{S}_4/(\mathbf{C}_2)$, we obtain $\tilde{\sigma}\hat{\mathbf{I}} = \hat{\mathbf{I}}\tilde{\sigma}$. This means that we may adopt a group $\{I, \tilde{\sigma}\hat{\mathbf{I}}, \tilde{\sigma}, \hat{\mathbf{I}}\}$ in place of the transversal. More complicated cases are open to the future investigation.

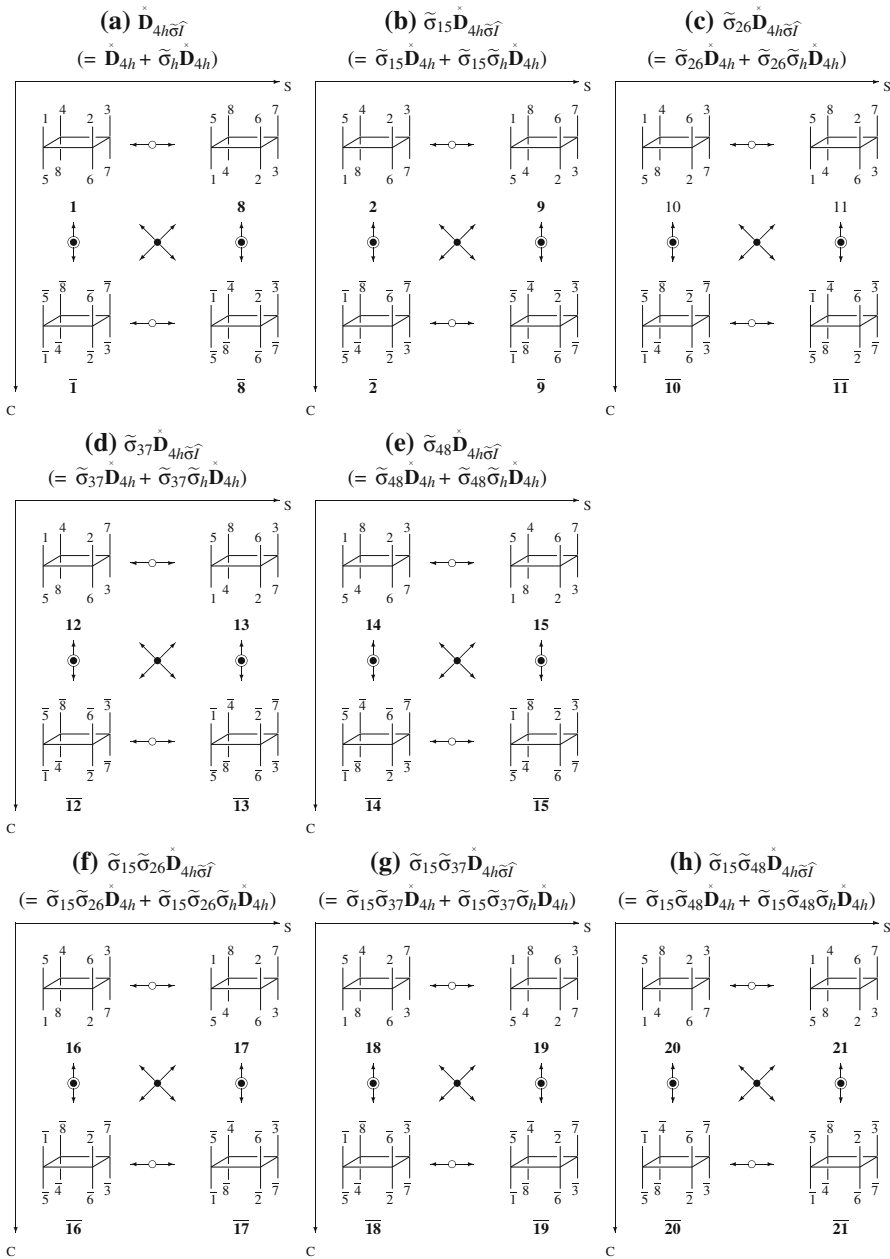


Fig. 4 Numbering of a cyclobutane stereoskeleton for specifying stereoisomeric cyclobutane derivatives

By starting from the permutations of I and σ_h , we obtain the following permutations:

$$\tilde{\sigma}_h = \begin{pmatrix} 1 & 2 & 3 & 4 & 5 & 6 & 7 & 8 \\ 5 & 6 & 7 & 8 & 1 & 2 & 3 & 4 \end{pmatrix} = (1\ 5)(2\ 6)(3\ 7)(4\ 8) \quad (29)$$

$$\widehat{I} = \left(\begin{array}{cccccccc} 1 & 2 & 3 & 4 & 5 & 6 & 7 & 8 \\ \bar{1} & \bar{2} & \bar{3} & \bar{4} & \bar{5} & \bar{6} & \bar{7} & \bar{8} \end{array} \right) = \overline{(1)(2)(3)(4)(5)(6)(7)(8)} \quad (30)$$

in order to construct the corresponding *RS*-stereoisomeric group and related groups:

$$\mathbf{D}_{4\tilde{\sigma}_h} = \mathbf{D}_4 + \tilde{\sigma}_h \mathbf{D}_4 \quad (31)$$

$$\mathbf{D}_{4\widehat{I}} = \mathbf{D}_4 + \widehat{I} \mathbf{D}_4 \quad (32)$$

$$\mathbf{D}_{4h\tilde{\sigma}_h\widehat{I}} = \mathbf{D}_4 + \sigma_h \mathbf{D}_4 + \tilde{\sigma}_h \mathbf{D}_4 + \widehat{I} \mathbf{D}_4 \quad (33)$$

Let the symbols $\tilde{\sigma}_{15}$, $\tilde{\sigma}_{26}$, $\tilde{\sigma}_{37}$, and $\tilde{\sigma}_{48}$ be epimerization operations of cyclopropane stereoskeletons, which respectively correspond to **2** (Fig. 4b), **10** (Fig. 4c), **12** (Fig. 4d), and **14** (Fig. 4e), as shown in Fig. 4. Then, Eqs. 16 and 17 for this case are obtained as follows:

$$\tilde{\sigma}_h = \tilde{\sigma}_{15}\tilde{\sigma}_{26}\tilde{\sigma}_{37}\tilde{\sigma}_{48} \quad (34)$$

$$\sigma_h = \tilde{\sigma}_h \widehat{I}, \quad (35)$$

where the element $\tilde{\sigma}_h$ corresponds to **8**, while the element σ_h corresponds to $\bar{\mathbf{1}}$ (Fig. 4a).

According to Eq. 15, the coset decomposition represented by Eq. 33 generates the following factor group:

$$\dot{\mathbf{D}}_{4h\tilde{\sigma}_h\widehat{I}} = \mathbf{D}_{4h\tilde{\sigma}_h\widehat{I}}/\mathbf{D}_4 = \{\mathbf{D}_4, \sigma_h \mathbf{D}_4, \tilde{\sigma}_h \mathbf{D}_4, \widehat{I} \mathbf{D}_4\}, \quad (36)$$

which is isomorphic to the factor group $\dot{\mathbf{G}}_{C\sigma\tilde{\sigma}\widehat{I}}$ (Eq. 15).

When the coset $I\mathbf{D}_4$ ($= \mathbf{D}_4$) appearing in Eq. 33 (or Eq. 36) corresponds to the numbering of **1**, the other cosets $\sigma_h \mathbf{D}_4$, $\tilde{\sigma}_h \mathbf{D}_4$, and $\widehat{I} \mathbf{D}_4$ correspond to $\bar{\mathbf{1}}$, **8**, and $\bar{\mathbf{8}}$, respectively, as found in Fig. 4a. The quadruplet of **1**, $\bar{\mathbf{1}}$, **8**, and $\bar{\mathbf{8}}$ constructs a stereoisogram according to the formulation of [16].

The groups corresponding to Eqs. 18–21 are also obtained for this case. In particular, the stereoisogram group \mathbf{H}_s for this case is obtained as follows:

$$\mathbf{H}_s = \{I, \sigma_h, \tilde{\sigma}_h, \widehat{I}\} = \{I, \tilde{\sigma}_h \widehat{I}, \tilde{\sigma}_h, \widehat{I}\}, \quad (37)$$

where the concrete forms of the elements are given by Eqs. 26, 27, 29, and 30. These elements again correspond to **1**, $\bar{\mathbf{1}}$, **8**, and $\bar{\mathbf{8}}$, which construct a quadruplet contained in the stereoisogram shown in Fig. 4a.

3.3 Epimerizations

In the next step of the present approach, each epimerization operation is taken into consideration so as to give a respective group:

Definition 5 (*Epimerization group*) Let us examine the effect of an epimerization which is represented by the symbol $\tilde{\sigma}_i$ ($i = 1, 2, \dots, n$):

$$\mathbf{H}_{\tilde{\sigma}_i} = \{I, \tilde{\sigma}_i\}, \quad (38)$$

which is called an epimerization group at the i -th RS -stereocenter.

Each epimerization group is combined with the RS -stereoisomeric group as follows:

Definition 6 (*Local symmetry group at an RS -stereogenic center*) The direct product of $\mathbf{H}_{\tilde{\sigma}_i}$ (Eq. 38) and $\mathbf{G}_{C\sigma\tilde{\sigma}\hat{I}}$ (Eq. 14 or Eq. 22) is constructed as follows:

$$\mathbf{G}_{C\sigma\tilde{\sigma}\hat{I}}^{\tilde{\sigma}_i} = \mathbf{H}_{\tilde{\sigma}_i} \times \mathbf{G}_{C\sigma\tilde{\sigma}\hat{I}}, \tag{39}$$

which is called a local symmetry group at an RS -stereogenic center.

It should be noted here that although $\mathbf{G}_{C\sigma\tilde{\sigma}\hat{I}}$ is a permutation group, a similar relationship to Eq. 7 is presumed because Eq. 39 is defined in terms of a direct product.

By keeping Eq. 38 in mind, the direct product represented by Eq. 39 is formally rewritten as follows:

$$\mathbf{G}_{C\sigma\tilde{\sigma}\hat{I}}^{\tilde{\sigma}_i} = (I + \tilde{\sigma}_i) \times \mathbf{G}_{C\sigma\tilde{\sigma}\hat{I}} \tag{40}$$

$$= I \times \mathbf{G}_{C\sigma\tilde{\sigma}\hat{I}} + \tilde{\sigma}_i \times \mathbf{G}_{C\sigma\tilde{\sigma}\hat{I}} \tag{41}$$

$$= \overset{\times}{\mathbf{G}}_{C\sigma\tilde{\sigma}\hat{I}} + \tilde{\sigma}_i \overset{\times}{\mathbf{G}}_{C\sigma\tilde{\sigma}\hat{I}}. \tag{42}$$

For the purpose of showing that Eq. 42 is a coset decomposition corresponding to Eq. 39, we adopt the following convention:

$$\overset{\times}{\mathbf{G}}_{C\sigma\tilde{\sigma}\hat{I}} = I \times \mathbf{G}_{C\sigma\tilde{\sigma}\hat{I}} = \{I\} \times \mathbf{G}_{C\sigma\tilde{\sigma}\hat{I}}. \tag{43}$$

This convention means that the identity group $\{I\}$ is a normal subgroup of $\mathbf{H}_{\tilde{\sigma}_i}$ and that $\mathbf{G}_{C\sigma\tilde{\sigma}\hat{I}}$ itself is a normal subgroup of $\mathbf{G}_{C\sigma\tilde{\sigma}\hat{I}}$. Hence, the resulting equation (Eq. 42) can be regarded as a coset decomposition of the direct product $\mathbf{G}_{C\sigma\tilde{\sigma}\hat{I}}^{\tilde{\sigma}_i}$ (Eq. 39) by $\overset{\times}{\mathbf{G}}_{C\sigma\tilde{\sigma}\hat{I}}$ (Eq. 43), which is a normal subgroup of $\mathbf{G}_{C\sigma\tilde{\sigma}\hat{I}}^{\tilde{\sigma}_i}$.

The coset decomposition (Eq. 42) generates the following set of cosets:

$$\mathbf{G}_{C\sigma\tilde{\sigma}\hat{I}}^{\tilde{\sigma}_i} / \overset{\times}{\mathbf{G}}_{C\sigma\tilde{\sigma}\hat{I}} = \{\overset{\times}{\mathbf{G}}_{C\sigma\tilde{\sigma}\hat{I}}, \tilde{\sigma}_i \overset{\times}{\mathbf{G}}_{C\sigma\tilde{\sigma}\hat{I}}\}, \tag{44}$$

which is a factor group of order 2. The set of cosets (Eq. 44) generates a coset representation $\mathbf{G}_{C\sigma\tilde{\sigma}\hat{I}}^{\tilde{\sigma}_i} \left(/ \overset{\times}{\mathbf{G}}_{C\sigma\tilde{\sigma}\hat{I}} \right)$, so that we are able to the subduction ($\downarrow \mathbf{H}_{\tilde{\sigma}_i}$) of the coset representation according to the USCI (unit-subduced-cycle-index) approach developed by Fujita [13]:

$$\begin{array}{c|cc} \downarrow \mathbf{H}_{\tilde{\sigma}_i} & \overset{\times}{\mathbf{G}}_{C\sigma\tilde{\sigma}\hat{I}} & \tilde{\sigma}_i \overset{\times}{\mathbf{G}}_{C\sigma\tilde{\sigma}\hat{I}} \\ \times I & \overset{\times}{\mathbf{G}}_{C\sigma\tilde{\sigma}\hat{I}} & \tilde{\sigma}_i \overset{\times}{\mathbf{G}}_{C\sigma\tilde{\sigma}\hat{I}} \\ \times \tilde{\sigma}_i & \tilde{\sigma}_i \overset{\times}{\mathbf{G}}_{C\sigma\tilde{\sigma}\hat{I}} & \overset{\times}{\mathbf{G}}_{C\sigma\tilde{\sigma}\hat{I}} \end{array} \tag{45}$$

Hence, the set represented by (Eq. 44) is transitive under the subduction ($\downarrow \mathbf{H}_{\tilde{\sigma}_i}$), where the group $\mathbf{H}_{\tilde{\sigma}_i}$ is equalized to $\mathbf{H}_{\tilde{\sigma}_i} \times \{I\}$ which is a normal subgroup of the direct product represented by Eq. 39. According to the notation of Fujita’s USCI approach, Eq. 45 is represented as follows:

$$\mathbf{G}_{C\sigma\tilde{\sigma}\hat{I}}^{\tilde{\sigma}_i} \left(/ \mathbf{G}_{C\sigma\tilde{\sigma}\hat{I}}^{\times} \right) \downarrow \mathbf{H}_{\tilde{\sigma}_i} = \mathbf{H}_{\tilde{\sigma}_i} (/ \{I\}). \tag{46}$$

The direct product represented by Eq. 39 is further expanded by means of Eq. 23 so as to generate the following equation:

$$\mathbf{G}_{C\sigma\tilde{\sigma}\hat{I}}^{\tilde{\sigma}_i} = \mathbf{H}_{\tilde{\sigma}_i} \times \mathbf{G}_{C\sigma\tilde{\sigma}\hat{I}} = \mathbf{H}_{\tilde{\sigma}_i} \times \mathbf{H}_{\sigma} \times \mathbf{H}_{\hat{I}} \times \mathbf{G}_C, \tag{47}$$

where a similar relationship to Eq. 7 is presumed because Eq. 47 is defined in terms of a direct product. The elements of the partial direct product ($\mathbf{H}_{\tilde{\sigma}_i} \times \mathbf{H}_{\sigma}$) contained in Eq. 47 can be obtained by collecting the terms appearing in a formal equation $(I + \tilde{\sigma}_i)(I + \sigma)$ so that we obtain:

Definition 7 (*Epimeric stereoisogram group*) An epimeric stereoisogram (defined below) is controlled by the following group:

$$\begin{aligned} \mathbf{H}_{\sigma}^{\tilde{\sigma}_i} &= \mathbf{H}_{\tilde{\sigma}_i} \times \mathbf{H}_{\sigma} \\ &= \{I, \tilde{\sigma}_i, \sigma, \tilde{\sigma}_i\sigma\} = \{I, \tilde{\sigma}_i, \tilde{\sigma}\hat{I}, \tilde{\sigma}_i\tilde{\sigma}\hat{I}\}, \end{aligned} \tag{48}$$

which is called an *epimeric stereoisogram group*.

On a similar line, the terms appearing in a formal equation $(I + \tilde{\sigma}_i)(I + \tilde{\sigma})(I + \hat{I})$ is collected to generate the elements of the direct product $\mathbf{H}_{\tilde{\sigma}_i} \times \mathbf{H}_{\sigma} \times \mathbf{H}_{\hat{I}}$ contained in Eq. 47 so that we obtain:

$$\begin{aligned} &(\mathbf{H}_{\tilde{\sigma}_i} \times \mathbf{H}_{\sigma}) \times \mathbf{H}_{\hat{I}} \\ &= \{I, \tilde{\sigma}_i, \sigma, \tilde{\sigma}_i\sigma; \hat{I}, \hat{I}\tilde{\sigma}_i, \hat{I}\sigma, \hat{I}\tilde{\sigma}_i\sigma\} = \{I, \tilde{\sigma}_i, \sigma, \tilde{\sigma}_i\sigma; \hat{I}, \hat{I}\tilde{\sigma}_i, \hat{I}\sigma, \hat{I}\tilde{\sigma}_i\sigma\}, \end{aligned} \tag{49}$$

which is a group of order 8. By keeping Eq. 49 in mind, the direct product represented by Eq. 47 is formally transformed into the following equation:

$$\mathbf{G}_{C\sigma\tilde{\sigma}\hat{I}}^{\tilde{\sigma}_i} = (I + \tilde{\sigma}_i)(I + \tilde{\sigma})(I + \hat{I}) \times \mathbf{G}_C \tag{50}$$

$$\begin{aligned} &= I \times \mathbf{G}_C + \tilde{\sigma}_i \times \mathbf{G}_C + \sigma \times \mathbf{G}_C + \tilde{\sigma}_i\sigma \times \mathbf{G}_C \\ &\quad + \hat{I} \times \mathbf{G}_C + \hat{I}\tilde{\sigma}_i \times \mathbf{G}_C + \hat{I}\sigma \times \mathbf{G}_C + \hat{I}\tilde{\sigma}_i\sigma \times \mathbf{G}_C \end{aligned} \tag{51}$$

$$= \overset{\times}{\mathbf{G}}_C + \tilde{\sigma}_i \overset{\times}{\mathbf{G}}_C + \sigma \overset{\times}{\mathbf{G}}_C + \tilde{\sigma}_i\sigma \overset{\times}{\mathbf{G}}_C + \hat{I} \overset{\times}{\mathbf{G}}_C + \hat{I}\tilde{\sigma}_i \overset{\times}{\mathbf{G}}_C + \hat{I}\sigma \overset{\times}{\mathbf{G}}_C + \hat{I}\tilde{\sigma}_i\sigma \overset{\times}{\mathbf{G}}_C \tag{52}$$

where we put

$$\overset{\times}{\mathbf{G}}_C = I \times \mathbf{G}_C = \{I\} \times \{I\} \times \{I\} \times \mathbf{G}_C \tag{53}$$

in accord with Eq. 47. The resulting equation (Eq. 52) can be regarded as a coset decomposition of the direct product $\mathbf{G}_{C\sigma\tilde{\sigma}\hat{I}}^{\tilde{\sigma}_i}$ (Eq. 47) by \mathbf{G}_C (Eq. 53), which is a normal subgroup of $\mathbf{G}_{C\sigma\tilde{\sigma}\hat{I}}^{\tilde{\sigma}_i}$. Note that each identity group $\{I\}$ is a normal subgroup of $\mathbf{H}_{\tilde{\sigma}_i}$, \mathbf{H}_σ , or $\mathbf{H}_{\hat{I}}$ and that \mathbf{G}_C itself is a normal subgroup of \mathbf{G}_C .

The coset decomposition (Eq. 52) generates the following set of cosets:

$$\mathbf{G}_{C\sigma\tilde{\sigma}\hat{I}}^{\tilde{\sigma}_i} / \mathbf{G}_C = \left\{ \begin{matrix} \mathbf{G}_C, & \tilde{\sigma}_i \mathbf{G}_C, & \sigma \mathbf{G}_C, & \tilde{\sigma}_i \sigma \mathbf{G}_C, & \hat{I} \mathbf{G}_C, & \hat{I} \tilde{\sigma}_i \mathbf{G}_C, & \tilde{\sigma} \mathbf{G}_C, & \tilde{\sigma}_i \tilde{\sigma} \mathbf{G}_C \\ 1 & 2 & 3 & 4 & 5 & 6 & 7 & 8 \end{matrix} \right\}, \tag{54}$$

where the eight cosets are numbered sequentially. The set of cosets (Eq. 54) is a factor group of order 8. The set of cosets (Eq. 54) generates a coset representation $\mathbf{G}_{C\sigma\tilde{\sigma}\hat{I}}^{\tilde{\sigma}_i} / (\mathbf{G}_C)$ so that we are able to the subduction ($\downarrow \mathbf{H}_\sigma^{\tilde{\sigma}_i} = \downarrow \mathbf{H}_{\tilde{\sigma}_i} \times \mathbf{H}_\sigma$) of the coset representation according to the USCI (unit-subduced-cycle-index) approach developed by Fujita [13]:

$\downarrow \mathbf{H}_\sigma^{\tilde{\sigma}_i}$ ($= \downarrow \mathbf{H}_{\tilde{\sigma}_i} \times \mathbf{H}_\sigma$)	\mathbf{G}_C	$\tilde{\sigma}_i \mathbf{G}_C$	$\sigma \mathbf{G}_C$	$\tilde{\sigma}_i \sigma \mathbf{G}_C$	$\hat{I} \mathbf{G}_C$	$\hat{I} \tilde{\sigma}_i \mathbf{G}_C$	$\tilde{\sigma} \mathbf{G}_C$	$\tilde{\sigma}_i \tilde{\sigma} \mathbf{G}_C$	(55)
$\times I$	1	2	3	4	5	6	7	8	
$\times \tilde{\sigma}_i$	2	1	4	3	6	5	8	7	
$\times \sigma$	3	4	1	2	7	8	5	6	
$\times \tilde{\sigma}_i \sigma$	4	3	2	1	8	7	6	5	

Hence, the set represented by Eq. 54 is divided into two sets of cosets according to the following subduction:

$$\mathbf{G}_{C\sigma\tilde{\sigma}\hat{I}}^{\tilde{\sigma}_i} / (\mathbf{G}_C) \downarrow \mathbf{H}_\sigma^{\tilde{\sigma}_i} = 2\mathbf{H}_\sigma^{\tilde{\sigma}_i} / (\{I\}), \tag{56}$$

where the right-hand side represents the regular representation of the group $\mathbf{H}_\sigma^{\tilde{\sigma}_i}$ ($= \mathbf{H}_{\tilde{\sigma}_i} \times \mathbf{H}_\sigma$). Note that $\mathbf{H}_\sigma^{\tilde{\sigma}_i} \times \{I\} \times \{I\}$ ($= \mathbf{H}_{\tilde{\sigma}_i} \times \mathbf{H}_\sigma \times \{I\} \times \{I\}$) is equalized to $\mathbf{H}_\sigma^{\tilde{\sigma}_i}$ ($= \mathbf{H}_{\tilde{\sigma}_i} \times \mathbf{H}_\sigma$). As a result, Eq. 52 is divided into two parts as follows:

$$\mathbf{G}_{C\sigma\tilde{\sigma}\hat{I}}^{\tilde{\sigma}_i} = \mathbf{H}_\sigma^{\tilde{\sigma}_i} \times \mathbf{G}_C + \hat{I} \times \mathbf{H}_\sigma^{\tilde{\sigma}_i} \times \mathbf{G}_C \tag{57}$$

$$\begin{aligned} &= \mathbf{H}_{\tilde{\sigma}_i} \times \mathbf{H}_\sigma \times \mathbf{G}_C + \hat{I} \times \mathbf{H}_{\tilde{\sigma}_i} \times \mathbf{H}_\sigma \times \mathbf{G}_C \\ &= \{ \mathbf{G}_C + \tilde{\sigma}_i \mathbf{G}_C + \sigma \mathbf{G}_C + \tilde{\sigma}_i \sigma \mathbf{G}_C \} + \{ \hat{I} \mathbf{G}_C + \hat{I} \tilde{\sigma}_i \mathbf{G}_C + \tilde{\sigma} \mathbf{G}_C + \tilde{\sigma}_i \tilde{\sigma} \mathbf{G}_C \}, \end{aligned} \tag{58}$$

where $\mathbf{H}_\sigma^{\tilde{\sigma}_i} \times \{I\} \times \mathbf{G}_C$ ($= \mathbf{H}_{\tilde{\sigma}_i} \times \mathbf{H}_\sigma \times \{I\} \times \mathbf{G}_C$) is equalized to $\mathbf{H}_\sigma^{\tilde{\sigma}_i} \times \mathbf{G}_C$ ($= \mathbf{H}_{\tilde{\sigma}_i} \times \mathbf{H}_\sigma \times \mathbf{G}_C$).

The first set of four cosets parenthesized by a pair of braces in Eq. 58 is combined by Eq. 48 to give the definition of epimeric *RS*-stereoisomeric group:

Definition 8 (*Epimeric RS-stereoisomeric group*)

$$\mathbf{G}_{C\sigma}^{\tilde{\sigma}_i} = \mathbf{H}_{\sigma}^{\tilde{\sigma}_i} \times \mathbf{G}_C \quad (59)$$

$$\begin{aligned} &= \mathbf{H}_{\tilde{\sigma}_i} \times \mathbf{H}_{\sigma} \times \mathbf{G}_C \\ &= \overset{\times}{\mathbf{G}}_C + \tilde{\sigma}_i \overset{\times}{\mathbf{G}}_C + \sigma \overset{\times}{\mathbf{G}}_C + \tilde{\sigma}_i \sigma \overset{\times}{\mathbf{G}}_C, \end{aligned} \quad (60)$$

where the epimeric stereoisogram group $\mathbf{H}_{\sigma}^{\tilde{\sigma}_i}$ has been defined by Eq. 48.

The epimeric RS-stereoisomeric group $\mathbf{G}_{C\sigma}^{\tilde{\sigma}_i}$ defined by Eq. 59 or Eq. 60 describes the symmetrical feature of the corresponding stereoisogram, which is named as follows:

Definition 9 (*Epimeric stereoisograms and holantimeric stereoisograms*)

A stereoisogram corresponding to the epimeric RS-stereoisomeric group $\mathbf{G}_{C\sigma}^{\tilde{\sigma}_i}$ defined by Eq. 59 or Eq. 60 (for the first set of four cosets appearing in Eq. 58) is called an *epimeric stereoisogram*. A stereoisogram corresponding to the second set of four cosets appearing in Eq. 58 is called a *holantimeric stereoisogram*.

The naming described in Definition 9 stems from the following examination. By combining Eq. 56 with Eq. 58 or by referring to Eq. 60, we obtain the following set of cosets:

$$\begin{aligned} \mathbf{G}_{C\sigma}^{\tilde{\sigma}_i} / \overset{\times}{\mathbf{G}}_C &= \mathbf{H}_{\sigma}^{\tilde{\sigma}_i} \times \mathbf{G}_C / \overset{\times}{\mathbf{G}}_C = \mathbf{H}_{\tilde{\sigma}_i} \times \mathbf{H}_{\sigma} \times \mathbf{G}_C / \overset{\times}{\mathbf{G}}_C \\ &= \left\{ \overset{\times}{\mathbf{G}}_C, \tilde{\sigma}_i \overset{\times}{\mathbf{G}}_C, \sigma \overset{\times}{\mathbf{G}}_C, \tilde{\sigma}_i \sigma \overset{\times}{\mathbf{G}}_C \right\}, \end{aligned} \quad (61)$$

where $\overset{\times}{\mathbf{G}}_C$ is equalized to $\{I\} \times \mathbf{G}_C$ or $\{I\} \times \{I\} \times \mathbf{G}_C$. Because the transitivity of Eq. 61 is shown in the left part of the table collected in Eq. 55, the set (Eq. 61) corresponds to a stereoisogram, which is called an *epimeric stereoisogram* (Definition 9). See also Eq. 48 (an epimeric stereoisogram group $\mathbf{H}_{\sigma}^{\tilde{\sigma}_i}$).

Moreover, the second coset of Eq. 57 is alternatively interpreted when it is converted into

$$\hat{I} \times \mathbf{H}_{\tilde{\sigma}_i} \times \mathbf{H}_{\sigma} \times \mathbf{G}_C = \mathbf{H}_{\tilde{\sigma}_i} \times \mathbf{H}_{\sigma} \times (\hat{I} \times \mathbf{G}_C). \quad (62)$$

Because the parenthesized direct product $\hat{I} \times \mathbf{G}_C$ corresponds to the holantimer of a molecule represented by \mathbf{G}_C , the holantimer belonging to $\hat{I} \times \mathbf{G}_C$ gives a stereoisogram (called a *holantimeric stereoisogram*), which corresponds to the stereoisogram for Eq. 61.

The two kinds of stereoisograms (epimeric stereoisograms and holantimeric stereoisograms) can be commonly discussed by taking account of Eq. 47. Thus, we construct a set of cosets as follows:

$$\begin{aligned}
 \mathbf{G}_{C\sigma\tilde{\sigma}\hat{I}}^{\tilde{\sigma}_i} / \overset{\times}{\mathbf{G}}_{C\hat{I}} &= \mathbf{G}_{C\sigma\tilde{\sigma}\hat{I}}^{\tilde{\sigma}_i} / \mathbf{H}_{\hat{I}} \times \mathbf{G}_C \\
 &= \mathbf{H}_{\tilde{\sigma}_i} \times \mathbf{H}_{\sigma} \times \mathbf{H}_{\hat{I}} \times \mathbf{G}_C / \mathbf{H}_{\hat{I}} \times \mathbf{G}_C \\
 &= \{I \times \mathbf{H}_{\hat{I}} \times \mathbf{G}_C, \tilde{\sigma}_i \times \mathbf{H}_{\hat{I}} \times \mathbf{G}_C, \sigma \times \mathbf{H}_{\hat{I}} \times \mathbf{G}_C, \tilde{\sigma}_i \times \sigma \mathbf{H}_{\hat{I}} \times \mathbf{G}_C\} \\
 &= \left\{ \overset{\times}{\mathbf{G}}_{C\hat{I}}, \tilde{\sigma}_i \overset{\times}{\mathbf{G}}_{C\hat{I}}, \sigma \overset{\times}{\mathbf{G}}_{C\hat{I}}, \tilde{\sigma}_i \sigma \overset{\times}{\mathbf{G}}_{C\hat{I}} \right\}, \tag{63}
 \end{aligned}$$

where $\overset{\times}{\mathbf{G}}_{C\hat{I}}$ is equalized to a formal direct product $\{I\} \times \{I\} \times \mathbf{H}_{\hat{I}} \times \mathbf{G}_C$, because $\mathbf{G}_{C\hat{I}}$ (Eq. 13) is regarded as being equal to $\mathbf{H}_{\hat{I}} \times \mathbf{G}_C$ or equivalently to $\overset{\times}{\mathbf{G}}_C + \hat{I}\overset{\times}{\mathbf{G}}_C$ selected from Eq. 58. Because of the nature of direct products, the sets of cosets represented by Eqs. 61 and 63 are factor groups of order 4, which are isomorphic to each other.

The factor groups $\mathbf{G}_{C\sigma}^{\tilde{\sigma}_i} / \overset{\times}{\mathbf{G}}_C$ (Eq. 61) and $\mathbf{G}_{C\sigma\tilde{\sigma}\hat{I}}^{\tilde{\sigma}_i} / \overset{\times}{\mathbf{G}}_{C\hat{I}}$ (Eq. 63) have a common transversal, which has appeared as $\mathbf{H}_{\sigma}^{\tilde{\sigma}_i}$ in Eq. 48. Because $\mathbf{H}_{\sigma}^{\tilde{\sigma}_i}$ specifies a pair of stereoisograms (an epimeric and an holantimeric stereoisogram), it is one of stereoisogram groups. Because the stereoisogram group $\mathbf{H}_{\sigma}^{\tilde{\sigma}_i}$ (Eq. 48) is concerned with the local symmetry of the stereoskeleton at issue, it is more specifically called an *epimeric stereoisogram group* if necessary (Definition 7).

For example, let us the symbol $\tilde{\sigma}_{15}$ represent an epimerization at the C_1 atom of 1. This epimerization converts the stereoisogram shown in Fig. 4a into another stereoisogram shown in Fig. 4b, which corresponds to the coset $\tilde{\sigma}_{15}\overset{\times}{\mathbf{D}}_{4h\tilde{\sigma}_h\hat{I}}$ by applying Eq. 42 to this case:

$$\mathbf{D}_{4h\tilde{\sigma}\hat{I}}^{\tilde{\sigma}_{15}} = \mathbf{H}_{\tilde{\sigma}_{15}} \times \mathbf{D}_{4h\tilde{\sigma}_h\hat{I}} = \underbrace{\overset{\times}{\mathbf{D}}_{4h\tilde{\sigma}\hat{I}}}_{1, \bar{1}, 8, \bar{8}} + \underbrace{\tilde{\sigma}_{15}\overset{\times}{\mathbf{D}}_{4h\tilde{\sigma}\hat{I}}}_{2, \bar{2}, 9, \bar{9}} \tag{64}$$

where the group $\mathbf{H}_{\tilde{\sigma}_{15}}$ ($= \{I, \tilde{\sigma}_{15}\}$) is used in agreement with Eq. 39. By applying Eq. 52 to this case, we obtain the following coset decomposition:

$$\begin{aligned}
 \mathbf{D}_{4h\tilde{\sigma}\hat{I}}^{\tilde{\sigma}_{15}} &= \left\{ \underbrace{\overset{\times}{\mathbf{D}}_4}_1 + \underbrace{\sigma_h \overset{\times}{\mathbf{D}}_4}_{\bar{1}} + \underbrace{\tilde{\sigma}_h \overset{\times}{\mathbf{D}}_4}_8 + \underbrace{\hat{I}\overset{\times}{\mathbf{D}}_4}_{\bar{8}} \right\} \\
 &+ \left\{ \underbrace{\tilde{\sigma}_{15}\overset{\times}{\mathbf{D}}_4}_2 + \underbrace{\tilde{\sigma}_{15}\sigma_h \overset{\times}{\mathbf{D}}_4}_{\bar{2}} + \underbrace{\tilde{\sigma}_{15}\tilde{\sigma}_h \overset{\times}{\mathbf{D}}_4}_9 + \underbrace{\tilde{\sigma}_{15}\hat{I}\overset{\times}{\mathbf{D}}_4}_{\bar{9}} \right\} \tag{65}
 \end{aligned}$$

$$\begin{aligned}
 &= \left\{ \underbrace{\overset{\times}{\mathbf{D}}_4}_1 + \underbrace{\tilde{\sigma}_{15}\overset{\times}{\mathbf{D}}_4}_2 + \underbrace{\sigma_h \overset{\times}{\mathbf{D}}_4}_{\bar{1}} + \underbrace{\tilde{\sigma}_{15}\sigma_h \overset{\times}{\mathbf{D}}_4}_{\bar{2}} \right\} \\
 &+ \left\{ \underbrace{\hat{I}\overset{\times}{\mathbf{D}}_4}_{\bar{8}} + \underbrace{\tilde{\sigma}_{15}\hat{I}\overset{\times}{\mathbf{D}}_4}_{\bar{9}} + \underbrace{\tilde{\sigma}_h \overset{\times}{\mathbf{D}}_4}_8 + \underbrace{\tilde{\sigma}_{15}\tilde{\sigma}_h \overset{\times}{\mathbf{D}}_4}_9 \right\} \tag{66}
 \end{aligned}$$

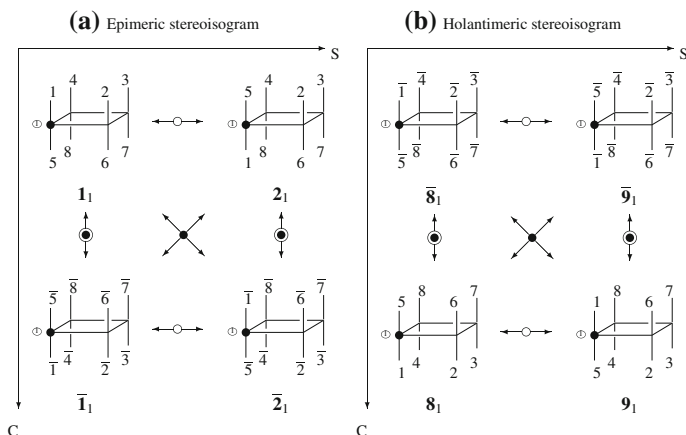


Fig. 5 Epimeric and holantimeric stereoisograms

The two parts appearing in Eq. 65 are generated by means of Eq. 64, while the two parts appearing in Eq. 66 are generated by applying Eq. 58 to this case.

The cosets appearing in the first part of Eq. 65, i.e., $\left\{ \overset{\times}{\mathbf{D}}_4, \sigma_h \overset{\times}{\mathbf{D}}_4, \tilde{\sigma}_h \overset{\times}{\mathbf{D}}_4, \widehat{\mathbf{T}} \overset{\times}{\mathbf{D}}_4 \right\}$ correspond respectively to **1**, **1**, **8**, and **8**, which are contained in the stereoisogram shown in Fig. 4a. On the other hand, the cosets appearing in the second part of Eq. 65, i.e., $\left\{ \tilde{\sigma}_{15} \overset{\times}{\mathbf{D}}_4, \tilde{\sigma}_{15} \sigma_h \overset{\times}{\mathbf{D}}_4, \tilde{\sigma}_{15} \tilde{\sigma}_h \overset{\times}{\mathbf{D}}_4, \tilde{\sigma}_{15} \widehat{\mathbf{T}} \overset{\times}{\mathbf{D}}_4 \right\}$, correspond respectively to **2**, **2**, **9**, and **9**, which are contained in the stereoisogram shown in Fig. 4b.

The set $\mathbf{D}_{4h\tilde{\sigma}\hat{\Gamma}}^{\tilde{\sigma}_{15}}$ (Eq. 64) has been noted in a previous report (Eq. 9 of [19]), where we put $\mathbf{D}_{4h\tilde{\sigma}\hat{\Gamma}}^{\tilde{\sigma}_{15}} = \mathbf{D}_{4h\tilde{\sigma}\hat{\Gamma}} + \tilde{\sigma}_{15} \mathbf{D}_{4h\tilde{\sigma}\hat{\Gamma}}$ in place of Eq. 64. Strictly speaking, however, the set due to the previous formulation does not necessarily construct a group because the equation $(1\ 5) \mathbf{D}_{4h\tilde{\sigma}\hat{\Gamma}} (1\ 5)$ (where $\tilde{\sigma}_{15} = (1\ 5)$) is not equal to $\mathbf{D}_{4h\tilde{\sigma}\hat{\Gamma}}$. The present formulation by using the direct product (Eq. 64) is suitable for investigating stereoisomerism by taking account of Eq. 7.

The first set of cosets of Eq. 66, i.e., $\left\{ \overset{\times}{\mathbf{D}}_4, \tilde{\sigma}_{15} \overset{\times}{\mathbf{D}}_4, \sigma_h \overset{\times}{\mathbf{D}}_4, \tilde{\sigma}_{15} \sigma_h \overset{\times}{\mathbf{D}}_4 \right\}$, corresponds to **1**, **2**, **1**, and **2**, which are collected to generate an epimeric stereoisogram shown in Fig. 5a. The conversion along with the horizontal axis (S-axis) corresponds to an epimerization at the C_1 atom ($\tilde{\sigma}_{15}$) so that the original stereoskeleton **1** is *RS*-diastereomeric to **2** at the C_1 atom. In other words, the epimeric stereoisogram (Fig. 5a) indicates the local symmetry at the C_1 atom. To clarify this feature, a solid circle is added at the C_1 atom and each skeleton number is attached by the subscript 1 for representing the C_1 atom (e.g., **1**₁).

On the other hand, the second set of cosets, i.e., $\left\{ \widehat{\mathbf{T}} \overset{\times}{\mathbf{D}}_4, \tilde{\sigma}_{15} \widehat{\mathbf{T}} \overset{\times}{\mathbf{D}}_4, \tilde{\sigma}_h \overset{\times}{\mathbf{D}}_4, \tilde{\sigma}_{15} \tilde{\sigma}_h \overset{\times}{\mathbf{D}}_4 \right\}$ which appears in Eq. 66, corresponds to **8**, **9**, **8**, and **9**. These stereoskeletons are collected to generate a holantimeric stereoisogram shown in Fig. 5b. Obviously, Fig. 5b

is available from Fig. 5a by changing each locant number into the one with an overbar (i.e., by alternating ligand configurations).

By applying Eq. 63 to this case, we obtain:

$$\mathbf{D}_{4\sigma\tilde{\sigma}\hat{I}}^{\tilde{\sigma}_{15}} / \mathbf{D}_{4\hat{I}}^{\times} = \left\{ \underbrace{\mathbf{D}_{4\hat{I}}^{\times}}_{\mathbf{1},\bar{\mathbf{8}}}, \underbrace{\tilde{\sigma}_{15}\mathbf{D}_{4\hat{I}}^{\times}}_{\mathbf{2},\bar{\mathbf{9}}}, \underbrace{\sigma_h\mathbf{D}_{4\hat{I}}^{\times}}_{\mathbf{1},\bar{\mathbf{8}}}, \underbrace{\tilde{\sigma}_{15}\sigma_h\mathbf{D}_{4\hat{I}}^{\times}}_{\mathbf{2},\bar{\mathbf{9}}} \right\}, \quad (67)$$

where we put $\mathbf{D}_{4\hat{I}} = \mathbf{H}_{\hat{I}} \times \mathbf{D}_4$ and $\mathbf{D}_{4\hat{I}}^{\times}$ is equalized to $\{I\} \times \{I\} \times \mathbf{D}_{4\hat{I}} (= \{I\} \times \{I\} \times \mathbf{H}_{\hat{I}} \times \mathbf{D}_4)$. Each of the cosets appearing in Eq. 67 correspond to each pair of a molecule and its holantimer, i.e., $\{\mathbf{1}, \bar{\mathbf{8}}\}, \{\mathbf{2}, \bar{\mathbf{9}}\}, \{\mathbf{1}, \bar{\mathbf{8}}\}$, and $\{\mathbf{2}, \bar{\mathbf{9}}\}$.

On a similar line, an epimerization $\tilde{\sigma}_{26}$ at the C₂ atom of **1** generates a stereoisogram shown in Fig. 4c. Similar results to Eqs. 64, 65, and 66 are obtained by applying Eq. 42 to this case:

$$\mathbf{D}_{4h\tilde{\sigma}\hat{I}}^{\tilde{\sigma}_{26}} = \mathbf{H}_{\tilde{\sigma}_{26}} \times \mathbf{D}_{4h\tilde{\sigma}\hat{I}} = \underbrace{\mathbf{D}_{4h\tilde{\sigma}\hat{I}}^{\times}}_{\mathbf{1},\bar{\mathbf{1}},\bar{\mathbf{8}},\bar{\mathbf{8}}} + \underbrace{\tilde{\sigma}_{26}\mathbf{D}_{4h\tilde{\sigma}\hat{I}}^{\times}}_{\mathbf{10},\bar{\mathbf{10}},\mathbf{11},\bar{\mathbf{11}}} \quad (68)$$

$$= \left\{ \underbrace{\mathbf{D}_4^{\times}}_{\mathbf{1}} + \underbrace{\sigma_h\mathbf{D}_4^{\times}}_{\bar{\mathbf{1}}} + \underbrace{\tilde{\sigma}_h\mathbf{D}_4^{\times}}_{\mathbf{8}} + \underbrace{\hat{I}\mathbf{D}_4^{\times}}_{\bar{\mathbf{8}}} \right\} + \left\{ \underbrace{\tilde{\sigma}_{26}\mathbf{D}_4^{\times}}_{\mathbf{10}} + \underbrace{\tilde{\sigma}_{26}\sigma_h\mathbf{D}_4^{\times}}_{\bar{\mathbf{10}}} + \underbrace{\tilde{\sigma}_{26}\tilde{\sigma}_h\mathbf{D}_4^{\times}}_{\mathbf{11}} + \underbrace{\tilde{\sigma}_{26}\hat{I}\mathbf{D}_4^{\times}}_{\bar{\mathbf{11}}} \right\} \quad (69)$$

$$= \left\{ \underbrace{\mathbf{D}_4^{\times}}_{\mathbf{1}} + \underbrace{\tilde{\sigma}_{26}\mathbf{D}_4^{\times}}_{\mathbf{10}} + \underbrace{\sigma_h\mathbf{D}_4^{\times}}_{\bar{\mathbf{1}}} + \underbrace{\tilde{\sigma}_{26}\sigma_h\mathbf{D}_4^{\times}}_{\bar{\mathbf{10}}} \right\} + \left\{ \underbrace{\hat{I}\mathbf{D}_4^{\times}}_{\bar{\mathbf{8}}} + \underbrace{\tilde{\sigma}_{26}\hat{I}\mathbf{D}_4^{\times}}_{\bar{\mathbf{11}}} + \underbrace{\tilde{\sigma}_h\mathbf{D}_4^{\times}}_{\mathbf{8}} + \underbrace{\tilde{\sigma}_{26}\tilde{\sigma}_h\mathbf{D}_4^{\times}}_{\mathbf{11}} \right\} \quad (70)$$

where the group $\mathbf{H}_{\tilde{\sigma}_{26}} (= \{I, \tilde{\sigma}_{26}\})$ is used in agreement with Eq. 39. The second set of cosets appearing in Eq. 69 corresponds to Fig. 4c. The two sets of cosets appearing in Eq. 70 generates epimeric and holantimeric stereoisograms in a parallel way to the derivation of Fig. 5a and b.

Similarly, an epimerization $\tilde{\sigma}_{37}$ at the C₃ atom of **1** generates a stereoisogram shown in Fig. 4d. On a similar line to Eqs. 64, 65, and 66, the application of Eq. 42 to this case gives:

$$\mathbf{D}_{4h\tilde{\sigma}\hat{I}}^{\tilde{\sigma}_{37}} = \mathbf{H}_{\tilde{\sigma}_{37}} \times \mathbf{D}_{4h\tilde{\sigma}\hat{I}} = \underbrace{\mathbf{D}_{4h\tilde{\sigma}\hat{I}}^{\times}}_{\mathbf{1},\bar{\mathbf{1}},\bar{\mathbf{8}},\bar{\mathbf{8}}} + \underbrace{\tilde{\sigma}_{37}\mathbf{D}_{4h\tilde{\sigma}\hat{I}}^{\times}}_{\mathbf{12},\bar{\mathbf{12}},\mathbf{13},\bar{\mathbf{13}}} \quad (71)$$

$$\begin{aligned}
&= \left\{ \underbrace{\overset{\times}{\mathbf{D}}_4}_{\mathbf{1}} + \underbrace{\sigma_h \overset{\times}{\mathbf{D}}_4}_{\bar{\mathbf{1}}} + \underbrace{\tilde{\sigma}_h \overset{\times}{\mathbf{D}}_4}_{\mathbf{8}} + \underbrace{\widehat{I} \overset{\times}{\mathbf{D}}_4}_{\bar{\mathbf{8}}} \right\} \\
&+ \left\{ \underbrace{\tilde{\sigma}_{37} \overset{\times}{\mathbf{D}}_4}_{\mathbf{12}} + \underbrace{\tilde{\sigma}_{37} \sigma_h \overset{\times}{\mathbf{D}}_4}_{\bar{\mathbf{12}}} + \underbrace{\tilde{\sigma}_{37} \tilde{\sigma}_h \overset{\times}{\mathbf{D}}_4}_{\mathbf{13}} + \underbrace{\tilde{\sigma}_{37} \widehat{I} \overset{\times}{\mathbf{D}}_4}_{\bar{\mathbf{13}}} \right\} \quad (72)
\end{aligned}$$

$$\begin{aligned}
&= \left\{ \underbrace{\overset{\times}{\mathbf{D}}_4}_{\mathbf{1}} + \underbrace{\tilde{\sigma}_{37} \overset{\times}{\mathbf{D}}_4}_{\mathbf{12}} + \underbrace{\sigma_h \overset{\times}{\mathbf{D}}_4}_{\bar{\mathbf{1}}} + \underbrace{\tilde{\sigma}_{37} \sigma_h \overset{\times}{\mathbf{D}}_4}_{\bar{\mathbf{12}}} \right\} \\
&+ \left\{ \underbrace{\widehat{I} \overset{\times}{\mathbf{D}}_4}_{\bar{\mathbf{8}}} + \underbrace{\tilde{\sigma}_{37} \widehat{I} \overset{\times}{\mathbf{D}}_4}_{\bar{\mathbf{13}}} + \underbrace{\tilde{\sigma}_h \overset{\times}{\mathbf{D}}_4}_{\mathbf{8}} + \underbrace{\tilde{\sigma}_{37} \tilde{\sigma}_h \overset{\times}{\mathbf{D}}_4}_{\mathbf{13}} \right\} \quad (73)
\end{aligned}$$

where the group $\mathbf{H}_{\tilde{\sigma}_{37}} (= \{I, \tilde{\sigma}_{37}\})$ is used in agreement with Eq. 39. The second set of cosets appearing in Eq. 72 corresponds to Fig. 4d. The two sets of cosets appearing in Eq. 73 generates epimeric and holantimeric stereoisograms in a parallel way to the derivation of Fig. 5a and b.

When a further epimerization at the C_4 atom of $\mathbf{1}$ is represented by the symbol $\tilde{\sigma}_{48}$, the corresponding stereoisogram is available as shown in Fig. 4d. On a similar line to Eqs. 64, 65, and 66, the application of Eq. 42 to this case gives:

$$\mathbf{D}_{4h\tilde{\sigma}I}^{\tilde{\sigma}_{48}} \hat{=} \mathbf{H}_{\tilde{\sigma}_{48}} \times \mathbf{D}_{4h\tilde{\sigma}I} \hat{=} \underbrace{\overset{\times}{\mathbf{D}}_{4h\tilde{\sigma}I}}_{\mathbf{1}, \bar{\mathbf{1}}, \mathbf{8}, \bar{\mathbf{8}}} + \underbrace{\tilde{\sigma}_{48} \overset{\times}{\mathbf{D}}_{4h\tilde{\sigma}I}}_{\mathbf{14}, \bar{\mathbf{14}}, \mathbf{15}, \bar{\mathbf{15}}} \quad (74)$$

$$\begin{aligned}
&= \left\{ \underbrace{\overset{\times}{\mathbf{D}}_4}_{\mathbf{1}} + \underbrace{\sigma_h \overset{\times}{\mathbf{D}}_4}_{\bar{\mathbf{1}}} + \underbrace{\tilde{\sigma}_h \overset{\times}{\mathbf{D}}_4}_{\mathbf{8}} + \underbrace{\widehat{I} \overset{\times}{\mathbf{D}}_4}_{\bar{\mathbf{8}}} \right\} \\
&+ \left\{ \underbrace{\tilde{\sigma}_{48} \overset{\times}{\mathbf{D}}_4}_{\mathbf{14}} + \underbrace{\tilde{\sigma}_{48} \sigma_h \overset{\times}{\mathbf{D}}_4}_{\bar{\mathbf{14}}} + \underbrace{\tilde{\sigma}_{48} \tilde{\sigma}_h \overset{\times}{\mathbf{D}}_4}_{\mathbf{15}} + \underbrace{\tilde{\sigma}_{48} \widehat{I} \overset{\times}{\mathbf{D}}_4}_{\bar{\mathbf{15}}} \right\} \quad (75)
\end{aligned}$$

$$\begin{aligned}
&= \left\{ \underbrace{\overset{\times}{\mathbf{D}}_4}_{\mathbf{1}} + \underbrace{\tilde{\sigma}_{48} \overset{\times}{\mathbf{D}}_4}_{\mathbf{14}} + \underbrace{\sigma_h \overset{\times}{\mathbf{D}}_4}_{\bar{\mathbf{1}}} + \underbrace{\tilde{\sigma}_{48} \sigma_h \overset{\times}{\mathbf{D}}_4}_{\bar{\mathbf{14}}} \right\} \\
&+ \left\{ \underbrace{\widehat{I} \overset{\times}{\mathbf{D}}_4}_{\bar{\mathbf{8}}} + \underbrace{\tilde{\sigma}_{48} \widehat{I} \overset{\times}{\mathbf{D}}_4}_{\bar{\mathbf{15}}} + \underbrace{\tilde{\sigma}_h \overset{\times}{\mathbf{D}}_4}_{\mathbf{8}} + \underbrace{\tilde{\sigma}_{48} \tilde{\sigma}_h \overset{\times}{\mathbf{D}}_4}_{\mathbf{15}} \right\} \quad (76)
\end{aligned}$$

where the group $\mathbf{H}_{\tilde{\sigma}_{48}} (= \{I, \tilde{\sigma}_{48}\})$ is used in agreement with Eq. 39. The second set of cosets appearing in Eq. 75 corresponds to Fig. 4e. The two sets of cosets appearing

in Eq. 76 generate epimeric and holantimeric stereoisograms in a parallel way to the derivation of Fig. 5a and b.

3.4 Stereoisomeric groups for stereoskeletons

3.4.1 Global symmetries of stereoskeletons

Multiple epimerization and formulation of stereoisomeric groups By starting from the epimerization groups $\mathbf{H}_{\tilde{\sigma}_i}$ (Eq. 38), the multiple epimerization group for a set of n *RS*-stereocenters is defined as the direct product of such epimerization groups:

Definition 10 (*Multiple epimerization groups*)

$$\tilde{\mathbf{H}} = \prod_{i=1}^n \mathbf{H}_{\tilde{\sigma}_i} = \mathbf{H}_{\tilde{\sigma}_1} \times \mathbf{H}_{\tilde{\sigma}_2} \times \cdots \times \mathbf{H}_{\tilde{\sigma}_n}, \quad (77)$$

where we employ Eq. 16. Each element of the multiple epimerization group (Eq. 77) is called a *multiple epimerization*.

Because each element of Eq. 77 can be represented by an appropriate product of epimerizations selected from $\tilde{\sigma}_i$ ($i = 1, 2, \dots, n$) (cf. Eq. 16), the coset decomposition of Eq. 77 by $\{I\}$ is formally represented by the following equation:

$$\tilde{\mathbf{H}} = \prod_{i=1}^n (I + \tilde{\sigma}_i). \quad (78)$$

Because all of the epimerizations ($\tilde{\sigma}_i, i = 1, 2, \dots, n$) are commutable and satisfy $\tilde{\sigma}_i^2 = I$, the 2^n terms generated by the expansion of the right-hand side of Eq. 78 are regarded as the elements (multiple epimerizations) contained in the group $\tilde{\mathbf{H}}$ of order 2^n . Then, the product represented by Eq. 78 is a coset decomposition of the group $\tilde{\mathbf{H}}$ by the trivial coset $\{I\}$ ($= \{I\} \times \cdots \times \{I\}$). By combining Eq. 3 with Eq. 78, we construct a direct product, which is important to discuss stereoisomerism comprehensively:

Definition 11 (*Stereoisomeric groups*) The direct product of Eqs. 3 and 78, i.e.,

$$\begin{aligned} \widehat{\mathbf{G}}_{C\sigma} &= \tilde{\mathbf{H}} \times \mathbf{G}_{C\sigma} & (79) \\ &= \tilde{\mathbf{H}} \times \mathbf{H}_{\sigma} \times \mathbf{G}_C = \left[\prod_{i=1}^n (I + \tilde{\sigma}_i) \right] \times \mathbf{G}_{C\sigma} = \left[\prod_{i=1}^n (I + \tilde{\sigma}_i) \right] \times \mathbf{H}_{\sigma} \times \mathbf{G}_C, & (80) \end{aligned}$$

is called a *stereoisomeric group*.

The definition of a stereoisomeric group (Eq. 79 or Eq. 80) does not explicitly contains an *RS*-stereoisomeric group defined by Eq. 14. As proven in the following paragraphs, however, such a stereoisomeric group contains an *RS*-stereoisomeric group as a subgroup. This fact provides us with a key for developing the theory of stereoisomerism in harmony of molecular symmetry.

RS-stereoisomeric groups versus stereoisomeric groups The expansion of Eq. 78 gives 2^n terms (multiple epimerizations), each of which is represented as follows:

$$\tilde{\sigma}_{[\omega]} = \prod_{i=1}^n \tilde{\sigma}_i^{\omega_i}, \quad (81)$$

where the symbol ω_i represents a bit and satisfies $\omega_i = 0$ or 1 ($i = 1, 2, \dots, n$) and where the $[\omega]$ represents an array of bits:

$$[\omega] = [\omega_1, \omega_2, \dots, \omega_n], \quad (82)$$

which is selected from the 2^n combinations of n bits. Let the symbol ω be the sum of the bits contained in the bit array $[\omega]$:

$$\omega = \omega_1 + \omega_2 + \dots + \omega_n, \quad (83)$$

which is an integer from 0 to n . The bit inversion of the bit array (Eq. 82) generates the complementary bit array $[\tilde{\omega}]$ as follows:

$$[\tilde{\omega}] = [\tilde{\omega}_1, \tilde{\omega}_2, \dots, \tilde{\omega}_n], \quad (84)$$

where we put $\tilde{\omega}_i = 0$ if $\omega_i = 1$, while $\tilde{\omega}_i = 1$ if $\omega_i = 0$. Thereby, we obtain the complementary multiple epimerization of $\tilde{\sigma}_{[\omega]}$ as follows:

$$\tilde{\sigma}_{[\tilde{\omega}]} = \prod_{i=1}^n \tilde{\sigma}_i^{\tilde{\omega}_i}, \quad (85)$$

where

$$\tilde{\omega} = \tilde{\omega}_1 + \tilde{\omega}_2 + \dots + \tilde{\omega}_n. \quad (86)$$

The definitions of ω (Eq. 83) and $\tilde{\omega}$ (Eq. 86) indicate the following obvious relationships:

$$\omega_i + \tilde{\omega}_i = 1 \text{ (for } i = 1, 2, \dots, n) \text{ and } \omega + \tilde{\omega} = n. \quad (87)$$

Because of Eq. 16 and $\tilde{\sigma}_i^2 = I$, we obtain:

$$\tilde{\sigma}_{[\tilde{\omega}]} = \tilde{\sigma}_{[\omega]} \tilde{\sigma}. \quad (88)$$

The multiple epimerization $\tilde{\sigma}_{[\omega]}$ (Eq. 81) and its complementary multiple epimerization $\tilde{\sigma}_{[\tilde{\omega}]}$ (Eq. 85) appear pairwise in Eq. 78 (or Eq. 80) so that $\tilde{\sigma}_{[\omega]}$ for $\omega \leq \frac{n}{2}$ corresponds to $\tilde{\sigma}_{[\tilde{\omega}]}$ for $\tilde{\omega} \geq \frac{n}{2}$ in a one-to-one fashion ($n \geq 2$). Because of Eq. 88, the set of $\tilde{\sigma}_{[\omega]}$ (Eq. 81) plus $\tilde{\sigma} \tilde{\sigma}_{[\omega]}$ (Eq. 88) for $\omega \leq \frac{n}{2}$ covers all of the terms contained

in Eq. 78 (or Eq. 80). Hence, the following equation is obtained as an alternative expression to Eq. 78:

$$\tilde{\mathbf{H}} = \sum_{\omega \leq n/2} (\tilde{\sigma}_{[\omega]} + \tilde{\sigma}_{[\tilde{\omega}]}) = \sum_{\omega \leq n/2} (\tilde{\sigma}_{[\omega]} + \tilde{\sigma}_{[\omega]}\tilde{\sigma}) = \sum_{\omega \leq n/2} \tilde{\sigma}_{[\omega]}(I + \tilde{\sigma}). \tag{89}$$

The range of summations should be noted. When $n = 1$ ($\omega = 0$), we obtain $\tilde{\sigma}_{[\omega]} = I$ and $\tilde{\sigma}_{[\tilde{\omega}]} = \tilde{\sigma}$, which can be regarded as an extreme case of Eq. 89. When n is odd ($n > 1$), we are able to select $\tilde{\sigma}_{[\omega]}$ for $\omega < \frac{n}{2}$ without ambiguity. On the other hand, when n is even, there is an ambiguity in the selection of $\tilde{\sigma}_{[\omega]}$ for $\omega = \frac{n}{2}$. Although either multiple epimerization of each pair (Eqs. 81 and 88) may be selected without losing generality, it is convenient to select a set of multiple epimerizations $\tilde{\sigma}_{[\omega]}$ (for $\omega = \frac{n}{2}$) which contain a fixed epimerization $\tilde{\sigma}_j$ (i.e., $\omega_j = 1$ for a fixed j in Eq. 81).

Definition 12 (*Pivot epimerizations*) As such a fixed epimerization, any epimerization can be selected from the n epimerizations (n : even) but it is temporarily fixed to continue further discussions. We refer to the fixed epimerization $\tilde{\sigma}_j$ as a *pivot epimerization*.

This selection is shown to be valid by the following examination. By selecting $n/2$ epimerizations among the n epimerizations (n : even) to generate multiple epimerizations of $\omega = n/2$ (and $\tilde{\omega} = n/2$), the number of such multiple epimerizations (Eq. 81 plus Eq. 88) is calculated to be:

$$n_A = \binom{n}{n/2} = \frac{n!}{(n/2)!(n/2)!} \tag{90}$$

By selecting a pivot epimerization $\tilde{\sigma}_j$ (i.e., $\omega_j = 1$ for a fixed j in Eq. 81) to be fixed, the number of the corresponding multiple epimerizations is reduced into the following one:

$$n_B = \binom{n-1}{n/2-1} = \frac{(n-1)!}{(n/2)!(n/2-1)!}. \tag{91}$$

Hence we obtain $n_A/n_B = 2$ so that we are able to select the n_B ($= n_A/2$) multiple epimerizations as $\tilde{\sigma}_{[\omega]}$ for $\omega = \frac{n}{2}$.

Let us select a multiple epimerization $\tilde{\sigma}_{[\omega^{(1)}]}$ which has the following array of bits:

$$[\omega^{(1)}] = [1, \omega_2, \dots, \omega_n], \tag{92}$$

where $\tilde{\sigma}_1$ (corresponding to $\omega_1 = 1$) is tentatively fixed as a pivot epimerization. Then, the corresponding complementary multiple epimerization $\tilde{\sigma}_{[\tilde{\omega}^{(1)}]}$ is determined to have the following array of bits:

$$[\tilde{\omega}^{(1)}] = [0, \tilde{\omega}_2, \dots, \tilde{\omega}_n]. \tag{93}$$

Obviously, such a pair of $\tilde{\sigma}_{[\omega^{(1)}]}$ and $\tilde{\sigma}_{[\tilde{\omega}^{(1)}]}$ appears concurrently when the bits ω_i ($i = 2, \dots, n$) run to cover all of the multiple epimerizations. This means that the

set of multiple epimerizations (Eq. 89) are divided into two sets, where either set is characterized by the presence of the pivot epimerization $\tilde{\sigma}_1$, while the other set is not. Although this fact seems to be trivial, it plays a crucial role in categorization of stereoisomers, e.g., the Fischer-Rosanoff convention for naming D- and L-glyceraldehydes and the relevant series of sugars [5]. Note that any epimerization other than $\tilde{\sigma}_1$ may be selected as a pivot epimerization without losing generality. This fact will be discussed after the introduction of Theorem 1.

The direct product of Eqs. 89 and 20 is calculated as follows:

$$\tilde{\mathbf{H}} \times \mathbf{H}_\sigma = \sum_{\omega \leq n/2} \tilde{\sigma}_{[\omega]}(I + \tilde{\sigma})(I + \sigma) = \sum_{\omega \leq n/2} \tilde{\sigma}_{[\omega]} \times \mathbf{H}_\sigma = \sum_{\omega \leq n/2} \tilde{\sigma}_{[\omega]} \times \mathbf{H}_\sigma \times \mathbf{H}_{\hat{\Gamma}}, \quad (94)$$

where we use Eq. 21. The meaning of Eq. 94 is that permutations ($\tilde{\mathbf{H}}$) and reflections (\mathbf{H}_σ) are combined to give a foundation for discussing stereoisomerism, where both mirror-image transformations of a given stereoskeleton (\mathbf{H}_σ) and alternations of ligand configurations ($\mathbf{H}_{\hat{\Gamma}}$) are taken into consideration.

Then, Eq. 94 is introduced into Eq. 80 to an alternative expression of the stereoisomeric group $\hat{\mathbf{G}}_{C\sigma}$ ($= \tilde{\mathbf{H}} \times \mathbf{G}_{C\sigma}$) as follows:

$$\hat{\mathbf{G}}_{C\sigma} = \tilde{\mathbf{H}} \times \mathbf{G}_{C\sigma} = \tilde{\mathbf{H}} \times \mathbf{H}_\sigma \times \mathbf{G}_C = \sum_{\omega \leq n/2} \tilde{\sigma}_{[\omega]} \times \mathbf{H}_\sigma \times \mathbf{H}_{\hat{\Gamma}} \times \mathbf{G}_C \quad (95)$$

$$= \sum_{\omega \leq n/2} \tilde{\sigma}_{[\omega]} \times \mathbf{G}_{C\sigma\hat{\Gamma}} = \sum_{\omega \leq n/2} \tilde{\sigma}_{[\omega]} \times \hat{\mathbf{G}}_{C\sigma\hat{\Gamma}} \quad (96)$$

where Eqs. 22 and 23 are used. The last equation of Eq. 96 can be regarded as a coset decomposition of the stereoisomeric group $\hat{\mathbf{G}}_{C\sigma}$ by its subgroup $\hat{\mathbf{G}}_{C\sigma\hat{\Gamma}}$ (Eq. 43), which is isomorphic to the *RS*-stereoisomeric group $\mathbf{G}_{C\sigma\hat{\Gamma}}$. Because of $|\hat{\mathbf{G}}_{C\sigma}| = 2^n |\mathbf{G}_{C\sigma}|$ and $|\hat{\mathbf{G}}_{C\sigma\hat{\Gamma}}| = 2 |\mathbf{G}_{C\sigma}|$, we obtain:

$$\left| \hat{\mathbf{G}}_{C\sigma} \right| / \left| \hat{\mathbf{G}}_{C\sigma\hat{\Gamma}} \right| = 2^{n-1}, \quad (97)$$

which represents the number of cosets contained in Eq. 96.

In the case of a cyclobutane stereoskeleton, Eq. 78 is calculated by means of Eq. 34 so as to generate the corresponding multiple epimerization group as follows:

$$\begin{aligned} \tilde{\mathbf{H}} &= (I + \tilde{\sigma}_{15})(I + \tilde{\sigma}_{26})(I + \tilde{\sigma}_{37})(I + \tilde{\sigma}_{48}) \quad (98) \\ &= (I + \tilde{\sigma}_h) + \tilde{\sigma}_{15}(I + \tilde{\sigma}_h) + \tilde{\sigma}_{26}(I + \tilde{\sigma}_h) + \tilde{\sigma}_{37}(I + \tilde{\sigma}_h) + \tilde{\sigma}_{48}(I + \tilde{\sigma}_h) \\ &\quad + \tilde{\sigma}_{15}\tilde{\sigma}_{26}(I + \tilde{\sigma}_h) + \tilde{\sigma}_{15}\tilde{\sigma}_{37}(I + \tilde{\sigma}_h) + \tilde{\sigma}_{15}\tilde{\sigma}_{48}(I + \tilde{\sigma}_h), \quad (99) \end{aligned}$$

where Eq. 88 for this case is obtained to be $\tilde{\sigma}_{[\omega]} = \tilde{\sigma}_{[\omega]}\tilde{\sigma}_h$ so that Eq. 99 corresponds to Eq. 89. Note that the three multiple epimerizations ($\tilde{\sigma}_{[\omega]}$) in the last row of Eq. 99, i.e.,

$\tilde{\sigma}_{15}\tilde{\sigma}_{26}$, $\tilde{\sigma}_{15}\tilde{\sigma}_{37}$, and $\tilde{\sigma}_{15}\tilde{\sigma}_{48}$, contain a common epimerization $\tilde{\sigma}_{15}$ as a pivot epimerization. Their complementary multiple enumerations ($\tilde{\sigma}_{[\omega]}$) which are not involved in Eq. 99 (i.e., $\tilde{\sigma}_{37}\tilde{\sigma}_{48}$, $\tilde{\sigma}_{26}\tilde{\sigma}_{48}$, and $\tilde{\sigma}_{26}\tilde{\sigma}_{37}$) do not contain the pivot epimerization $\tilde{\sigma}_{15}$.

The direct product of $\tilde{\mathbf{H}}$ (Eq. 99) and \mathbf{H}_{σ_h} according to Eq. 94 is calculated to give:

$$\begin{aligned} \tilde{\mathbf{H}} \times \mathbf{H}_{\sigma_h} &= \mathbf{H}_s + \tilde{\sigma}_{15} \times \mathbf{H}_s + \tilde{\sigma}_{26} \times \mathbf{H}_s + \tilde{\sigma}_{37} \times \mathbf{H}_s + \tilde{\sigma}_{48} \times \mathbf{H}_s \\ &\quad + \tilde{\sigma}_{15}\tilde{\sigma}_{26} \times \mathbf{H}_s + \tilde{\sigma}_{15}\tilde{\sigma}_{37} \times \mathbf{H}_s + \tilde{\sigma}_{15}\tilde{\sigma}_{48} \times \mathbf{H}_s, \end{aligned} \tag{100}$$

where we use $\mathbf{H}_s = (I + \tilde{\sigma})(I + \sigma_h)$ (cf. Eq. 37). Then, Eq. 96 is applied to this case so as to generate the corresponding stereoisomeric group:

$$\begin{aligned} \widehat{\mathbf{D}}_{4h} &= \tilde{\mathbf{H}} \times \mathbf{D}_{4h} = \tilde{\mathbf{H}} \times \mathbf{H}_{\sigma_h} \times \mathbf{D}_4 \\ &= \mathbf{D}_{4h\tilde{\sigma}I} + \tilde{\sigma}_{15} \times \mathbf{D}_{4h\tilde{\sigma}I} + \tilde{\sigma}_{26} \times \mathbf{D}_{4h\tilde{\sigma}I} + \tilde{\sigma}_{37} \times \mathbf{D}_{4h\tilde{\sigma}I} + \tilde{\sigma}_{48} \times \mathbf{D}_{4h\tilde{\sigma}I} \\ &\quad + \tilde{\sigma}_{15}\tilde{\sigma}_{26} \times \mathbf{D}_{4h\tilde{\sigma}I} + \tilde{\sigma}_{15}\tilde{\sigma}_{37} \times \mathbf{D}_{4h\tilde{\sigma}I} + \tilde{\sigma}_{15}\tilde{\sigma}_{48} \times \mathbf{D}_{4h\tilde{\sigma}I}, \\ &= \underbrace{\mathbf{D}_{4h\tilde{\sigma}I}^\times}_{1, \bar{1}, 8, \bar{8}} + \underbrace{\tilde{\sigma}_{15}\mathbf{D}_{4h\tilde{\sigma}I}^\times}_{2, \bar{2}, 9, \bar{9}} + \underbrace{\tilde{\sigma}_{26}\mathbf{D}_{4h\tilde{\sigma}I}^\times}_{10, \bar{10}, 11, \bar{11}} + \underbrace{\tilde{\sigma}_{37}\mathbf{D}_{4h\tilde{\sigma}I}^\times}_{12, \bar{12}, 13, \bar{13}} + \underbrace{\tilde{\sigma}_{48}\mathbf{D}_{4h\tilde{\sigma}I}^\times}_{14, \bar{14}, 15, \bar{15}} \\ &\quad + \underbrace{\tilde{\sigma}_{15}\tilde{\sigma}_{26}\mathbf{D}_{4h\tilde{\sigma}I}^\times}_{16, \bar{16}, 17, \bar{17}} + \underbrace{\tilde{\sigma}_{15}\tilde{\sigma}_{37}\mathbf{D}_{4h\tilde{\sigma}I}^\times}_{18, \bar{18}, 19, \bar{19}} + \underbrace{\tilde{\sigma}_{15}\tilde{\sigma}_{48}\mathbf{D}_{4h\tilde{\sigma}I}^\times}_{20, \bar{20}, 21, \bar{21}}, \end{aligned} \tag{101}$$

Equation 101 is regarded as a coset decomposition of the stereoisomeric group $\widehat{\mathbf{D}}_{4h}$ by its subgroup $\mathbf{D}_{4h\tilde{\sigma}I}^\times$, which is isomorphic to the *RS*-stereoisomeric group $\mathbf{D}_{4h\tilde{\sigma}I}$. Each coset appearing in Eq. 101 corresponds to a quadruplet of stereoskeletons, whose skeleton numbers are shown below a brace. The stereoskeletons of the quadruplet are contained in each of the stereoisograms listed in Fig. 4a–h.

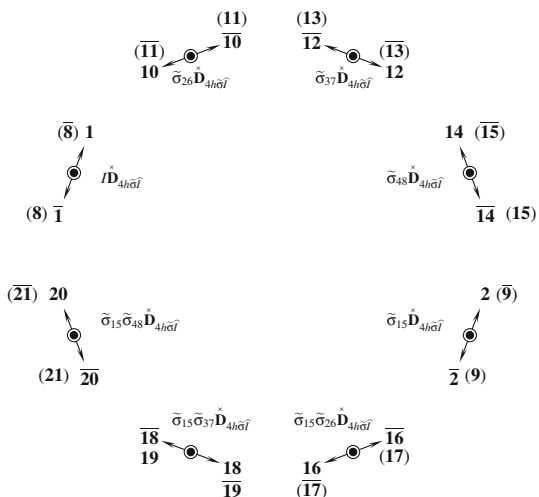
Correlation diagrams for characterizing global symmetries The coset decomposition defined by Eq. 96 generates a coset representation of $\widehat{\mathbf{G}}_{C\sigma}$ by $\mathbf{G}_{C\sigma\tilde{\sigma}I}^\times$, i.e., $\widehat{\mathbf{G}}_{C\sigma} \left(/ \mathbf{G}_{C\sigma\tilde{\sigma}I}^\times \right)$, by referring to Fujita’s USCI approach [13].

Definition 13 (*Stereoisomeric Representations*) The coset representation represented by the symbol $\widehat{\mathbf{G}}_{C\sigma} \left(/ \mathbf{G}_{C\sigma\tilde{\sigma}I}^\times \right)$ governs a main correlation diagram of stereoisograms so as to control the stereoisomeric behavior of the stereoisograms (the relevant quadruplets of *RS*-stereoisomers which belong to $\mathbf{G}_{C\sigma\tilde{\sigma}I}^\times$). The coset representation is called a *stereoisomeric representation* of the stereoisomeric group $\widehat{\mathbf{G}}_{C\sigma}$.

It should be noted that the set of permutations $\tilde{\sigma}_{[\omega]}$ in Eq. 96 is arbitrarily selected under the condition $\omega \leq \frac{n}{2}$ (without losing generality), where the set is not a group. This means that the set of $\widehat{\mathbf{G}}_{C\sigma} / \mathbf{G}_{C\sigma\tilde{\sigma}I}^\times$ is not a group. However, the coset representation

Fig. 6 Main correlation diagram for characterizing the global symmetry of a cyclobutane stereoskeleton.

Quadruplets of *RS*-stereoisomeric stereoskeletons (e.g., **1**, **1̄**, **8**, and **8̄**), whose stereoisograms are shown in Fig. 4, correspond to respective cosets appearing in Eq. 101



$\widehat{\mathbf{G}}_{C\sigma} \left(/ \overset{\times}{\widehat{\mathbf{G}}}_{C\sigma\tilde{\tau}} \right)$ is transitive under the action of the multiple epimerization group $\widehat{\mathbf{H}}$ (Eq. 77), which is a subgroup of $\widehat{\mathbf{G}}_{C\sigma}$.

For example, the coset decomposition of the stereoisomeric group $\widehat{\mathbf{D}}_{4h}$ (Eq. 101) generates the corresponding coset representation $\widehat{\mathbf{D}}_{4h} \left(/ \overset{\times}{\widehat{\mathbf{D}}}_{4h\tilde{\tau}} \right)$. Thus, the cosets $\overset{\times}{\widehat{\mathbf{D}}}_{4h\tilde{\tau}}$, $\tilde{\sigma}_{15}\overset{\times}{\widehat{\mathbf{D}}}_{4h\tilde{\tau}}$, $\tilde{\sigma}_{26}\overset{\times}{\widehat{\mathbf{D}}}_{4h\tilde{\tau}}$, $\tilde{\sigma}_{37}\overset{\times}{\widehat{\mathbf{D}}}_{4h\tilde{\tau}}$, and $\tilde{\sigma}_{48}\overset{\times}{\widehat{\mathbf{D}}}_{4h\tilde{\tau}}$ in Eq. 101 correspond to the stereoisograms shown in Fig. 4a–e. The remaining cosets $\tilde{\sigma}_{15}\tilde{\sigma}_{26}\overset{\times}{\widehat{\mathbf{D}}}_{4h\tilde{\tau}}$, $\tilde{\sigma}_{15}\tilde{\sigma}_{37}\overset{\times}{\widehat{\mathbf{D}}}_{4h\tilde{\tau}}$, and $\tilde{\sigma}_{15}\tilde{\sigma}_{48}\overset{\times}{\widehat{\mathbf{D}}}_{4h\tilde{\tau}}$ in Eq. 101 correspond to the stereoisograms shown in Fig. 4f–h. These cosets are transitive under the action of the multiple epimerization group $\widehat{\mathbf{H}}$ (Eq. 99), which is a subgroup of $\widehat{\mathbf{D}}_{4h}$.

To visualize the correspondence due to Eq. 101, a correlation diagram for characterizing the global symmetry of a cyclobutane stereoskeleton is depicted in Fig. 6. Each quadruplet of *RS*-stereoisomeric stereoskeletons (e.g., **1**, **1̄**, **8**, and **8̄**) constructs a stereoisogram shown in Fig. 4. For the sake of simplicity, each stereoisogram in Fig. 6 is depicted in a simplified form, in which two holantimeric pairs (e.g., **1̄/8** and **1̄/8̄**) are placed one by one at respective nodes.

By starting from Eq. 23, the following equation is obtained:

$$\begin{aligned} \mathbf{G}_{C\sigma\tilde{\tau}} &= \mathbf{H}_{\tilde{\sigma}} \times \mathbf{H}_{\tilde{\tau}} \times \mathbf{G}_C = \mathbf{H}_{\tilde{\sigma}} \times \mathbf{G}_{C\tilde{\tau}} \\ &= I \times \mathbf{G}_{C\tilde{\tau}} + \tilde{\sigma} \times \mathbf{G}_{C\tilde{\tau}} = \overset{\times}{\mathbf{G}}_{C\tilde{\tau}} + \tilde{\sigma} \overset{\times}{\mathbf{G}}_{C\tilde{\tau}} \end{aligned} \tag{102}$$

On the other hand, Eq. 23 is alternatively converted into another expression:

$$\begin{aligned} \mathbf{G}_{C\sigma\tilde{\tau}} &= \mathbf{H}_{\sigma} \times \mathbf{H}_{\tilde{\tau}} \times \mathbf{G}_C = \mathbf{H}_{\sigma} \times \mathbf{G}_{C\tilde{\tau}} \\ &= I \times \mathbf{G}_{C\tilde{\tau}} + \sigma \times \mathbf{G}_{C\tilde{\tau}} = \overset{\times}{\mathbf{G}}_{C\tilde{\tau}} + \sigma \overset{\times}{\mathbf{G}}_{C\tilde{\tau}} \end{aligned} \tag{103}$$

Because $\mathbf{G}_{C\hat{I}}$ (e.g., $\mathbf{D}_{4\hat{I}}$) corresponds to a pair of a molecule and its holantimer (e.g., **1** and $\bar{\mathbf{8}}$), Eqs. 102 and 103 means that such a pair is regarded as being *RS*-diastereomeric as well as enantiomeric to the complementary pair (e.g., $\bar{\mathbf{1}}$ and **8**). Note that Fig. 6 shows enantiomeric relationships only, which are tentatively regarded as having precedence over the superposed *RS*-diastereomeric relationships.

3.4.2 Local symmetries of stereoskeletons

Local symmetry groups in a stereoisomeric group Let us examine how a local symmetry group $\mathbf{G}_{C\sigma\tilde{\sigma}\hat{I}}^{\tilde{\sigma}_i}$ (Eq. 39 or 42) is contained in the stereomeric group $\widehat{\mathbf{G}}_{C\sigma}$ (Eq. 80 or Eq. 96).

When we put $\tilde{\sigma}_{[0,0,\dots,0]} = I$, the term $\tilde{\sigma}_{[0,0,\dots,0]} \times \mathbf{G}_{C\sigma\tilde{\sigma}\hat{I}}$ appearing in Eq. 96 corresponds to the *RS*-stereoisomeric group represented by Eq. 22 or the term contained in Eq. 42. When we put

$$[\omega'] = [0, 0, \dots, 0, \overset{j}{1}, 0, \dots, 0], \tag{104}$$

the term $\tilde{\sigma}_{[\omega']}$ is identical with $\tilde{\sigma}_j$ (cf. Eq. 81), so that the term $\tilde{\sigma}_{[\omega']} \times \mathbf{G}_{C\sigma\tilde{\sigma}\hat{I}}$ appearing in Eq. 96 is identical with $\tilde{\sigma}_j \times \mathbf{G}_{C\sigma\tilde{\sigma}\hat{I}}$ appearing in Eq. 41. The two terms are added to give the group $\mathbf{G}_{C\sigma\tilde{\sigma}\hat{I}}^{\tilde{\sigma}_j}$ (Eq. 41) as follows:

$$\tilde{\sigma}_{[0,0,\dots,0]} \times \mathbf{G}_{C\sigma\tilde{\sigma}\hat{I}} + \tilde{\sigma}_{[\omega']} \times \mathbf{G}_{C\sigma\tilde{\sigma}\hat{I}} = I \times \mathbf{G}_{C\sigma\tilde{\sigma}\hat{I}} + \tilde{\sigma}_j \times \mathbf{G}_{C\sigma\tilde{\sigma}\hat{I}} = \mathbf{G}_{C\sigma\tilde{\sigma}\hat{I}}^{\tilde{\sigma}_j}, \tag{105}$$

when $n \geq 2$. Hence, the group $\mathbf{G}_{C\sigma\tilde{\sigma}\hat{I}}^{\tilde{\sigma}_j}$ ($j = 1, 2, \dots, n$; Eq. 41) is contained in the stereoisomeric group $\widehat{\mathbf{G}}_{C\sigma}$ ($= \tilde{\mathbf{H}} \times \mathbf{G}_{C\sigma}$; Eq. 96). When $n = 2$, $\mathbf{G}_{C\sigma\tilde{\sigma}\hat{I}}^{\tilde{\sigma}_j}$ is identical with $\widehat{\mathbf{G}}_{C\sigma}$. When $n = 1$, $\mathbf{G}_{C\sigma\tilde{\sigma}\hat{I}}$ is identical with $\widehat{\mathbf{G}}_{C\sigma}$.

Let next consider a coset decomposition of the stereoisomeric group $\widehat{\mathbf{G}}_{C\sigma}$ by its subgroup $\mathbf{G}_{C\sigma\tilde{\sigma}\hat{I}}^{\tilde{\sigma}_j}$ (a local symmetry group), where j is tentatively fixed. By starting from Eq. 80, we obtain the following equation:

$$\begin{aligned} \widehat{\mathbf{G}}_{C\sigma} &= \tilde{\mathbf{H}} \times \mathbf{H}_\sigma \times \mathbf{G}_C = \left[\prod_{\substack{i=1 \\ i \neq j}}^n (I + \tilde{\sigma}_i) \right] \times (I + \tilde{\sigma}_j) \times \mathbf{G}_{C\sigma} \\ &= \left[\prod_{\substack{i=1 \\ i \neq j}}^n (I + \tilde{\sigma}_i) \right] \times (I + \tilde{\sigma}_j) \times \mathbf{H}_\sigma \times \mathbf{G}_C, \end{aligned} \tag{106}$$

where the product in the pair of brackets is concerned with epimerizations except $\tilde{\sigma}_j$. By putting $\omega_j = 0$ in Eq. 82, the following array of bits is obtained.

$$[\omega^{(j)}] = [\omega_1, \omega_2, \dots, \omega_{j-1}, \overset{j}{0}, \omega_{j+1}, \dots, \omega_n], \tag{107}$$

where ω_j is always equal to zero. Let the symbol $\omega^{(j)}$ be the sum of the bits contained in the bit array $[\omega^{(j)}]$:

$$\omega^{(j)} = \omega_1 + \omega_2 + \dots + \omega_n, \tag{108}$$

which is an integer from 0 to $n - 1$. A parallel procedure to the one for deriving Eq. 96 from Eq. 80 is effective to this case, so that Eq. 106 is similarly converted so as to give the following result:

$$\begin{aligned} \widehat{\mathbf{G}}_{C\sigma} &= \sum_{\omega^{(j)} \leq \frac{n-1}{2}} \tilde{\sigma}_{[\omega^{(j)}]} \times (I + \tilde{\sigma}_j) \times \mathbf{H}_\sigma \times \mathbf{H}_{\widehat{\Gamma}} \times \mathbf{G}_C \\ &= \sum_{\omega^{(j)} \leq \frac{n-1}{2}} \tilde{\sigma}_{[\omega^{(j)}]} \times \mathbf{H}_{\tilde{\sigma}_j} \times \mathbf{G}_{C\sigma\tilde{\sigma}\widehat{\Gamma}} = \sum_{\omega^{(j)} \leq \frac{n-1}{2}} \tilde{\sigma}_{[\omega^{(j)}]} \times \mathbf{G}_{C\sigma\tilde{\sigma}\widehat{\Gamma}}^{\tilde{\sigma}_j} \\ &= \sum_{\omega^{(j)} \leq \frac{n-1}{2}} \tilde{\sigma}_{[\omega^{(j)}]} \times \mathbf{G}_{C\sigma\tilde{\sigma}\widehat{\Gamma}}^{\tilde{\sigma}_j} \end{aligned} \tag{109}$$

for $j = 1, 2, \dots, n$, where the summation is effective for $n \geq 2$. Note that $\mathbf{G}_{C\sigma\tilde{\sigma}\widehat{\Gamma}}^{\tilde{\sigma}_j}$ is identical with $\widehat{\mathbf{G}}_{C\sigma}$ itself in the case of $n = 2$. The following discussions are effective even for such an extreme case ($n = 2$).

Obviously, Eq. 109 is a coset decomposition of $\widehat{\mathbf{G}}_{C\sigma}$ by the subgroup $\mathbf{G}_{C\sigma\tilde{\sigma}\widehat{\Gamma}}^{\tilde{\sigma}_j}$ which is a direct-product equivalent to $\mathbf{G}_{C\sigma\tilde{\sigma}\widehat{\Gamma}}^{\tilde{\sigma}_j}$. Because of $|\widehat{\mathbf{G}}_{C\sigma}| = 2^n |\mathbf{G}_{C\sigma}|$ and $|\mathbf{G}_{C\sigma\tilde{\sigma}\widehat{\Gamma}}^{\tilde{\sigma}_j}| = 2^2 |\mathbf{G}_{C\sigma}|$, we obtain:

$$\left| \widehat{\mathbf{G}}_{C\sigma} \middle/ \left| \mathbf{G}_{C\sigma\tilde{\sigma}\widehat{\Gamma}}^{\tilde{\sigma}_j} \right. \right| = 2^{n-2}, \tag{110}$$

which represents the number of cosets contained in Eq. 109.

Subductions of a stereoisomeric group for characterizing local symmetries The relationship between the coset decomposition by $\mathbf{G}_{C\sigma\tilde{\sigma}\widehat{\Gamma}}^{\tilde{\sigma}_j}$ (Eq. 109) and the counterpart by $\mathbf{G}_{C\sigma\tilde{\sigma}\widehat{\Gamma}}^{\times}$ (Eq. 96) can be investigated by following Fujita’s USCI approach [13], where the concept of *subductions of coset representations* is a key to examine such a relationship.

The latter coset decomposition (Eq. 96) generates a coset representation denoted by the symbol $\widehat{\mathbf{G}}_{C\sigma} \left(/ \mathbf{G}_{C\sigma\tilde{\sigma}\widehat{\Gamma}}^{\times} \right)$, where the representative of each coset is an element involved in the summation $\sum_{\omega \leq n/2} \tilde{\sigma}_{[\omega]}$. Then subduction of $\widehat{\mathbf{G}}_{C\sigma} \left(/ \mathbf{G}_{C\sigma\tilde{\sigma}\widehat{\Gamma}}^{\times} \right)$

by $\mathbf{G}_{C\sigma\tilde{\sigma}\hat{I}}^{\tilde{\sigma}_j}$ (or simply by \mathbf{H}_{σ_j}) generates orbits, each of which provides a grouping of cosets contained in Eq. 96 in accord with the grouping shown by Eq. 109. This discussion is summarized to give the following equation:

$$\widehat{\mathbf{G}}_{C\sigma} \left(/ \overset{\times}{\mathbf{G}}_{C\sigma\tilde{\sigma}\hat{I}} \right) \downarrow \mathbf{G}_{C\sigma\tilde{\sigma}\hat{I}}^{\tilde{\sigma}_j} = 2^{n-2} \mathbf{G}_{C\sigma\tilde{\sigma}\hat{I}}^{\tilde{\sigma}_j} \left(/ \overset{\times}{\mathbf{G}}_{C\sigma\tilde{\sigma}\hat{I}} \right), \tag{111}$$

or its simplified alternative:

$$\widehat{\mathbf{G}}_{C\sigma} \left(/ \overset{\times}{\mathbf{G}}_{C\sigma\tilde{\sigma}\hat{I}} \right) \downarrow \mathbf{H}_{\sigma_j} = 2^{n-2} \mathbf{H}_{\sigma_j} (/ \{I\}), \tag{112}$$

where the common coefficient 2^{n-2} is obtained because the degree of the coset representation $\widehat{\mathbf{G}}_{C\sigma} \left(/ \overset{\times}{\mathbf{G}}_{C\sigma\tilde{\sigma}\hat{I}} \right)$ is calculated to be $|\widehat{\mathbf{G}}_{C\sigma}| / |\overset{\times}{\mathbf{G}}_{C\sigma\tilde{\sigma}\hat{I}}| = 2^{n-1}$ (cf. Eq. 97), while the degree of the coset representation $\mathbf{G}_{C\sigma\tilde{\sigma}\hat{I}}^{\tilde{\sigma}_j} \left(/ \overset{\times}{\mathbf{G}}_{C\sigma\tilde{\sigma}\hat{I}} \right)$ (or $\mathbf{H}_{\sigma_j} (/ \{I\})$) is calculated to be 2. Note that the coefficient 2^{n-2} in Eqs. 111 and 112 is in agreement with Eq. 110.

Note that the coset representation $\mathbf{G}_{C\sigma\tilde{\sigma}\hat{I}}^{\tilde{\sigma}_j} \left(/ \overset{\times}{\mathbf{G}}_{C\sigma\tilde{\sigma}\hat{I}} \right)$ appearing in the right-hand side of Eq. 111 is closely related to, or essentially equivalent to the factor group $\mathbf{G}_{C\sigma\tilde{\sigma}\hat{I}}^{\tilde{\sigma}_j} / \overset{\times}{\mathbf{G}}_{C\sigma\tilde{\sigma}\hat{I}}$ shown in Eq. 44 (where the subscript i is changed to j without losing generality), because $\overset{\times}{\mathbf{G}}_{C\sigma\tilde{\sigma}\hat{I}}^{\tilde{\sigma}_j}$ can be equalized to $\mathbf{G}_{C\sigma\tilde{\sigma}\hat{I}}^{\tilde{\sigma}_j}$. Hence, the discussions on the factor group (before or after Eq. 44) are also effective to the coset representation appearing in the right-hand side of Eq. 111. Thus, the use of Eq. 112 in place of Eq. 111 is rationalized by the discussion on the derivation of Eq. 46.

By referring to Eq. 109, the 2^{n-2} cosets which correspond to the coset representations appearing in Eq. 111 are governed by the coset representation $\widehat{\mathbf{G}}_{C\sigma} \left(/ \overset{\times}{\mathbf{G}}_{C\sigma\tilde{\sigma}\hat{I}}^{\tilde{\sigma}_j} \right)$. The abovementioned discussions are summarized to give a theorem:

Theorem 1 *The 2^{n-2} sets of stereoisograms, where each set belongs to the local symmetry group $\mathbf{G}_{C\sigma\tilde{\sigma}\hat{I}}^{\tilde{\sigma}_j}$ (Definition 6), construct an orbit governed by the coset representation $\widehat{\mathbf{G}}_{C\sigma} \left(/ \overset{\times}{\mathbf{G}}_{C\sigma\tilde{\sigma}\hat{I}}^{\tilde{\sigma}_j} \right)$, which is generated by Eq. 109. Each of the 2^{n-2} sets of stereoisograms is governed by the coset representation $\mathbf{G}_{C\sigma\tilde{\sigma}\hat{I}}^{\tilde{\sigma}_j} \left(/ \overset{\times}{\mathbf{G}}_{C\sigma\tilde{\sigma}\hat{I}} \right)$ (Eq. 111, cf. Eq. 44).*

For example, the cosets appearing in Eq. 101 are converted into others by multiplication of $\tilde{\sigma}_{15}$, $\tilde{\sigma}_{26}$, $\tilde{\sigma}_{37}$, or $\tilde{\sigma}_{48}$ as follows:

$\downarrow \mathbf{H}_{\tilde{\sigma}_i}$	$\overset{\times}{\mathbf{D}}_{4h\tilde{\sigma}1}$	$\tilde{\sigma}_{15}\overset{\times}{\mathbf{D}}_{4h\tilde{\sigma}1}$	$\tilde{\sigma}_{26}\overset{\times}{\mathbf{D}}_{4h\tilde{\sigma}1}$	$\tilde{\sigma}_{37}\overset{\times}{\mathbf{D}}_{4h\tilde{\sigma}1}$	$\tilde{\sigma}_{48}\overset{\times}{\mathbf{D}}_{4h\tilde{\sigma}1}$	$\tilde{\sigma}_{15}\tilde{\sigma}_{26}\overset{\times}{\mathbf{D}}_{4h\tilde{\sigma}1}$	$\tilde{\sigma}_{15}\tilde{\sigma}_{37}\overset{\times}{\mathbf{D}}_{4h\tilde{\sigma}1}$	$\tilde{\sigma}_{15}\tilde{\sigma}_{48}\overset{\times}{\mathbf{D}}_{4h\tilde{\sigma}1}$	
	1	2	3	4	5	6	7	8	
$\times I$	1	2	3	4	5	6	7	8	
$\times \tilde{\sigma}_{15}$	2	1	6	7	8	3	4	5	(113)
$\times \tilde{\sigma}_{26}$	3	6	1	8	7	2	5	4	
$\times \tilde{\sigma}_{37}$	4	7	8	1	6	5	2	3	
$\times \tilde{\sigma}_{48}$	5	8	7	6	1	4	3	2	

where the cosets are numbered sequentially.

According to Eq. 112, the results shown in the $(\times I)$ - and the $(\times \tilde{\sigma}_{15})$ -rows of Eq. 113 indicate the subduction of the coset representation $\widehat{\mathbf{D}}_{4h} \left(/ \overset{\times}{\mathbf{D}}_{4h\tilde{\sigma}1} \right)$ by $\mathbf{H}_{\tilde{\sigma}_{15}}$ ($= \{I, \tilde{\sigma}_{15}\}$). Thereby, four modes of grouping appear to give the corresponding orbits, i.e., $\{1, 2\}$, $\{3, 6\}$, $\{4, 7\}$, and $\{5, 8\}$, where the numbering of the cosets is shown in Eq. 113. Note that the number of orbits is calculated to be $2^{4-2} = 4$ according to Eq. 112. By referring to Eqs. 109 and 96, the cosets appearing in Eq. 101 are rearranged to generate the four orbits:

$$\begin{aligned}
 \widehat{\mathbf{D}}_{4h} &= \overset{\times}{\mathbf{D}}_{4h\tilde{\sigma}1}^{15} + \tilde{\sigma}_{26}\overset{\times}{\mathbf{D}}_{4h\tilde{\sigma}1}^{15} + \tilde{\sigma}_{37}\overset{\times}{\mathbf{D}}_{4h\tilde{\sigma}1}^{15} + \tilde{\sigma}_{48}\overset{\times}{\mathbf{D}}_{4h\tilde{\sigma}1}^{15} \tag{114} \\
 &= \left\{ \overset{\times}{\mathbf{D}}_{4h\tilde{\sigma}1} + \tilde{\sigma}_{15}\overset{\times}{\mathbf{D}}_{4h\tilde{\sigma}1} \right\} + \left\{ \tilde{\sigma}_{26}\overset{\times}{\mathbf{D}}_{4h\tilde{\sigma}1} + \tilde{\sigma}_{15}\tilde{\sigma}_{26}\overset{\times}{\mathbf{D}}_{4h\tilde{\sigma}1} \right\} \\
 &\quad + \left\{ \tilde{\sigma}_{37}\overset{\times}{\mathbf{D}}_{4h\tilde{\sigma}1} + \tilde{\sigma}_{15}\tilde{\sigma}_{37}\overset{\times}{\mathbf{D}}_{4h\tilde{\sigma}1} \right\} + \left\{ \tilde{\sigma}_{48}\overset{\times}{\mathbf{D}}_{4h\tilde{\sigma}1} + \tilde{\sigma}_{15}\tilde{\sigma}_{48}\overset{\times}{\mathbf{D}}_{4h\tilde{\sigma}1} \right\} \tag{115}
 \end{aligned}$$

where a pair parenthesized by braces represents each one of the four orbits (cf. Fig. 4) and corresponds to a set of an epimeric stereoisogram and a holantimeric one. For example, the set of $\overset{\times}{\mathbf{D}}_{4h\tilde{\sigma}1}$ (for $1, \bar{1}, 8, \bar{8}$) and $\tilde{\sigma}_{15}\overset{\times}{\mathbf{D}}_{4h\tilde{\sigma}1}$ (for $2, \bar{2}, 9, \bar{9}$) represents the set of two stereoisograms shown in Fig. 4a and b. The conversion of Eq. 65 into Eq. 66 shows the rearrangement of inner cosets, which causes the conversion of the stereoisograms of Fig. 4a and b into those of Fig. 5a and b (an epimeric stereoisogram and a holantimeric stereoisogram). Each of the resulting stereoisograms contains a quadruplet of numbered stereoskeletons, i.e., $\{1_1, \bar{1}_1, 2_1, \bar{2}_1\}$ or $\{8_1, \bar{8}_1, 9_1, \bar{9}_1\}$, where the subscript 1 denotes the local symmetry at the C_1 atom. This type of rearrangements will be discussed more strictly from a different point of view.

The subduction $\widehat{\mathbf{D}}_{4h} \left(/ \overset{\times}{\mathbf{D}}_{4h\tilde{\sigma}1} \right) \downarrow \mathbf{H}_{\tilde{\sigma}_{26}}$ (where $\mathbf{H}_{\tilde{\sigma}_{26}} = \{I, \tilde{\sigma}_{26}\}$) generates another set of four orbits, $\{1, 3\}$, $\{2, 6\}$, $\{4, 8\}$, and $\{5, 7\}$, where the numbering of the cosets

is shown in Eq. 113. The cosets appearing in Eq. 101 are rearranged to generate the four orbits:

$$\begin{aligned} \widehat{\mathbf{D}}_{4h} &= \overset{\times}{\mathbf{D}}_{4h\tilde{\sigma}I}^{\tilde{\sigma}_{26}} + \tilde{\sigma}_{15}\overset{\times}{\mathbf{D}}_{4h\tilde{\sigma}I}^{\tilde{\sigma}_{26}} + \tilde{\sigma}_{37}\overset{\times}{\mathbf{D}}_{4h\tilde{\sigma}I}^{\tilde{\sigma}_{26}} + \tilde{\sigma}_{48}\overset{\times}{\mathbf{D}}_{4h\tilde{\sigma}I}^{\tilde{\sigma}_{26}} \tag{116} \\ &= \left\{ \begin{array}{c} \overset{\times}{\mathbf{D}}_{4h\tilde{\sigma}I} + \tilde{\sigma}_{26}\overset{\times}{\mathbf{D}}_{4h\tilde{\sigma}I} \\ \underline{1, \bar{1}, 8, \bar{8}} \quad \underline{10, \bar{10}, 11, \bar{11}} \end{array} \right\} + \left\{ \begin{array}{c} \tilde{\sigma}_{15}\overset{\times}{\mathbf{D}}_{4h\tilde{\sigma}I} + \tilde{\sigma}_{15}\tilde{\sigma}_{26}\overset{\times}{\mathbf{D}}_{4h\tilde{\sigma}I} \\ \underline{2, \bar{2}, 9, \bar{9}} \quad \underline{16, \bar{16}, 17, \bar{17}} \end{array} \right\} \\ &+ \left\{ \begin{array}{c} \tilde{\sigma}_{37}\overset{\times}{\mathbf{D}}_{4h\tilde{\sigma}I} + \tilde{\sigma}_{15}\tilde{\sigma}_{48}\overset{\times}{\mathbf{D}}_{4h\tilde{\sigma}I} \\ \underline{12, \bar{12}, 13, \bar{13}} \quad \underline{20, \bar{20}, 21, \bar{21}} \end{array} \right\} + \left\{ \begin{array}{c} \tilde{\sigma}_{48}\overset{\times}{\mathbf{D}}_{4h\tilde{\sigma}I} + \tilde{\sigma}_{15}\tilde{\sigma}_{37}\overset{\times}{\mathbf{D}}_{4h\tilde{\sigma}I} \\ \underline{14, \bar{14}, 15, \bar{15}} \quad \underline{18, \bar{18}, 19, \bar{19}} \end{array} \right\} \tag{117} \end{aligned}$$

where each pair parenthesized by braces represents one of the four orbits (cf. Fig. 4) and corresponds to a set of an epimeric stereoisogram and a holantimeric one (via Eqs. 69 and 70).

The subduction by $\mathbf{H}_{\tilde{\sigma}_{37}}$ ($= \{I, \tilde{\sigma}_{37}\}$) causes a rearrangement to generate a further set of four orbits, {1, 4}, {2, 7}, {3, 8}, and {5, 6}, where the numbering of the cosets is shown in Eq. 113. The cosets appearing in Eq. 101 are rearranged to generate the four orbits:

$$\begin{aligned} \widehat{\mathbf{D}}_{4h} &= \overset{\times}{\mathbf{D}}_{4h\tilde{\sigma}I}^{\tilde{\sigma}_{37}} + \tilde{\sigma}_{15}\overset{\times}{\mathbf{D}}_{4h\tilde{\sigma}I}^{\tilde{\sigma}_{37}} + \tilde{\sigma}_{26}\overset{\times}{\mathbf{D}}_{4h\tilde{\sigma}I}^{\tilde{\sigma}_{37}} + \tilde{\sigma}_{48}\overset{\times}{\mathbf{D}}_{4h\tilde{\sigma}I}^{\tilde{\sigma}_{37}} \tag{118} \\ &= \left\{ \begin{array}{c} \overset{\times}{\mathbf{D}}_{4h\tilde{\sigma}I} + \tilde{\sigma}_{37}\overset{\times}{\mathbf{D}}_{4h\tilde{\sigma}I} \\ \underline{1, \bar{1}, 8, \bar{8}} \quad \underline{12, \bar{12}, 13, \bar{13}} \end{array} \right\} + \left\{ \begin{array}{c} \tilde{\sigma}_{15}\overset{\times}{\mathbf{D}}_{4h\tilde{\sigma}I} + \tilde{\sigma}_{15}\tilde{\sigma}_{37}\overset{\times}{\mathbf{D}}_{4h\tilde{\sigma}I} \\ \underline{2, \bar{2}, 9, \bar{9}} \quad \underline{18, \bar{18}, 19, \bar{19}} \end{array} \right\} \\ &+ \left\{ \begin{array}{c} \tilde{\sigma}_{26}\overset{\times}{\mathbf{D}}_{4h\tilde{\sigma}I} + \tilde{\sigma}_{15}\tilde{\sigma}_{48}\overset{\times}{\mathbf{D}}_{4h\tilde{\sigma}I} \\ \underline{10, \bar{10}, 11, \bar{11}} \quad \underline{20, \bar{20}, 21, \bar{21}} \end{array} \right\} + \left\{ \begin{array}{c} \tilde{\sigma}_{48}\overset{\times}{\mathbf{D}}_{4h\tilde{\sigma}I} + \tilde{\sigma}_{15}\tilde{\sigma}_{26}\overset{\times}{\mathbf{D}}_{4h\tilde{\sigma}I} \\ \underline{14, \bar{14}, 15, \bar{15}} \quad \underline{16, \bar{16}, 17, \bar{17}} \end{array} \right\} \tag{119} \end{aligned}$$

where each pair parenthesized by braces represents one of the four orbits (cf. Fig. 4) and corresponds to a set of an epimeric stereoisogram and a holantimeric one (via Eqs. 72 and 73).

The subduction of the coset representation $\widehat{\mathbf{D}}_{4h} \left(\overset{\times}{\mathbf{D}}_{4h\tilde{\sigma}I} \right)$ by $\mathbf{H}_{\tilde{\sigma}_{48}}$ ($= \{I, \tilde{\sigma}_{48}\}$) causes a rearrangement to generate a further set of four orbits, {1, 5}, {2, 8}, {3, 7}, and {4, 6}, where the numbering of the cosets is shown in Eq. 113. The cosets appearing in Eq. 101 are rearranged to generate the four orbits:

$$\widehat{\mathbf{D}}_{4h} = \overset{\times}{\mathbf{D}}_{4h\tilde{\sigma}\hat{I}}^{\tilde{\sigma}_{48}} + \tilde{\sigma}_{15}\overset{\times}{\mathbf{D}}_{4h\tilde{\sigma}\hat{I}}^{\tilde{\sigma}_{48}} + \tilde{\sigma}_{26}\overset{\times}{\mathbf{D}}_{4h\tilde{\sigma}\hat{I}}^{\tilde{\sigma}_{48}} + \tilde{\sigma}_{37}\overset{\times}{\mathbf{D}}_{4h\tilde{\sigma}\hat{I}}^{\tilde{\sigma}_{48}} \quad (120)$$

$$= \left\{ \overset{\times}{\mathbf{D}}_{4h\tilde{\sigma}\hat{I}} + \overset{\times}{\mathbf{D}}_{4h\tilde{\sigma}\hat{I}}^{\tilde{\sigma}_{48}} \right\} + \left\{ \tilde{\sigma}_{15}\overset{\times}{\mathbf{D}}_{4h\tilde{\sigma}\hat{I}} + \tilde{\sigma}_{15}\tilde{\sigma}_{48}\overset{\times}{\mathbf{D}}_{4h\tilde{\sigma}\hat{I}} \right\} \\ + \left\{ \tilde{\sigma}_{26}\overset{\times}{\mathbf{D}}_{4h\tilde{\sigma}\hat{I}} + \tilde{\sigma}_{15}\tilde{\sigma}_{37}\overset{\times}{\mathbf{D}}_{4h\tilde{\sigma}\hat{I}} \right\} + \left\{ \tilde{\sigma}_{37}\overset{\times}{\mathbf{D}}_{4h\tilde{\sigma}\hat{I}} + \tilde{\sigma}_{15}\tilde{\sigma}_{26}\overset{\times}{\mathbf{D}}_{4h\tilde{\sigma}\hat{I}} \right\} \quad (121)$$

where each pair parenthesized by braces represents one of the four orbits (cf. Fig. 4) and corresponds to a set of an epimeric stereoisogram and a holantimeric one (via Eqs. 75 and 76).

It should be added here that Theorem 1 is a foundation of traditional categorizations of stereoisomers, e.g., the Fischer-Rosanoff convention for naming the DL-series of sugars by starting from D- and L-glyceraldehydes [5]. The selection of the local symmetry group $\mathbf{G}_{C_{\sigma}\tilde{\sigma}\hat{I}}^{\tilde{\sigma}_j}$ (Definition 6) in Theorem 1 corresponds to the selection of D- or L-glyceraldehyde as an initial standard configuration, where the corresponding pivot epimerization (Definition 12) is concerned with the *RS*-diastereomeric relationship between D- and L-glyceraldehydes (not to the enantiomeric relationship between them). Note that any *RS*-stereogenic center can be selected as the center of such a pivot epimerization ($\tilde{\sigma}_j$). As for cyclobutane stereoisomers, any one of C_1 – C_4 can be selected as such a pivot epimerization so as to result in Eq. 115, 117, 119, or 121.

Correlation diagrams for characterizing local symmetries As clarified by Theorem 1 (Eq. 111 or Eq. 112), the group $\mathbf{G}_{C_{\sigma}\tilde{\sigma}\hat{I}}^{\tilde{\sigma}_j}$ appearing in Eq. 109 corresponds to a pair of stereoisograms (an epimeric stereoisogram and a holantimeric stereoisogram, e.g., Fig. 5a and b). Thereby the coset decomposition represented by Eq. 109 determines the behavior of 2^{n-2} pairs of such stereoisograms, where each coset of Eq. 109 is correlated to a pair of stereoisograms. Each pair of stereoisograms represents the local symmetries at the C_j atoms of relevant stereoskeletons ($j = 1, 2, \dots, n$). The behavior of the 2^{n-2} pairs of stereoisograms at a fixed C_j atom is visualized by correlation diagrams of stereoisograms. For example, the coset decompositions represented by Eq. 114 (or Eq. 115) for C_1 , Eq. 116 (or Eq. 117) for C_2 , Eq. 116 (or Eq. 119) for C_3 , and Eq. 114 (or Eq. 121) for C_4 are visualized by correlation diagrams of stereoisograms, as shown in Fig. 7.

We are able to discuss the local symmetries at the C_1 atoms of cyclobutane stereoskeletons on the basis of Eq. 114 (or Eq. 115). By starting from the correlation diagram for characterizing the global symmetry of a cyclobutane stereoskeleton (Fig. 6), enantiomeric, *RS*-diastereomeric, and holantimeric relationships are drawn in agreement with Eq. 114 (as well as with Eq. 115) so as to generate the corresponding correlation diagram, as shown in Fig. 7a. Thus, the coset $\overset{\times}{\mathbf{D}}_{4h\tilde{\sigma}\hat{I}}^{\tilde{\sigma}_{15}}$ contained in Eq. 114 corresponds to Stereoisogram #1 of Fig. 7a. Stereoisogram #1 of Fig. 7a is concerned with a

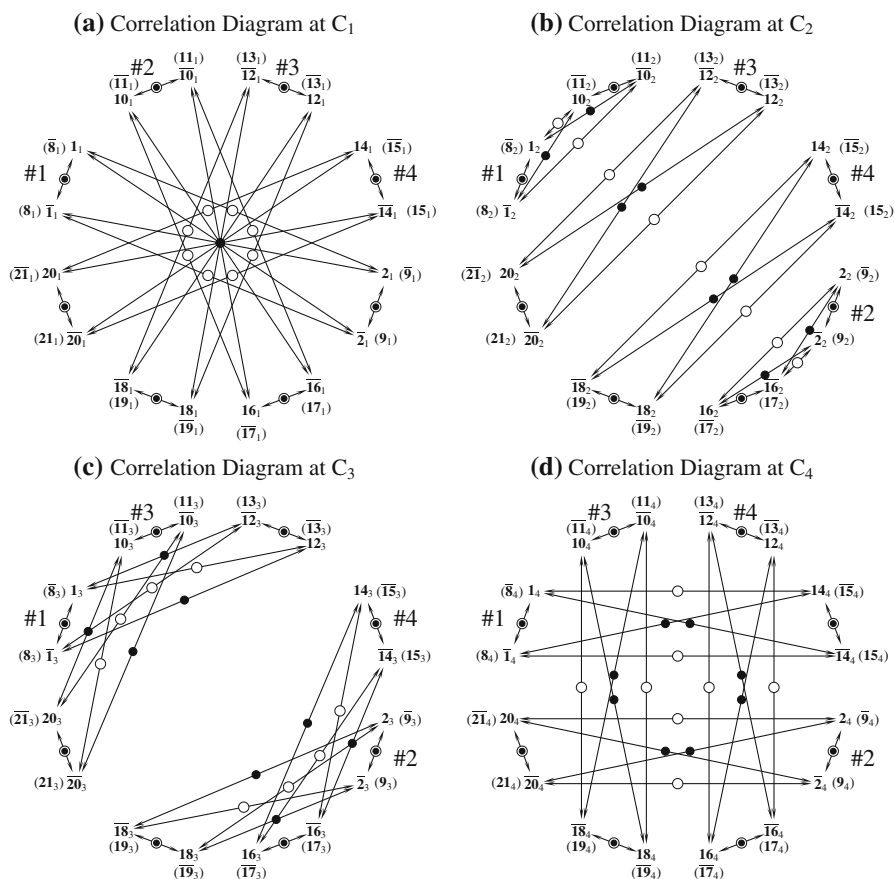


Fig. 7 Correlation diagrams of stereoisograms for cyclobutane stereoskeletons: **a** for C_1 (cf. Eq. 115), **b** for C_2 (cf. Eq. 117), **c** for C_3 (cf. Eq. 119), and **d** for C_4 (cf. Eq. 121)

quadruplet of stereoskeletons, i.e., 1_1 and $\bar{1}_1$ (corresponding to the coset $\times D_{4h\tilde{\sigma}I}$ in Eq. 115) as well as 2_1 and $\bar{2}_1$ (corresponding to the coset $\times \tilde{\sigma}_{15} D_{4h\tilde{\sigma}I}$ in Eq. 115). Note that the subscript 1 of each stereoskeleton number emphasizes the consideration of the local symmetry at the C_1 atom. The concrete form of Stereoisogram #1 is shown as an epimeric stereoisogram in Fig. 5a. Stereoisogram #1 of Fig. 7a is also concerned with another quadruplet of stereoskeletons, i.e., 8_1 and $\bar{8}_1$ (corresponding to the coset $\times D_{4h\tilde{\sigma}I}$ as well as 9_1 and $\bar{9}_1$ (corresponding to the coset $\times \tilde{\sigma}_{15} D_{4h\tilde{\sigma}I}$ in Eq. 115). The concrete form of Stereoisogram #1 of this case is shown as a holantimeric stereoisogram in Fig. 5b.

Similarly, the coset $\times \tilde{\sigma}_{26} D_{4h\tilde{\sigma}I}^{\times 15}$ contained in Eq. 114 corresponds to Stereoisogram #2 of Fig. 7a, where relevant stereoskeletons are collected in Eq. 115; the coset $\times \tilde{\sigma}_{37} D_{4h\tilde{\sigma}I}^{\times 15}$

contained in Eq. 114 corresponds to Stereoisogram #3 of Fig. 7a, where relevant stereoskeletons are collected in Eq. 115; and the coset $\tilde{\sigma}_{48} \times \tilde{\mathbf{D}}_{4h\tilde{\sigma}\hat{I}}^{\tilde{\sigma}_{15}}$ contained in Eq. 114 corresponds to Stereoisogram #4 of Fig. 7a, where relevant stereoskeletons are collected in Eq. 115. The corresponding concrete forms of epimeric and holantimeric stereoisograms can be depicted in a parallel way to Fig. 5a and b.

The local symmetries at the C_2 atoms of cyclobutane stereoskeletons are examined by means of Eq. 116 (or Eq. 117). Thus, the behavior of the cosets contained in Eq. 116 are correlated to Stereoisogram #1–#4, which are contained in the correlation diagram of stereoisograms shown in Fig. 7b. The coset $\tilde{\sigma}_{48} \times \tilde{\mathbf{D}}_{4h\tilde{\sigma}\hat{I}}^{\tilde{\sigma}_{26}}$ contained in Eq. 116 corresponds to Stereoisogram #1 of Fig. 7b. The remaining cosets contained in Eq. 116 correspond respectively to Stereoisogram #2–#4 of Fig. 7b.

When we focus our attention on the C_3 atoms of cyclobutane stereoskeletons, we use Eq. 118 (or Eq. 119) to discuss the local symmetries at the C_3 atoms. The behavior of the cosets contained in Eq. 118 are correlated to Stereoisogram #1–#4, which are contained in the correlation diagram of stereoisograms shown in Fig. 7c. The coset $\tilde{\sigma}_{37} \times \tilde{\mathbf{D}}_{4h\tilde{\sigma}\hat{I}}$ contained in Eq. 118 corresponds to Stereoisogram #1 of Fig. 7c. The remaining cosets contained in Eq. 118 correspond respectively to Stereoisogram #2–#4 of Fig. 7c.

The correlation diagram of stereoisograms for determining the local symmetries at the C_4 atoms of cyclobutane stereoskeletons is illustrated in Fig. 7d, where each stereoisogram is correlated to a coset appearing in Eq. 120 (or Eq. 121). Thus, the coset $\tilde{\sigma}_{48} \times \tilde{\mathbf{D}}_{4h\tilde{\sigma}\hat{I}}$ contained in Eq. 120 corresponds to Stereoisogram #1 of Fig. 7d. The remaining cosets contained in Eq. 120 correspond respectively to Stereoisogram #2–#4 of Fig. 7d.

By means Eq. 111, a quadruplet of *RS*-stereoisomers (e.g., $\mathbf{1}_1, \bar{\mathbf{1}}_1, \mathbf{8}_1,$ and $\bar{\mathbf{8}}_1$) and another quadruplet (e.g., $\mathbf{2}_1, \bar{\mathbf{2}}_1, \mathbf{9}_1,$ and $\bar{\mathbf{9}}_1$) construct a two-membered orbit governed by the coset representation $\tilde{\mathbf{G}}_{C\sigma\tilde{\sigma}\hat{I}}^{\tilde{\sigma}_j} \left(/ \tilde{\mathbf{G}}_{C\sigma\tilde{\sigma}\hat{I}}^{\times} \right)$, where each quadruplet belongs to $\tilde{\mathbf{G}}_{C\sigma\tilde{\sigma}\hat{I}}^{\times}$. On the other hand, Eq. 112 indicates that the two quadruplets are regarded as abstract entities belonging to $\{I\}$ so as to construct a two-membered orbit governed by the coset representation $\mathbf{H}_{\tilde{\sigma}_j} / \{I\}$.

Strictly speaking, there appears one more subduction between Eqs. 111 and 112, i.e.,

$$\widehat{\mathbf{G}}_{C\sigma} \left(/ \tilde{\mathbf{G}}_{C\sigma\tilde{\sigma}\hat{I}}^{\times} \right) \downarrow \mathbf{H}_{\sigma}^{\tilde{\sigma}_j} = 2^{n-2} \mathbf{H}_{\sigma}^{\tilde{\sigma}_j} / \{ \mathbf{H}_{\sigma} \}, \quad (122)$$

where $\widehat{\mathbf{H}}_{\sigma}^{\tilde{\sigma}_j}$ is an epimeric stereoisogram group defined by Eq. 48 and \mathbf{H}_{σ} is given by Eq. 20. By following Eq. 122, the two quadruplets belonging to $\tilde{\mathbf{G}}_{C\sigma\tilde{\sigma}\hat{I}}^{\times}$ are reduced into two enantiomeric pairs belonging to \mathbf{H}_{σ} (e.g., one pair: $\mathbf{1}_1 (\bar{\mathbf{8}}_1) / \bar{\mathbf{1}}_1 (\mathbf{8}_1)$ and the other pair: $\mathbf{2}_1 (\bar{\mathbf{9}}_1) / \bar{\mathbf{2}}_1 (\mathbf{9}_1)$).

Because we obtain the following subduction:

$$\mathbf{H}_{\sigma}^{\tilde{\sigma}_j} (/ \mathbf{H}_{\sigma}) \downarrow \mathbf{H}_{\tilde{\sigma}_j} = \mathbf{H}_{\tilde{\sigma}_j} (/ \{I\}), \tag{123}$$

Equation 122 gives apparently an equivalent result to Eq. 112. The two modes of results can be equalized so long as we take account of the *RS*-stereoisomeric group $\overset{\times}{\mathbf{G}}_{C\sigma\tilde{\sigma}\hat{I}}$, which is contained in the coset representation $\widehat{\mathbf{G}}_{C\sigma} \left(/ \overset{\times}{\mathbf{G}}_{C\sigma\tilde{\sigma}\hat{I}} \right)$.

Definition 8 combined with Eq. 60 indicates that the epimeric *RS*-stereoisomeric group $\mathbf{G}_{C\sigma}^{\tilde{\sigma}_j} (= \mathbf{H}_{\sigma}^{\tilde{\sigma}_j} \times \mathbf{G}_C)$ corresponds to an epimeric stereoisogram. Thereby, Eq. 122 is converted into the following subduction:

$$\begin{aligned} \widehat{\mathbf{G}}_{C\sigma} \left(/ \overset{\times}{\mathbf{G}}_{C\sigma\tilde{\sigma}\hat{I}} \right) \downarrow \mathbf{G}_{C\sigma}^{\tilde{\sigma}_j} &= \widehat{\mathbf{G}}_{C\sigma} \left(/ \overset{\times}{\mathbf{G}}_{C\sigma\tilde{\sigma}\hat{I}} \right) \downarrow \mathbf{H}_{\sigma}^{\tilde{\sigma}_j} \times \mathbf{G}_C \\ &= 2^{n-2} \mathbf{H}_{\sigma}^{\tilde{\sigma}_j} \times \mathbf{G}_C (/ \mathbf{H}_{\sigma} \times \mathbf{G}_C) = 2^{n-2} \mathbf{G}_{C\sigma}^{\tilde{\sigma}_j} (/ \mathbf{G}_{C\sigma}). \end{aligned} \tag{124}$$

The coset representation $\mathbf{G}_{C\sigma}^{\tilde{\sigma}_j} (/ \mathbf{G}_{C\sigma})$ means that an epimeric stereoisogram controlled by $\mathbf{G}_{C\sigma}^{\tilde{\sigma}_j} (/ \mathbf{G}_{C\sigma})$ is regarded as being composed of two enantiomeric pairs belonging to $\mathbf{G}_{C\sigma}$, where the two enantiomeric pairs are converted into each other by $\tilde{\sigma}_j$.

4 Stereoisomers derived from a stereoskeleton

4.1 Pairwise appearance of epimeric and holantimeric stereoisograms

The combination of Eq. 57 with Eq. 59 gives the following equation:

$$\mathbf{G}_{C\sigma\tilde{\sigma}\hat{I}}^{\tilde{\sigma}_i} = I \times \mathbf{G}_{C\sigma}^{\tilde{\sigma}_i} + \hat{I} \times \mathbf{G}_{C\sigma}^{\tilde{\sigma}_i} = \overset{\times}{\mathbf{G}}_{C\sigma}^{\tilde{\sigma}_i} + \hat{I} \overset{\times}{\mathbf{G}}_{C\sigma}^{\tilde{\sigma}_i}, \tag{125}$$

which is regarded as a coset decomposition of the local symmetry group $\mathbf{G}_{C\sigma\tilde{\sigma}\hat{I}}^{\tilde{\sigma}_i}$ by the epimeric *RS*-stereoisomeric group $\mathbf{G}_{C\sigma}^{\tilde{\sigma}_i}$. The coset decomposition (Eq. 125) generates the corresponding coset representation $\mathbf{G}_{C\sigma\tilde{\sigma}\hat{I}}^{\tilde{\sigma}_i} \left(/ \overset{\times}{\mathbf{G}}_{C\sigma}^{\tilde{\sigma}_i} \right)$ of degree 2, which is calculated as follows: $|\mathbf{G}_{C\sigma\tilde{\sigma}\hat{I}}^{\tilde{\sigma}_i} / | \overset{\times}{\mathbf{G}}_{C\sigma}^{\tilde{\sigma}_i} | = 2 \times 2^2 | \mathbf{G}_C | / 2^2 | \mathbf{G}_C | = 2$. The group $\overset{\times}{\mathbf{G}}_{C\sigma}^{\tilde{\sigma}_i}$ of the coset representation $\mathbf{G}_{C\sigma\tilde{\sigma}\hat{I}}^{\tilde{\sigma}_i} \left(/ \overset{\times}{\mathbf{G}}_{C\sigma}^{\tilde{\sigma}_i} \right)$ (Eq. 125) indicates the group governing an epimeric stereoisogram (or a holantimeric stereoisogram) as shown in Eq. 60 and Definition 9. Hence, the coset representation $\mathbf{G}_{C\sigma\tilde{\sigma}\hat{I}}^{\tilde{\sigma}_i} \left(/ \overset{\times}{\mathbf{G}}_{C\sigma}^{\tilde{\sigma}_i} \right)$ (Eq. 125) generates a two-membered orbit, whose members are correlated to an epimeric stereoisogram and a holantimeric stereoisogram (Definition 9).

By introducing Eq. 125 (the subscript i is changed to a fixed j) into Eq. 109, we obtain the following equation:

$$\begin{aligned}\widehat{\mathbf{G}}_{C\sigma} &= \sum_{\omega^{(j)} \leq \frac{n-1}{2}} \widetilde{\sigma}_{[\omega^{(j)}]} \times \widetilde{\sigma}_j \widehat{\mathbf{G}}_{C\sigma\widehat{I}} \\ &= \sum_{\omega^{(j)} \leq \frac{n-1}{2}} \widetilde{\sigma}_{[\omega^{(j)}]} \times \widetilde{\sigma}_j \mathbf{G}_{C\sigma} + \sum_{\omega^{(j)} \leq \frac{n-1}{2}} \widetilde{\sigma}_{[\omega^{(j)}]} \widehat{I} \times \widetilde{\sigma}_j \mathbf{G}_{C\sigma} = \sum_{\omega^{(j)} \leq \frac{n-1}{2}} \widetilde{\sigma}_{[\omega^{(j)}]} (I + \widehat{I}) \times \widetilde{\sigma}_j \mathbf{G}_{C\sigma},\end{aligned}\quad (126)$$

which is regarded as a coset decomposition of the stereoisomeric group $\widehat{\mathbf{G}}_{C\sigma}$ by the epimeric RS -stereoisomeric group $\mathbf{G}_{C\sigma}^{\widetilde{\sigma}_j}$. Note that the expansion of $\sum_{\omega^{(j)} \leq \frac{n-1}{2}} \widetilde{\sigma}_{[\omega^{(j)}]} (I + \widehat{I})$ generates 2^{n-1} terms. The coset decomposition (Eq. 126) generates the corresponding coset representation $\widehat{\mathbf{G}}_{C\sigma} \left(/ \mathbf{G}_{C\sigma}^{\widetilde{\sigma}_j} \right)$, the degree of which is calculated to be $|\widehat{\mathbf{G}}_{C\sigma}| / |\mathbf{G}_{C\sigma}^{\widetilde{\sigma}_j}| = 2^n |\mathbf{G}_C| / 2^2 |\mathbf{G}_C| = 2^{n-2}$.

By keeping Eqs. 125 and 126 in mind, we obtain the following subduction for a fixed j :

$$\widehat{\mathbf{G}}_{C\sigma} \left(/ \mathbf{G}_{C\sigma}^{\widetilde{\sigma}_j} \right) \downarrow \mathbf{G}_{C\sigma\widehat{I}}^{\widetilde{\sigma}_j} = 2^{n-2} \mathbf{G}_{C\sigma\widehat{I}}^{\widetilde{\sigma}_j} \left(/ \mathbf{G}_{C\sigma}^{\widetilde{\sigma}_j} \right). \quad (127)$$

On a similar line to the derivation of Eq. 125, the omission of \mathbf{G}_C is allowed to give a coset decomposition:

$$\mathbf{H}_{\sigma\widehat{I}}^{\widetilde{\sigma}_i} = I \times \mathbf{H}_{\sigma}^{\widetilde{\sigma}_i} + \widehat{I} \times \mathbf{H}_{\sigma}^{\widetilde{\sigma}_i}, = \mathbf{H}_{\sigma}^{\widetilde{\sigma}_i} + \widehat{I} \mathbf{H}_{\sigma}^{\widetilde{\sigma}_i}, \quad (128)$$

which generates a coset representation of degree 2, i.e., $\mathbf{H}_{\sigma\widehat{I}}^{\widetilde{\sigma}_i} \left(/ \mathbf{H}_{\sigma}^{\widetilde{\sigma}_i} \right)$. Thereby, a parallel derivation to Eq. 127 is allowed so as to generate the following equations:

$$\widehat{\mathbf{G}}_{C\sigma} \left(/ \mathbf{G}_{C\sigma}^{\widetilde{\sigma}_j} \right) \downarrow \mathbf{H}_{\sigma\widehat{I}}^{\widetilde{\sigma}_j} = 2^{n-2} \mathbf{H}_{\sigma\widehat{I}}^{\widetilde{\sigma}_j} \left(/ \mathbf{H}_{\sigma}^{\widetilde{\sigma}_j} \right) \quad (129)$$

$$\widehat{\mathbf{G}}_{C\sigma} \left(/ \mathbf{G}_{C\sigma}^{\widetilde{\sigma}_j} \right) \downarrow \mathbf{H}_{\widehat{I}} = 2^{n-2} \mathbf{H}_{\widehat{I}} \left(/ \{I\} \right). \quad (130)$$

For example, the data of Eqs. 114 and 115 are alternatively analyzed in accord with Eq. 127, which is calculated for characterizing this case as follows:

$$\widehat{\mathbf{D}}_{4h} \left(/ \mathbf{D}_{4\sigma}^{\widetilde{\sigma}_{15}} \right) \downarrow \mathbf{D}_{4h\sigma\widehat{I}}^{\widetilde{\sigma}_{15}} = 4 \mathbf{D}_{4h\sigma\widehat{I}}^{\widetilde{\sigma}_{15}} \left(/ \mathbf{D}_{4\sigma}^{\widetilde{\sigma}_{15}} \right), \quad (131)$$

where we put $\widehat{\mathbf{D}}_{4h\tilde{\sigma}\tilde{I}}^{\tilde{\sigma}_{15}} = \overset{\times}{\mathbf{D}}_{4\sigma}^{\tilde{\sigma}_{15}} + \widehat{\overset{\times}{\mathbf{I}}\mathbf{D}}_{4\sigma}^{\tilde{\sigma}_{15}}$ in accord with Eq. 125. In addition, Eqs. 129 and 130 are applied to this case to give the following subductions:

$$\widehat{\mathbf{D}}_{4h} \left(/ \overset{\times}{\mathbf{D}}_{4\sigma}^{\tilde{\sigma}_{15}} \right) \downarrow \mathbf{H}_{\sigma\tilde{I}}^{\tilde{\sigma}_{15}} = 4\mathbf{H}_{\sigma\tilde{I}}^{\tilde{\sigma}_{15}} \left(/ \overset{\times}{\mathbf{H}}_{\sigma}^{\tilde{\sigma}_{15}} \right) \tag{132}$$

$$\widehat{\mathbf{D}}_{4h} \left(/ \overset{\times}{\mathbf{D}}_{4\sigma}^{\tilde{\sigma}_{15}} \right) \downarrow \mathbf{H}_{\tilde{I}} = 4\mathbf{H}_{\tilde{I}} \left(/ \{I\} \right), \tag{133}$$

where we put $\mathbf{H}_{\sigma\tilde{I}}^{\tilde{\sigma}_{15}} = \overset{\times}{\mathbf{H}}_{\sigma}^{\tilde{\sigma}_{15}} + \widehat{\overset{\times}{\mathbf{I}}\mathbf{H}}_{\sigma}^{\tilde{\sigma}_{15}}$ in accord with Eq. 128. For the sake of simplicity, Eq. 132 is applied to the eight cosets governed by the coset representation $\widehat{\mathbf{D}}_{4h} \left(/ \overset{\times}{\mathbf{D}}_{4\sigma}^{\tilde{\sigma}_{15}} \right)$ so that the cosets are converted into one another by the multiplication of each operation of Eq. 132 as follows:

$\downarrow \overset{\times}{\mathbf{H}}_{\sigma\tilde{I}}^{\tilde{\sigma}_{15}}$	$\overset{\times}{\mathbf{D}}_{4\sigma}^{\tilde{\sigma}_{15}}$	$\widehat{\overset{\times}{\mathbf{I}}\mathbf{D}}_{4\sigma}^{\tilde{\sigma}_{15}}$	$\tilde{\sigma}_{26}\overset{\times}{\mathbf{D}}_{4\sigma}^{\tilde{\sigma}_{15}}$	$\tilde{\sigma}_{26}\widehat{\overset{\times}{\mathbf{I}}\mathbf{D}}_{4\sigma}^{\tilde{\sigma}_{15}}$	$\tilde{\sigma}_{37}\overset{\times}{\mathbf{D}}_{4\sigma}^{\tilde{\sigma}_{15}}$	$\tilde{\sigma}_{37}\widehat{\overset{\times}{\mathbf{I}}\mathbf{D}}_{4\sigma}^{\tilde{\sigma}_{15}}$	$\tilde{\sigma}_{48}\overset{\times}{\mathbf{D}}_{4\sigma}^{\tilde{\sigma}_{15}}$	$\tilde{\sigma}_{48}\widehat{\overset{\times}{\mathbf{I}}\mathbf{D}}_{4\sigma}^{\tilde{\sigma}_{15}}$
$\times I$	1	2	3	4	5	6	7	8
$\times \tilde{\sigma}_{15}$	1	2	3	4	5	6	7	8
$\times \sigma$	1	2	3	4	5	6	7	8
$\times \tilde{\sigma}_{15}\sigma$	1	2	3	4	5	6	7	8
$\times \tilde{I}$	2	1	4	3	6	5	8	7
$\times \widehat{\tilde{I}}\tilde{\sigma}_{15}$	2	1	4	3	6	5	8	7
$\times \widehat{\tilde{I}}\sigma$	2	1	4	3	6	5	8	7
$\times \widehat{\tilde{I}}\tilde{\sigma}_{15}\sigma$	2	1	4	3	6	5	8	7

(134)

As a result, the eight cosets numbered sequentially are divided according to Eq. 132 so as to generate four ($= 2^{4-2}$) orbits governed by the coset representation $\mathbf{H}_{\sigma\tilde{I}}^{\tilde{\sigma}_{15}} \left(/ \overset{\times}{\mathbf{H}}_{\sigma}^{\tilde{\sigma}_{15}} \right)$, i.e., {1, 2}, {3, 4}, {5, 6}, and {7, 8}. This division is interpreted to be equal to Eq. 131. Thereby, the data of Eqs. 114 and 115 are rearranged to generate four orbits governed by the coset representation $\mathbf{D}_{4h\tilde{\sigma}\tilde{I}}^{\tilde{\sigma}_{15}} \left(/ \overset{\times}{\mathbf{D}}_{4\sigma}^{\tilde{\sigma}_{15}} \right)$.

$$\widehat{\mathbf{D}}_{4h} = \overset{\times}{\mathbf{D}}_{4h\tilde{\sigma}\tilde{I}}^{\tilde{\sigma}_{15}} + \tilde{\sigma}_{26}\overset{\times}{\mathbf{D}}_{4h\tilde{\sigma}\tilde{I}}^{\tilde{\sigma}_{15}} + \tilde{\sigma}_{37}\overset{\times}{\mathbf{D}}_{4h\tilde{\sigma}\tilde{I}}^{\tilde{\sigma}_{15}} + \tilde{\sigma}_{48}\overset{\times}{\mathbf{D}}_{4h\tilde{\sigma}\tilde{I}}^{\tilde{\sigma}_{15}} \tag{135}$$

$$= \left\{ \begin{matrix} \overset{\times}{\mathbf{D}}_{4\sigma}^{\tilde{\sigma}_{15}} + \widehat{\overset{\times}{\mathbf{I}}\mathbf{D}}_{4\sigma}^{\tilde{\sigma}_{15}} \\ \underline{1, \bar{1}, 2, \bar{2}} \quad \underline{8, \bar{8}, 9, \bar{9}} \end{matrix} \right\} + \left\{ \begin{matrix} \tilde{\sigma}_{26}\overset{\times}{\mathbf{D}}_{4\sigma}^{\tilde{\sigma}_{15}} + \tilde{\sigma}_{26}\widehat{\overset{\times}{\mathbf{I}}\mathbf{D}}_{4\sigma}^{\tilde{\sigma}_{15}} \\ \underline{10, \bar{10}, 16, \bar{16}} \quad \underline{11, \bar{11}, 17, \bar{17}} \end{matrix} \right\} \\ + \left\{ \begin{matrix} \tilde{\sigma}_{37}\overset{\times}{\mathbf{D}}_{4\sigma}^{\tilde{\sigma}_{15}} + \tilde{\sigma}_{37}\widehat{\overset{\times}{\mathbf{I}}\mathbf{D}}_{4\sigma}^{\tilde{\sigma}_{15}} \\ \underline{12, 12, 18, \bar{18}} \quad \underline{13, \bar{13}, 19, \bar{19}} \end{matrix} \right\} + \left\{ \begin{matrix} \tilde{\sigma}_{48}\overset{\times}{\mathbf{D}}_{4\sigma}^{\tilde{\sigma}_{15}} + \tilde{\sigma}_{48}\widehat{\overset{\times}{\mathbf{I}}\mathbf{D}}_{4\sigma}^{\tilde{\sigma}_{15}} \\ \underline{14, 14, 20, \bar{20}} \quad \underline{15, \bar{15}, 21, \bar{21}} \end{matrix} \right\}. \tag{136}$$

Note that Eq. 135 is identical with Eq. 114. The coset representation $\mathbf{D}_{4h\tilde{\sigma}\hat{I}}^{\tilde{\sigma}_{15}} \left(/ \mathbf{D}_{4\sigma}^{\tilde{\sigma}_{15}} \right)$ indicates the relationships between the cosets of Eq. 135 and those of Eq. 136. Thus, the coset $\mathbf{D}_{4h\tilde{\sigma}\hat{I}}^{\tilde{\sigma}_{15}}$ (Eq. 135) is divided into $\mathbf{D}_{4\sigma}^{\tilde{\sigma}_{15}}$ and $\widehat{\mathbf{I}}\mathbf{D}_{4\sigma}^{\tilde{\sigma}_{15}}$ (Eq. 136) and so on. In other words, an epimeric stereoisogram is paired with an holantimeric stereoisogram in accord with $\mathbf{D}_{4\sigma}^{\tilde{\sigma}_{15}}$ and $\widehat{\mathbf{I}}\mathbf{D}_{4\sigma}^{\tilde{\sigma}_{15}}$.

The result shown in Eq. 136 provides us with an alternative interpretation of the correlation diagram of stereoisograms shown in Fig. 7a. Thus, each pair parenthesized by braces represents an orbit governed by the coset representation $\mathbf{D}_{4h\tilde{\sigma}\hat{I}}^{\tilde{\sigma}_{15}} \left(/ \mathbf{D}_{4\sigma}^{\tilde{\sigma}_{15}} \right)$, which shows a set of two types of stereoisograms, i.e., an epimeric stereoisogram (e.g., the coset $\mathbf{D}_{4\sigma}^{\tilde{\sigma}_{15}}$ for a quadruplet $\mathbf{1}_1, \bar{\mathbf{1}}_1, \mathbf{2}_1, \bar{\mathbf{2}}_1$) and a holantimeric one (e.g., the coset $\widehat{\mathbf{I}}\mathbf{D}_{4\sigma}^{\tilde{\sigma}_{15}}$ for a quadruplet $\mathbf{8}_1, \bar{\mathbf{8}}_1, \mathbf{9}_1, \bar{\mathbf{9}}_1$). Although the two types of stereoisograms should be depicted separately as exemplified in Fig. 5a and b, they are illustrated by a single stereoisogram in Fig. 7a (e.g. Stereoisogram #1) for the sake of saving space.

The data of Eqs. 116 and 117 are rearranged in accord with Eq. 127 so as to generate four orbits ($= 2^{4-2}$), each of which is governed by the coset representation $\mathbf{D}_{4h\tilde{\sigma}\hat{I}}^{\tilde{\sigma}_{26}} \left(/ \mathbf{D}_{4\sigma}^{\tilde{\sigma}_{26}} \right)$ of degree 2.

$$\widehat{\mathbf{D}}_{4h} = \mathbf{D}_{4h\tilde{\sigma}\hat{I}}^{\tilde{\sigma}_{26}} + \tilde{\sigma}_{15} \mathbf{D}_{4h\tilde{\sigma}\hat{I}}^{\tilde{\sigma}_{26}} + \tilde{\sigma}_{37} \mathbf{D}_{4h\tilde{\sigma}\hat{I}}^{\tilde{\sigma}_{26}} + \tilde{\sigma}_{48} \mathbf{D}_{4h\tilde{\sigma}\hat{I}}^{\tilde{\sigma}_{26}} \quad (137)$$

$$= \left\{ \underbrace{\mathbf{D}_{4\sigma}^{\tilde{\sigma}_{26}}}_{\mathbf{1}, \bar{\mathbf{1}}, \mathbf{10}, \bar{\mathbf{10}}} + \underbrace{\widehat{\mathbf{I}}\mathbf{D}_{4\sigma}^{\tilde{\sigma}_{26}}}_{\mathbf{8}, \bar{\mathbf{8}}, \mathbf{11}, \bar{\mathbf{11}}} \right\} + \left\{ \underbrace{\tilde{\sigma}_{15} \mathbf{D}_{4\sigma}^{\tilde{\sigma}_{26}} + \tilde{\sigma}_{26} \widehat{\mathbf{I}}\mathbf{D}_{4\sigma}^{\tilde{\sigma}_{26}}}_{\mathbf{2}, \bar{\mathbf{2}}, \mathbf{16}, \bar{\mathbf{16}}} + \underbrace{\tilde{\sigma}_{37} \mathbf{D}_{4\sigma}^{\tilde{\sigma}_{26}} + \tilde{\sigma}_{48} \widehat{\mathbf{I}}\mathbf{D}_{4\sigma}^{\tilde{\sigma}_{26}}}_{\mathbf{14}, \bar{\mathbf{14}}, \mathbf{18}, \bar{\mathbf{18}}} \right\} + \left\{ \underbrace{\tilde{\sigma}_{37} \mathbf{D}_{4\sigma}^{\tilde{\sigma}_{26}} + \tilde{\sigma}_{48} \widehat{\mathbf{I}}\mathbf{D}_{4\sigma}^{\tilde{\sigma}_{26}}}_{\mathbf{12}, \bar{\mathbf{12}}, \mathbf{20}, \bar{\mathbf{20}}} + \underbrace{\tilde{\sigma}_{15} \mathbf{D}_{4\sigma}^{\tilde{\sigma}_{26}} + \tilde{\sigma}_{26} \widehat{\mathbf{I}}\mathbf{D}_{4\sigma}^{\tilde{\sigma}_{26}}}_{\mathbf{13}, \bar{\mathbf{13}}, \mathbf{21}, \bar{\mathbf{21}}} \right\} + \left\{ \underbrace{\tilde{\sigma}_{15} \mathbf{D}_{4\sigma}^{\tilde{\sigma}_{26}} + \tilde{\sigma}_{26} \widehat{\mathbf{I}}\mathbf{D}_{4\sigma}^{\tilde{\sigma}_{26}}}_{\mathbf{9}, \bar{\mathbf{9}}, \mathbf{17}, \bar{\mathbf{17}}} + \underbrace{\tilde{\sigma}_{37} \mathbf{D}_{4\sigma}^{\tilde{\sigma}_{26}} + \tilde{\sigma}_{48} \widehat{\mathbf{I}}\mathbf{D}_{4\sigma}^{\tilde{\sigma}_{26}}}_{\mathbf{15}, \bar{\mathbf{15}}, \mathbf{19}, \bar{\mathbf{19}}} \right\} \quad (138)$$

where a pair parenthesized by braces represents each one of the four orbits and corresponds to a set of an epimeric stereoisogram and a holantimeric one. These data provide us with an alternative interpretation of the correlation diagram of stereoisograms shown in Fig. 7b.

On a similar line, the data of Eqs. 119 and 121 are rearranged in accord with Eq. 127 so that the results enable us to obtain alternative interpretations of the correlation diagrams shown in Fig. 7c and d.

4.2 Coincidence of epimeric and holantimeric stereoisograms

4.2.1 Functions for determining stereoisomers with achiral substituents only

Because an epimeric stereoisogram and its holantimeric counterpart appear pairwise, each pair of such stereoisograms can be treated as a single entity. This type of treatment is versatile to discuss special cases having achiral substituents only, because each pair is reduced into a single stereoisogram.

Let us consider a function having the following components:

$$\begin{aligned} f(1) &= \text{Br}, f(2) = \text{Cl}, f(3) = \text{F}, f(4) = \text{F}, \\ f(5) &= \text{H}, f(6) = \text{H}, f(7) = \text{H}, f(8) = \text{H}, \end{aligned} \quad (139)$$

which produces chiral stereoisomers of 1-bromo-2-chloro-3,4-difluorocyclobutane. They are depicted in Fig. 8.

The molecule **22** is generated by applying the function Eq. 139 to the stereoskeleton **1**. The molecule **22** belongs to C_1 , which is a subgroup of the molecular-symmetry group D_{4h} assigned to the stereoskeleton **1**. The corresponding enantiomer $\overline{\mathbf{22}}$ also belongs to C_1 . The pair of **22** and $\overline{\mathbf{22}}$ is regarded as a single entity of $\overline{C_s}$, which is a subgroup of D_{4h} . Moreover, a quadruplet of stereoisomers (e.g., **22**, $\overline{\mathbf{22}}$, **23** and $\overline{\mathbf{23}}$) is regarded as a single entity of $C_{s\tilde{\sigma}\tilde{I}}$ ($\subset D_{4h\tilde{\sigma}\tilde{I}}$). Similarly, the other stereoisomeric molecules collected in Fig. 8 are obtained by applying the function Eq. 139 to the stereoskeletons shown in Fig. 4. Each of the stereoisograms collected in Fig. 8 belongs to the *RS*-stereoisomeric group $C_{s\tilde{\sigma}\tilde{I}}$ and is categorized to Type I [16]. In spite of the symmetry reduction, the action of the multiple epimerization group \tilde{H} (Eq. 77) and its derived group (Eq. 94) are also effective to examine the stereoisomerism of such a C_1 -promolecule.

As exemplified by this case (Fig. 8), stereoisomers with achiral substituents only correspond to main stereoisograms of Type I. The Type I nature of each stereoisogram produces remarkable features of correlation diagrams of epimeric stereoisograms, which can be discussed in general by pairing a promolecule with its holantimer.

4.2.2 Global symmetries for special cases

When all substituents are achiral in isolation, a molecule is identical with its holantimer (i.e., a self-holantimer) so that they are identical under the action of $G_{C\tilde{I}}$ (Eq. 13). To treat such cases, we adopt the coset representation of degree 2, i.e., $G_{C\sigma\tilde{\sigma}\tilde{I}} \left(/ \overset{\times}{G_{C\tilde{I}}} \right)$, which is derived from Eq. 103. Each of the two cosets relevant to the degree 2 corresponds to a pair of skeletons to give a molecule (and its self-holantimer).

The stereoisomeric group defined by Eq. 80 is represented by the following coset decomposition:

$$\widehat{G}_{C\sigma} = \tilde{H} \times G_{C\sigma} = \left[\prod_{i=1}^n (I + \tilde{\sigma}_i) \right] \times G_{C\sigma} = \left[\prod_{i=1}^n (I + \tilde{\sigma}_i) \right] \times G_{C\tilde{I}}$$

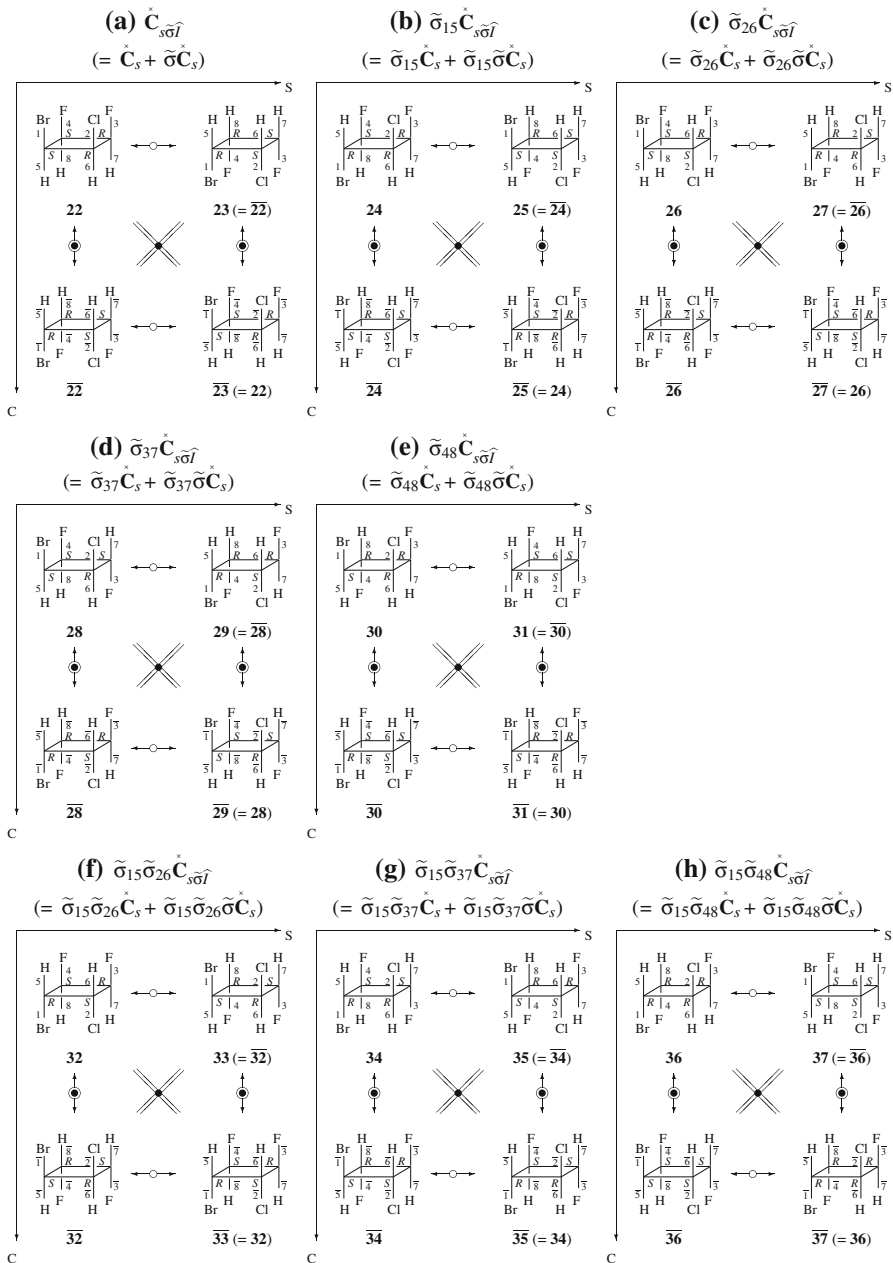


Fig. 8 Main stereoisograms for specifying stereoisomeric 1-bromo-2-chloro-3,4-difluorocyclobutanes. All of the stereoisograms belong to Type I

$$= \left[\prod_{i=1}^n (I + \tilde{\sigma}_i) \right] \times \mathbf{G}_{C\hat{T}}, \tag{140}$$

where the number of cosets contained in the last side is calculated to be 2^n , which is equal to the order of the multiple epimerization group $\tilde{\mathbf{H}}$ (Eq. 78). Note that Eq. 140 is based on two alternative ways for defining the stereoisomeric group $\widehat{\mathbf{G}}_{C\sigma}$, i.e.,

$$\widehat{\mathbf{G}}_{C\sigma} = \tilde{\mathbf{H}} \times \mathbf{G}_{C\sigma} = \tilde{\mathbf{H}} \times \mathbf{G}_{C\hat{I}}, \tag{141}$$

which is correlated to the following relationship:

$$\left[\prod_{i=1}^n (I + \tilde{\sigma}_i) \right] \sigma = \left[\prod_{i=1}^n (I + \tilde{\sigma}_i) \right] \tilde{\sigma} \hat{I} = \left[\prod_{i=1}^n (I + \tilde{\sigma}_i) \right] \hat{I}, \tag{142}$$

where we use Eq. 16 by keeping Eq. 80 in mind. As a result, Eq. 140 can be regarded as a coset decomposition of $\widehat{\mathbf{G}}_{C\sigma}$ by $\overset{\times}{\mathbf{G}}_{C\hat{I}}$ so as to generate a coset representation $\widehat{\mathbf{G}}_{C\sigma} \left(/ \overset{\times}{\mathbf{G}}_{C\hat{I}} \right)$, the degree of which is equal to the number of cosets, i.e., 2^n . The degree 2^n is calculated by starting from the orders of the relevant groups, i.e., $|\widehat{\mathbf{G}}_{C\sigma}| = 2^n |\overset{\times}{\mathbf{G}}_{C\hat{I}}|$.

By following Fujita’s USCI approach [13], let us consider the subduction of the coset representation $\widehat{\mathbf{G}}_{C\sigma} \left(/ \overset{\times}{\mathbf{G}}_{C\hat{I}} \right)$ by the *RS*-stereoisomeric group $\mathbf{G}_{C\sigma\tilde{\sigma}\hat{I}}$. Thereby, we obtain the following equation:

$$\widehat{\mathbf{G}}_{C\sigma} \left(/ \overset{\times}{\mathbf{G}}_{C\hat{I}} \right) \downarrow \mathbf{G}_{C\sigma\tilde{\sigma}\hat{I}} = 2^{n-1} \mathbf{G}_{C\sigma\tilde{\sigma}\hat{I}} \left(/ \overset{\times}{\mathbf{G}}_{C\hat{I}} \right), \tag{143}$$

where the coefficient 2^{n-1} is calculated by using $|\widehat{\mathbf{G}}_{C\sigma}| = 2^n |\overset{\times}{\mathbf{G}}_{C\sigma}|$, $|\overset{\times}{\mathbf{G}}_{C\hat{I}}| = |\overset{\times}{\mathbf{G}}_{C\sigma}|$, and $|\mathbf{G}_{C\sigma\tilde{\sigma}\hat{I}}| = 2 |\overset{\times}{\mathbf{G}}_{C\sigma}|$. Note that the coset representation $\mathbf{G}_{C\sigma\tilde{\sigma}\hat{I}} \left(/ \overset{\times}{\mathbf{G}}_{C\hat{I}} \right)$ is of degree 2.

The stereoisogram group \mathbf{H}_s (Eq. 21) and its subgroup $\mathbf{H}_{\hat{I}}$ (Eq. 18) generate a coset representation $\mathbf{H}_s (/ \mathbf{H}_{\hat{I}})$, which can be used in place of $\overset{\times}{\mathbf{G}}_{C\sigma\tilde{\sigma}\hat{I}} \left(/ \overset{\times}{\mathbf{G}}_{C\hat{I}} \right)$ because the omission of $\overset{\times}{\mathbf{G}}_{C\sigma}$ is allowed without losing generality. Thereby Eq. 143 is simplified to give:

$$\widehat{\mathbf{G}}_{C\sigma} \left(/ \overset{\times}{\mathbf{G}}_{C\hat{I}} \right) \downarrow \mathbf{H}_s = 2^{n-1} \mathbf{H}_s (/ \mathbf{H}_{\hat{I}}), \tag{144}$$

where the coset representation $\mathbf{H}_s (/ \mathbf{H}_{\hat{I}})$ is equalized to the corresponding direct-product expression $\mathbf{H}_s (/ \overset{\times}{\mathbf{H}}_{\hat{I}})$.

The meaning of Eq. 143 is that 2^n holantimeric pairs governed by $\widehat{\mathbf{G}}_{C\sigma} \left(/ \overset{\times}{\mathbf{G}}_{C\hat{I}} \right)$ are divided into 2^{n-1} quadruplets of *RS*-stereoisomers governed by $\mathbf{G}_{C\sigma\tilde{\sigma}\hat{I}} \left(/ \overset{\times}{\mathbf{G}}_{C\hat{I}} \right)$. The coset representation $\mathbf{G}_{C\sigma\tilde{\sigma}\hat{I}} \left(/ \overset{\times}{\mathbf{G}}_{C\hat{I}} \right)$ means that each quadruplet is regarded as being composed of two holantimeric pairs belonging to $\overset{\times}{\mathbf{G}}_{C\hat{I}}$. The two holantimeric pairs are enantiomeric and *RS*-diastereomeric to each other (cf. Eqs. 102 and 103). Each holantimeric pair belonging to $\overset{\times}{\mathbf{G}}_{C\hat{I}}$ represents a single molecule if only achiral substituents are taken into consideration. It should be emphasized that the 2^{n-1} quadruplets of *RS*-stereoisomers, each of which is governed by $\mathbf{G}_{C\sigma\tilde{\sigma}\hat{I}} \left(/ \overset{\times}{\mathbf{G}}_{C\hat{I}} \right)$, appear as stereoisograms in a main correlation diagrams of stereoisograms. The 2^{n-1} stereoisograms are transitive under the action of $\widehat{\mathbf{G}}_{C\sigma} \left(/ \overset{\times}{\mathbf{G}}_{C\hat{I}} \right)$ while each of them is fixed under the action of the *RS*-stereoisomeric group $\mathbf{G}_{C\sigma\tilde{\sigma}\hat{I}}$.

For example, Eq. 101 is interpreted by the procedure described in the preceding paragraphs. Thus, Eqs. 143 and 144 are applied to this case so as to give the following subductions:

$$\widehat{\mathbf{D}}_{4h} \left(/ \overset{\times}{\mathbf{D}}_{4\hat{I}} \right) \downarrow \mathbf{D}_{4h\tilde{\sigma}\hat{I}} = 8\mathbf{D}_{4h\tilde{\sigma}\hat{I}} \left(/ \overset{\times}{\mathbf{D}}_{4\hat{I}} \right) \quad (145)$$

$$\widehat{\mathbf{D}}_{4h} \left(/ \overset{\times}{\mathbf{D}}_{4\hat{I}} \right) \downarrow \mathbf{H}_s = 8\mathbf{H}_s \left(/ \mathbf{H}_{\hat{I}} \right). \quad (146)$$

Thereby, each of the eight cosets contained in Eq. 101 is divided into two cosets governed by $\mathbf{D}_{4h\tilde{\sigma}\hat{I}} \left(/ \overset{\times}{\mathbf{D}}_{4\hat{I}} \right)$ in accord with Eq. 145.

$$\begin{aligned} \widehat{\mathbf{D}}_{4h} &= \overset{\times}{\mathbf{D}}_{4h\tilde{\sigma}\hat{I}} + \tilde{\sigma}_{15}\overset{\times}{\mathbf{D}}_{4h\tilde{\sigma}\hat{I}} + \tilde{\sigma}_{26}\overset{\times}{\mathbf{D}}_{4h\tilde{\sigma}\hat{I}} + \tilde{\sigma}_{37}\overset{\times}{\mathbf{D}}_{4h\tilde{\sigma}\hat{I}} + \tilde{\sigma}_{48}\overset{\times}{\mathbf{D}}_{4h\tilde{\sigma}\hat{I}} \\ &\quad + \tilde{\sigma}_{15}\tilde{\sigma}_{26}\overset{\times}{\mathbf{D}}_{4h\tilde{\sigma}\hat{I}} + \tilde{\sigma}_{15}\tilde{\sigma}_{37}\overset{\times}{\mathbf{D}}_{4h\tilde{\sigma}\hat{I}} + \tilde{\sigma}_{15}\tilde{\sigma}_{48}\overset{\times}{\mathbf{D}}_{4h\tilde{\sigma}\hat{I}}, \quad (147) \\ &= \left\{ \begin{array}{c} \overset{\times}{\mathbf{D}}_{4\hat{I}} + \sigma\overset{\times}{\mathbf{D}}_{4\hat{I}} \\ \underline{1,8} \quad \underline{1,8} \end{array} \right\} + \left\{ \begin{array}{c} \tilde{\sigma}_{15}\overset{\times}{\mathbf{D}}_{4\hat{I}} + \tilde{\sigma}_{15}\sigma\overset{\times}{\mathbf{D}}_{4\hat{I}} \\ \underline{2,9} \quad \underline{2,9} \end{array} \right\} \\ &\quad + \left\{ \begin{array}{c} \tilde{\sigma}_{26}\overset{\times}{\mathbf{D}}_{4\hat{I}} + \tilde{\sigma}_{26}\sigma\overset{\times}{\mathbf{D}}_{4\hat{I}} \\ \underline{10,11} \quad \underline{10,11} \end{array} \right\} + \left\{ \begin{array}{c} \tilde{\sigma}_{37}\overset{\times}{\mathbf{D}}_{4\hat{I}} + \tilde{\sigma}_{37}\sigma\overset{\times}{\mathbf{D}}_{4\hat{I}} \\ \underline{12,13} \quad \underline{12,13} \end{array} \right\} + \left\{ \begin{array}{c} \tilde{\sigma}_{48}\overset{\times}{\mathbf{D}}_{4\hat{I}} + \tilde{\sigma}_{48}\sigma\overset{\times}{\mathbf{D}}_{4\hat{I}} \\ \underline{14,15} \quad \underline{14,15} \end{array} \right\} \\ &\quad + \left\{ \begin{array}{c} \tilde{\sigma}_{15}\tilde{\sigma}_{26}\overset{\times}{\mathbf{D}}_{4\hat{I}} + \tilde{\sigma}_{15}\tilde{\sigma}_{26}\sigma\overset{\times}{\mathbf{D}}_{4\hat{I}} \\ \underline{16,17} \quad \underline{16,17} \end{array} \right\} + \left\{ \begin{array}{c} \tilde{\sigma}_{15}\tilde{\sigma}_{37}\overset{\times}{\mathbf{D}}_{4\hat{I}} + \tilde{\sigma}_{15}\tilde{\sigma}_{37}\sigma\overset{\times}{\mathbf{D}}_{4\hat{I}} \\ \underline{18,19} \quad \underline{18,19} \end{array} \right\} \end{aligned}$$

$$+ \left\{ \underbrace{\tilde{\sigma}_{15}\tilde{\sigma}_{48}\overset{\times}{\mathbf{D}}_{4\hat{T}}}_{20, \bar{2}\bar{1}} + \underbrace{\tilde{\sigma}_{15}\tilde{\sigma}_{48}\sigma\overset{\times}{\mathbf{D}}_{4\hat{T}}}_{20, 21} \right\}, \quad (148)$$

where Eq. 147 is identical with Eq. 101. Comparison between Eq. 147 (Eq. 101) and Eq. 148 indicates the meaning of Eq. 145. Thus, eight parenthesized couples of two cosets contained in Eq. 148 correspond to eight-times appearance of the coset representations $\mathbf{D}_{4h\tilde{\sigma}\hat{T}}(\overset{\times}{\mathbf{D}}_{4\hat{T}})$ in the right-hand side of Eq. 145. As found easily, these couples of two cosets contained in Eq. 148 correspond to the stereoisograms of Fig. 4a–h. Their transitivity is depicted in the main correlation diagram shown in Fig. 6. Because each of the eight couples belongs to the group $\overset{\times}{\mathbf{D}}_{4\hat{T}}$ contained in the coset representation $\widehat{\mathbf{D}}_{4h}(\overset{\times}{\mathbf{D}}_{4\hat{T}})$, they are transitive under the action of $\widehat{\mathbf{D}}_{4h}(\overset{\times}{\mathbf{D}}_{4\hat{T}})$. After the subduction into $\mathbf{D}_{4h\tilde{\sigma}\hat{T}}$ (Eq. 145), their transitivity is, on the other hand, reduced to permit changeability only under the action of $\mathbf{D}_{4h\tilde{\sigma}\hat{T}}(\overset{\times}{\mathbf{D}}_{4\hat{T}})$.

As shown by the groups $\overset{\times}{\mathbf{G}}_{C\hat{T}}$ (Eq. 143) and $\mathbf{H}_{\hat{T}}$ (Eq. 144), the Eqs. 143 and 144 are concerned with holantimeric pairs as well as with self-holantimeric pairs for characterizing stereoskeletons. For example, Eq. 148 for a cyclobutane stereoskeleton contains the group $\overset{\times}{\mathbf{D}}_{4\hat{T}}$ corresponding to a holantimeric pair of stereoskeletons, **1** and $\bar{\mathbf{8}}$.

The derivations of cyclobutane derivatives on the basis of such stereoskeletons as **1** and $\bar{\mathbf{8}}$ are categorized to five types by following Fujita's formulation [16]. Let us examine the five types by paying attention to holantimeric relationships appearing in Fig. 4.

1. When the function represented by Eq. 139 is applied to the holantimeric pair **1** and $\bar{\mathbf{8}}$, there emerge a self-holantimeric pair of **22** and $\bar{\mathbf{23}}$ (=22), which are identical with each other, as shown in Fig. 8a. As a result, the stereoisogram of Fig. 8a belongs to Type I. All of the relevant stereoisograms collected in Fig. 8 belongs also to Type I.
2. When the function represented by Eq. 10 is applied to the holantimeric pair **1** and $\bar{\mathbf{8}}$, there emerge a pair of holantimers, which are different from each other (cf. **6** and $\bar{\mathbf{6}}$ for the corresponding enantiomeric pair). The corresponding stereoisogram belongs to Type II.
3. When the function represented by Eq. 8 is applied to the holantimeric pair **1** and $\bar{\mathbf{8}}$, there emerge a pair of holantimers, which are different from each other (cf. **5** and $\bar{\mathbf{5}}$ for the corresponding enantiomeric pair). The corresponding stereoisogram belongs to Type III.
4. When the function represented by Eq. 11 is applied to the holantimeric pair **1** and $\bar{\mathbf{8}}$, there emerge an self-enantiomeric pair, which indicates a single molecule (i.e., cyclobutane itself; cf. **7**). The corresponding stereoisogram belongs to Type IV.
5. The remaining type is generated, for example, by the following function:

$$\begin{aligned} f(1) &= \mathbf{a}, f(2) = \text{Cl}, f(3) = \text{H}, f(4) = \text{H}, \\ f(5) &= \bar{\mathbf{a}}, f(6) = \text{Cl}, f(7) = \text{H}, f(8) = \text{H}. \end{aligned} \quad (149)$$

By applying this function to the holantimeric pair **1** and $\bar{\mathbf{8}}$, there emerge a pair of holantimers, which are different from each other. This case exhibits pseudoasymmetry so that the corresponding stereoisogram belongs to Type V.

When all of the substituents are achiral, there appear stereoisograms of Types I and IV for investigating stereoisomerism. As for the case of Eqs. 139, 148 is converted into the following equation:

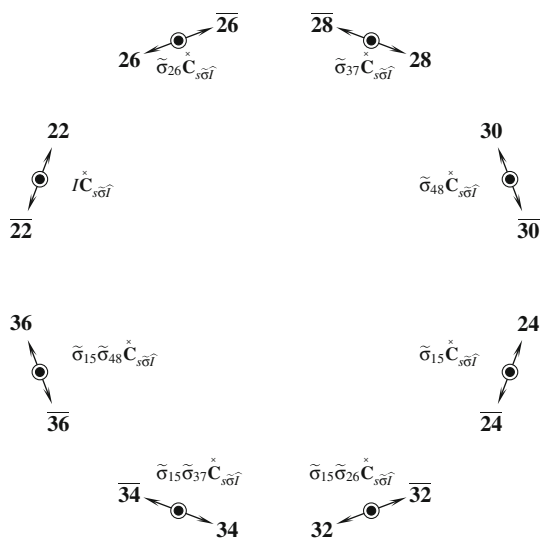
$$\begin{aligned}
 \widehat{\mathbf{C}}_s &= \overset{\times}{\mathbf{C}}_{s\bar{\sigma}\hat{I}} + \tilde{\sigma}_{15}\overset{\times}{\mathbf{C}}_{s\bar{\sigma}\hat{I}} + \tilde{\sigma}_{26}\overset{\times}{\mathbf{C}}_{s\bar{\sigma}\hat{I}} + \tilde{\sigma}_{37}\overset{\times}{\mathbf{C}}_{s\bar{\sigma}\hat{I}} + \tilde{\sigma}_{48}\overset{\times}{\mathbf{C}}_{s\bar{\sigma}\hat{I}} \\
 &\quad + \tilde{\sigma}_{15}\tilde{\sigma}_{26}\overset{\times}{\mathbf{C}}_{s\bar{\sigma}\hat{I}} + \tilde{\sigma}_{15}\tilde{\sigma}_{37}\overset{\times}{\mathbf{C}}_{s\bar{\sigma}\hat{I}} + \tilde{\sigma}_{15}\tilde{\sigma}_{48}\overset{\times}{\mathbf{C}}_{s\bar{\sigma}\hat{I}}, \quad (150) \\
 &= \left\{ \overset{\times}{\mathbf{C}}_{\hat{I}} + \sigma\overset{\times}{\mathbf{C}}_{\hat{I}} \right\} + \left\{ \tilde{\sigma}_{15}\overset{\times}{\mathbf{C}}_{\hat{I}} + \tilde{\sigma}_{15}\sigma\overset{\times}{\mathbf{C}}_{\hat{I}} \right\} \\
 &\quad + \left\{ \tilde{\sigma}_{26}\overset{\times}{\mathbf{C}}_{\hat{I}} + \tilde{\sigma}_{26}\sigma\overset{\times}{\mathbf{C}}_{\hat{I}} \right\} + \left\{ \tilde{\sigma}_{37}\overset{\times}{\mathbf{C}}_{\hat{I}} + \tilde{\sigma}_{37}\sigma\overset{\times}{\mathbf{C}}_{\hat{I}} \right\} + \left\{ \tilde{\sigma}_{48}\overset{\times}{\mathbf{C}}_{\hat{I}} + \tilde{\sigma}_{48}\sigma\overset{\times}{\mathbf{C}}_{\hat{I}} \right\} \\
 &\quad + \left\{ \tilde{\sigma}_{15}\tilde{\sigma}_{26}\overset{\times}{\mathbf{C}}_{\hat{I}} + \tilde{\sigma}_{15}\tilde{\sigma}_{26}\sigma\overset{\times}{\mathbf{C}}_{\hat{I}} \right\} + \left\{ \tilde{\sigma}_{15}\tilde{\sigma}_{37}\overset{\times}{\mathbf{C}}_{\hat{I}} + \tilde{\sigma}_{15}\tilde{\sigma}_{37}\sigma\overset{\times}{\mathbf{C}}_{\hat{I}} \right\} \\
 &\quad + \left\{ \tilde{\sigma}_{15}\tilde{\sigma}_{48}\overset{\times}{\mathbf{C}}_{\hat{I}} + \tilde{\sigma}_{15}\tilde{\sigma}_{48}\sigma\overset{\times}{\mathbf{C}}_{\hat{I}} \right\}, \quad (151)
 \end{aligned}$$

because the resulting molecule (**22** of the \mathbf{C}_1 -point group) and its enantiomer ($\bar{\mathbf{22}}$ of the \mathbf{C}_1 -point group) construct an enantiomeric pair, which is tentatively regarded as a single entity (equivalence class) belonging to \mathbf{C}_s -point-group symmetry.

In the present context, the molecule **22** is regarded as belonging to the $\overset{\times}{\mathbf{C}}_{\hat{I}}$ group (cf. Eq. 151) and its enantiomer $\bar{\mathbf{22}}$ also regarded as belonging to the $\overset{\times}{\mathbf{C}}_{\hat{I}}$ group (cf. the coset $\sigma\overset{\times}{\mathbf{C}}_{\hat{I}}$ in Eq. 151). Hence, the corresponding stereoisogram (Fig. 8a) belongs to $\overset{\times}{\mathbf{C}}_{s\bar{\sigma}\hat{I}}$ (cf. Eq. 150), which is more specifically categorized into Type I. Note that $\overset{\times}{\mathbf{C}}_{s\bar{\sigma}\hat{I}}$ may involve cases of Types I, III, IV, and V (except Type II), because a quadruplet contained in a stereoisogram is regarded as an equivalence class to be recognized as a single entity under the present viewpoint.

The other stereoisograms listed in Fig. 8b–d can be discussed in a parallel way to Fig. 8a by referring to Eq. 151. As a result, the main correlation diagram for the stereoskeleton **1** and related stereoskeletons (Fig. 6) is converted to the counterpart for the derivative **22** and related stereoisomers, as shown in Fig. 9.

Fig. 9 Main correlation diagram for characterizing the global symmetries of 1-bromo-2-chloro-3,4-difluorocyclobutanes. Quadruplets of *RS*-stereoisomeric stereoskeletons (e.g., **22**, $\overline{\mathbf{22}}$, **23**, and $\overline{\mathbf{23}}$), whose stereoisograms are shown in Fig. 8, correspond to respective cosets appearing in Eq. 151



By comparison between Eq. 148 (for the cyclopropane skeleton) and Eq. 151 (for cyclopropane derivatives such as **22**), the action of $\mathbf{D}_{4\hat{I}}$ on **1** generates its homomers, just as the action of $\mathbf{C}_{\hat{I}}$ on **22** generates its homomers. More generally speaking to permit chiral substituents, the action of \mathbf{D}_4 on **1** generates its homomers, just as the action of \mathbf{C}_1 on **22** generates its homomer (the same entity in this case).

4.2.3 Local symmetries for special cases

To treat the local symmetries of the cases with achiral substituents only, we adopt the coset representation of degree 4, i.e., $\mathbf{G}_{C\sigma\hat{I}}^{\tilde{\sigma}_j} \left(/ \mathbf{G}_{C\hat{I}}^{\times} \right)$, which is derived from Eq. 63. Each of the four cosets relevant to the degree 4 corresponds to a pair of skeletons to give a molecule (and its self-holantimer).

Thereby, according to a similar procedure for deriving Eq. 111, we obtain the following subduction:

$$\widehat{\mathbf{G}}_{C\sigma} \left(/ \mathbf{G}_{C\hat{I}}^{\times} \right) \downarrow \mathbf{G}_{C\sigma\hat{I}}^{\tilde{\sigma}_j} = 2^{n-2} \mathbf{G}_{C\sigma\hat{I}}^{\tilde{\sigma}_j} \left(/ \mathbf{G}_{C\hat{I}}^{\times} \right), \quad (152)$$

where the coefficient 2^{n-2} is calculated by using $|\widehat{\mathbf{G}}_{C\sigma}| = 2^n |\mathbf{G}_{C\sigma}|$, $|\mathbf{G}_{C\hat{I}}^{\times}| = |\mathbf{G}_{C\sigma}|$, and $|\mathbf{G}_{C\sigma\hat{I}}^{\tilde{\sigma}_j}| = 2^2 |\mathbf{G}_{C\sigma}|$. Note that the coset representation $\mathbf{G}_{C\sigma\hat{I}}^{\tilde{\sigma}_j} \left(/ \mathbf{G}_{C\hat{I}}^{\times} \right)$ has degree 4.

According to a similar procedure for deriving Eq. 122, we obtain the following subduction:

$$\widehat{\mathbf{G}}_{C\sigma} \left(/ \overset{\times}{\mathbf{G}}_{C\hat{I}} \right) \downarrow \mathbf{H}_{\sigma}^{\tilde{\sigma}j} = 2^{n-2} \mathbf{H}_{\sigma}^{\tilde{\sigma}j} (/ \{I\}) \quad (153)$$

where the coset representation $\mathbf{H}_{\sigma}^{\tilde{\sigma}j} (/ \{I\})$ has degree 4 because of Eq. 48.

The discussions subsequent to Eq. 152 are summarized to give the following theorem:

Theorem 2 Suppose that 2^n holantimeric pairs each belonging to $\mathbf{G}_{C\hat{I}}$ are governed by the coset representation $\widehat{\mathbf{G}}_{C\sigma} \left(/ \overset{\times}{\mathbf{G}}_{C\hat{I}} \right)$, which is generated by Eq. 140. They are divided into 2^{n-2} stereoisograms of $\mathbf{G}_{C\sigma\tilde{\sigma}\hat{I}}^{\tilde{\sigma}j}$ (the local symmetry group of Definition 6), where each quadruplet in a stereoisogram is concerned with four holantimeric pairs. The 2^{n-2} stereoisograms construct an orbit governed by the coset representation $\widehat{\mathbf{G}}_{C\sigma} (/ \overset{\times}{\mathbf{G}}_{C\sigma\tilde{\sigma}\hat{I}}^{\tilde{\sigma}j})$. Each of the 2^{n-2} stereoisograms is governed by the coset representation $\mathbf{G}_{C\sigma\tilde{\sigma}\hat{I}}^{\tilde{\sigma}j} (/ \overset{\times}{\mathbf{G}}_{C\hat{I}})$ of degree 4 (cf. Eq. 63).

For example, the data of Eqs. 114 and 115 are alternatively analyzed in accord with Eq. 152, which is applied to this case to give the following equation:

$$\widehat{\mathbf{D}}_{4h} (/ \overset{\times}{\mathbf{D}}_{4\hat{I}}) \downarrow \mathbf{D}_{4h\tilde{\sigma}\hat{I}}^{\tilde{\sigma}15} = 4\mathbf{D}_{4h\tilde{\sigma}\hat{I}}^{\tilde{\sigma}15} (/ \overset{\times}{\mathbf{D}}_{4\hat{I}}), \quad (154)$$

where the coset representation in the right-hand side corresponds to the following coset decomposition:

$$\mathbf{D}_{4h\tilde{\sigma}\hat{I}}^{\tilde{\sigma}15} = \overset{\times}{\mathbf{D}}_{4\hat{I}} + \sigma \overset{\times}{\mathbf{D}}_{4\hat{I}} + \tilde{\sigma}_{15} \overset{\times}{\mathbf{D}}_{4\hat{I}} + \tilde{\sigma}_{15} \sigma \overset{\times}{\mathbf{D}}_{4\hat{I}}. \quad (155)$$

Note that the four cosets in the right-hand side of Eq. 155 correspond to four holantimeric pairs which are contained as the quadruplet of a stereoisogram at the C_j atom. Theorem 2 teaches us that sixteen ($= 2^4$) holantimeric pairs are divided into four stereoisograms, where the number 4 of the stereoisograms is confirmed by the coefficient 4 ($= 2^{4-2}$) appearing in the right-hand side of Eq. 154.

For practical purposes, a more simplified equation is derived from Eq. 153 as follows:

$$\widehat{\mathbf{D}}_{4h} (/ \overset{\times}{\mathbf{D}}_{4\hat{I}}) \downarrow \mathbf{H}_{\sigma}^{\tilde{\sigma}15} = 4\mathbf{H}_{\sigma}^{\tilde{\sigma}15} (/ \{I\}), \quad (156)$$

which is conveniently used in place of Eq. 154. The coset representation $\mathbf{H}_{\sigma}^{\tilde{\sigma}15} (/ \{I\})$ corresponds to the coset decomposition of the epimeric stereoisogram group (Eq. 48) by the identity group.

The stereoisogram corresponding to Eq. 155 is regarded as an initial stereoisogram, which is transformed under the action of $\widehat{\mathbf{D}}_{4h}$ so as to give four stereoisograms accord-

ing to Eq. 154 (cf. Theorem 2). Thereby, the data of Eqs. 114 and 115 are rearranged to generate four orbits governed by the coset representation $\mathbf{D}_{4h\tilde{\sigma}\hat{I}}^{\tilde{\sigma}_{15}}(/|\mathbf{D}_{4\hat{I}}^{\times})$.

$$\widehat{\mathbf{D}}_{4h} = \mathbf{D}_{4h\tilde{\sigma}\hat{I}}^{\tilde{\sigma}_{15}} + \tilde{\sigma}_{26}\mathbf{D}_{4h\tilde{\sigma}\hat{I}}^{\tilde{\sigma}_{15}} + \tilde{\sigma}_{37}\mathbf{D}_{4h\tilde{\sigma}\hat{I}}^{\tilde{\sigma}_{15}} + \tilde{\sigma}_{48}\mathbf{D}_{4h\tilde{\sigma}\hat{I}}^{\tilde{\sigma}_{15}} \tag{157}$$

$$= \left\{ \begin{array}{c} \mathbf{D}_{4\hat{I}}^{\times} \\ \underline{1,8} \end{array} + \underbrace{\sigma\mathbf{D}_{4\hat{I}}^{\times}}_{\underline{1,8}} + \underbrace{\tilde{\sigma}_{15}\mathbf{D}_{4\hat{I}}^{\times}}_{\underline{2,9}} + \underbrace{\tilde{\sigma}_{15}\sigma\mathbf{D}_{4\hat{I}}^{\times}}_{\underline{2,9}} \right\}$$

$$+ \left\{ \begin{array}{c} \tilde{\sigma}_{26}\mathbf{D}_{4\hat{I}}^{\times} \\ \underline{10,11} \end{array} + \begin{array}{c} \tilde{\sigma}_{26}\sigma\mathbf{D}_{4\hat{I}}^{\times} \\ \underline{10,11} \end{array} + \begin{array}{c} \tilde{\sigma}_{15}\tilde{\sigma}_{26}\mathbf{D}_{4\hat{I}}^{\times} \\ \underline{16,17} \end{array} + \begin{array}{c} \tilde{\sigma}_{15}\tilde{\sigma}_{26}\sigma\mathbf{D}_{4\hat{I}}^{\times} \\ \underline{16,17} \end{array} \right\}$$

$$+ \left\{ \begin{array}{c} \tilde{\sigma}_{37}\mathbf{D}_{4\hat{I}}^{\times} \\ \underline{12,13} \end{array} + \begin{array}{c} \tilde{\sigma}_{37}\sigma\mathbf{D}_{4\hat{I}}^{\times} \\ \underline{12,13} \end{array} + \begin{array}{c} \tilde{\sigma}_{15}\tilde{\sigma}_{37}\mathbf{D}_{4\hat{I}}^{\times} \\ \underline{18,19} \end{array} + \begin{array}{c} \tilde{\sigma}_{15}\tilde{\sigma}_{37}\sigma\mathbf{D}_{4\hat{I}}^{\times} \\ \underline{18,19} \end{array} \right\}$$

$$+ \left\{ \begin{array}{c} \tilde{\sigma}_{48}\mathbf{D}_{4\hat{I}}^{\times} \\ \underline{14,15} \end{array} + \begin{array}{c} \tilde{\sigma}_{48}\sigma\mathbf{D}_{4\hat{I}}^{\times} \\ \underline{14,15} \end{array} + \begin{array}{c} \tilde{\sigma}_{15}\tilde{\sigma}_{48}\mathbf{D}_{4\hat{I}}^{\times} \\ \underline{20,21} \end{array} + \begin{array}{c} \tilde{\sigma}_{15}\tilde{\sigma}_{48}\sigma\mathbf{D}_{4\hat{I}}^{\times} \\ \underline{20,21} \end{array} \right\}, \tag{158}$$

where $\mathbf{D}_{4h\tilde{\sigma}\hat{I}}^{\tilde{\sigma}_{15}}$ is equalized to $\mathbf{D}_{4h\tilde{\sigma}\hat{I}}^{\tilde{\sigma}_{15}}$ which appears in Eq. 155. Note that Eq. 157 is identical with Eq. 114, although they are interpreted differently.

According to Theorem 2, the four cosets appearing in Eq. 157 construct an orbit governed by the coset representation $\widehat{\mathbf{D}}_{4h}(/|\mathbf{D}_{4h\tilde{\sigma}\hat{I}}^{\tilde{\sigma}_{15}})$. The first coset $\mathbf{D}_{4h\tilde{\sigma}\hat{I}}^{\tilde{\sigma}_{15}}$ (Eq. 157) is divided into four cosets appearing in the first pair of braces in Eq. 158, where the four cosets are contained in an orbit governed by the coset representation $\mathbf{D}_{4h\tilde{\sigma}\hat{I}}^{\tilde{\sigma}_{15}}(/|\mathbf{D}_{4\hat{I}}^{\times})$. Similarly, each of the remaining cosets (Eq. 157) is divided into four cosets, as surrounded by a pair of braces in Eq. 158. They are also correlated to the coset representation $\mathbf{D}_{4h\tilde{\sigma}\hat{I}}^{\tilde{\sigma}_{15}}(/|\mathbf{D}_{4\hat{I}}^{\times})$. The value 4 is consistent with the degree of the coset representation because it is calculated to be $|\mathbf{D}_{4h\tilde{\sigma}\hat{I}}^{\tilde{\sigma}_{15}}|/|\mathbf{D}_{4\hat{I}}^{\times}| = (4 \times 2|\mathbf{D}_4|)/(2|\mathbf{D}_4|) = 4$.

The modes of division shown by Eq. 158 can be interpreted in a more detailed fashion. The four cosets in the first pair of braces of Eq. 158 (cf. Eq. 155) correspond to four holantimeric pairs of skeletons, i.e., $\underline{1,8}$, $\underline{1,8}$, $\underline{2,9}$, and $\underline{2,9}$. The four holantimeric pairs are correlated to Fig. 5, where the epimeric stereoisogram (Fig. 5a) and the holantimeric stereoisogram (Fig. 5b) are superposed. The superposed result has been already adopted in Stereoisogram #1 contained in the correlation diagram of Fig. 7a. The other parenthesized sets of four cosets in Eq. 158 can be also illustrated in a similar way so as to give Stereoisograms #2–#4 contained in the correlation diagram of Fig. 7a.

On a similar line, the data of Eqs. 117, 119, and 121 are rearranged in accord with Eq. 154 so that the results enable us to obtain additional interpretations of the correlation diagrams shown in Fig. 7b, c, and d.

In Theorem 2, each holantimeric pair of skeletons is regarded to be a hypothetically single entity. In other words, Eqs. 152 and 153 are concerned with holantimeric pairs as well as with self-holantimeric pairs, as shown in the groups $G_{C\hat{I}}$ (Eq. 152) and $H_{\hat{I}}$ (Eq. 153). When all of the substituents are achiral, two molecules derived from such a holantimeric pair of skeletons are really reduced into a single molecular entity, i.e., a self-holantimeric pair. For example, the function represented by Eq. 139 is applied to a holantimeric pair of **1** and **8** to give holantimeric 1-bromo-2-chloro-3,4-difluorocyclobutanes, i.e., **22** and **23**, which are identical with each other (cf. Fig. 8).

As a result, in the case of 1-bromo-2-chloro-3,4-difluorocyclobutanes, Eq. 158 is converted into the following equation:

$$\begin{aligned} \widehat{C}_s &= \overset{\times}{C}_{s\hat{I}}^{\tilde{\sigma}_{15}} + \tilde{\sigma}_{26} \overset{\times}{C}_{s\hat{I}}^{\tilde{\sigma}_{15}} + \tilde{\sigma}_{37} \overset{\times}{C}_{s\hat{I}}^{\tilde{\sigma}_{15}} + \tilde{\sigma}_{48} \overset{\times}{C}_{s\hat{I}}^{\tilde{\sigma}_{15}} & (159) \\ &= \left\{ \overset{\times}{C}_{\hat{I}} + \underbrace{\sigma \overset{\times}{C}_{\hat{I}}}_{22} + \underbrace{\tilde{\sigma}_{15} \overset{\times}{C}_{\hat{I}}}_{24} + \underbrace{\tilde{\sigma}_{15} \sigma \overset{\times}{C}_{\hat{I}}}_{24} \right\} \\ &\quad + \left\{ \underbrace{\tilde{\sigma}_{26} \overset{\times}{C}_{\hat{I}}}_{26} + \underbrace{\tilde{\sigma}_{26} \sigma \overset{\times}{C}_{\hat{I}}}_{\overline{26}} + \underbrace{\tilde{\sigma}_{15} \tilde{\sigma}_{26} \overset{\times}{C}_{\hat{I}}}_{32} + \underbrace{\tilde{\sigma}_{15} \tilde{\sigma}_{26} \sigma \overset{\times}{C}_{\hat{I}}}_{\overline{32}} \right\} \\ &\quad + \left\{ \underbrace{\tilde{\sigma}_{37} \overset{\times}{C}_{\hat{I}}}_{28} + \underbrace{\tilde{\sigma}_{37} \sigma \overset{\times}{C}_{\hat{I}}}_{\overline{28}} + \underbrace{\tilde{\sigma}_{15} \tilde{\sigma}_{37} \overset{\times}{C}_{\hat{I}}}_{34} + \underbrace{\tilde{\sigma}_{15} \tilde{\sigma}_{37} \sigma \overset{\times}{C}_{\hat{I}}}_{\overline{34}} \right\} \\ &\quad + \left\{ \underbrace{\tilde{\sigma}_{48} \overset{\times}{C}_{\hat{I}}}_{30} + \underbrace{\tilde{\sigma}_{48} \sigma \overset{\times}{C}_{\hat{I}}}_{\overline{30}} + \underbrace{\tilde{\sigma}_{15} \tilde{\sigma}_{48} \overset{\times}{C}_{\hat{I}}}_{36} + \underbrace{\tilde{\sigma}_{15} \tilde{\sigma}_{48} \sigma \overset{\times}{C}_{\hat{I}}}_{\overline{36}} \right\}. & (160) \end{aligned}$$

The resulting equation (Eq. 160) is illustrated by applying the function (Eq. 139) to the correlation diagram shown in Fig. 7a, so that the counterpart diagram is generated as shown in Fig. 10a. The first pair of braces of Eq. 160 contains four cosets, which respectively corresponds to a promolecule (22_1), its enantiomer ($\overline{22}_1$), its *RS*-diastereomer (24_1), and its holantimer ($\overline{24}_1$), where the subscript emphasizes the fixation at the C_1 -position. The quadruplet constructs Stereoisogram #1 of Fig. 10a, where Stereoisogram #1 is controlled by $\overset{\times}{C}_{s\hat{I}}^{\tilde{\sigma}_{15}}$ appearing in Eq. 159, while each of the *RS*-stereoisomers (22_1 , $\overline{22}_1$, 24_1 , and $\overline{24}_1$) is controlled by $\overset{\times}{C}_{\hat{I}}$ appearing in Eq. 160. As for an intervening group $\overset{\times}{C}_{s\hat{I}}$, see Eq. 150.

Similarly, the other sets of four cosets in Eq. 160 illustrated by the remaining stereoisograms (#2–#4) contained in Fig. 10a. Moreover, the other correlation diagrams (Fig. 10b–d) can be interpreted in a similar way.

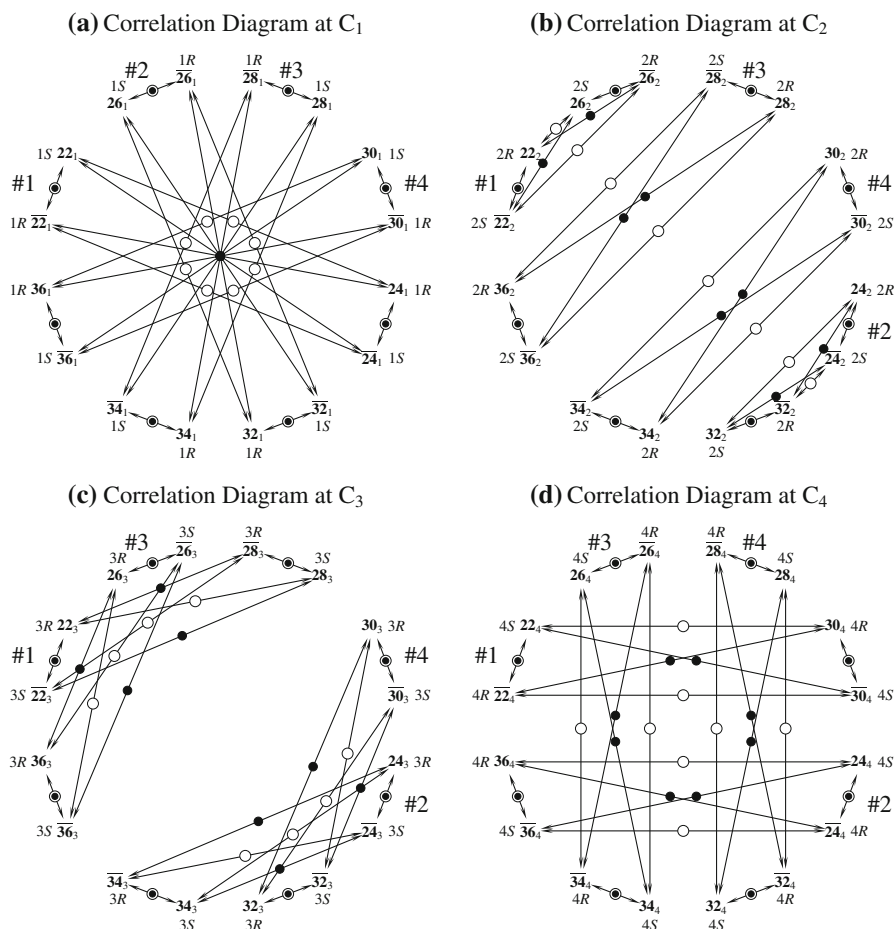


Fig. 10 Correlation diagrams of stereoisograms for 1-bromo-2-chloro-3,4-difluorocyclobutanes: **a** for C_1 (cf. Eq. 160), **b** for C_2 , **c** for C_3 , and **d** for C_4

4.3 Epimeric stereoisograms and RS -stereodescriptors

4.3.1 Conversion of epimeric stereoisograms into Fischer-like projections

The discussions described above indicate that stereoisomerism can be investigated by using stereoisograms and their correlation diagrams without examining the molecular-symmetry group $G_{C\sigma}$ detailedly. Such stereoisograms and their correlation diagrams are mainly controlled by the stereoisogram group (Eq. 21) or the epimeric stereoisogram group (Eq. 48) so that the use of the epimeric RS -stereoisomeric group (Eq. 60) or the corresponding factor group of order 4 (Eq. 61) is sufficient to discuss stereoisomerism. Even if any molecular-symmetry group $G_{C\sigma}$ is selected, its factor group of order 4 (Eq. 61) is isomorphic to the epimeric stereoisogram group (Eq. 48). In fact, the factor group based on the tetrahedral point group T_d has been implicitly

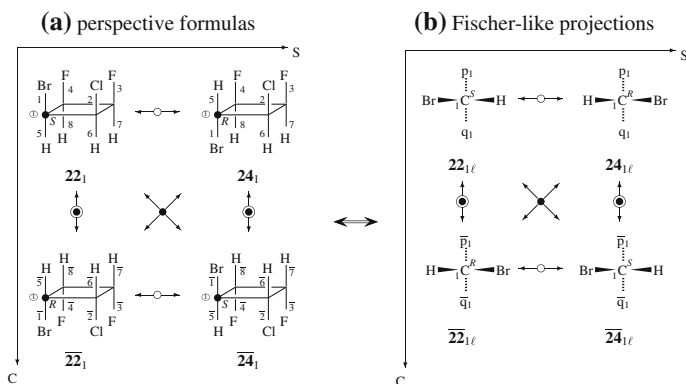


Fig. 11 Epimeric stereoisograms for specifying stereoisomeric 1-bromo-2-chloro-3,4-difluorocyclobutanes: **a** perspective formulas, **b** Fischer-like projections. The two stereoisograms belong to Type I. Each *R*- or *S*-stereodescriptor is determined by employing the priority sequence, $\text{Br} > p_1 > q_1 > \text{H}$ or $\text{Br} > \overline{p}_1 > \overline{q}_1 > \text{H}$

used in place of any of the groups $\mathbf{G}_{C\sigma}$, although this fact has been overlooked by organic chemists in practices of determining *RS*-stereodescriptors of the CIP system. The present subsection is devoted to clarify how such practices depend on the factor group of order 4 and on stereoisograms and correlation diagrams.

Let us examine Stereoisogram #1 contained in the correlation diagram for determining the configurations of the C_1 atom (Fig. 10a). The full expression of Stereoisogram #1 is shown in Fig. 11a, where four molecules, 22_1 , 22_1 , 24_1 , and 24_1 , are depicted by perspective formulas with a solid circle at the C_1 atom. The quadruplet corresponds to the cosets contained in the first pair of braces in Eq. 160. The resulting epimeric stereoisogram (Fig. 11a) belongs to Type III.

The procedure for determining *RS*-stereodescriptors is more clearly traced by using Fischer-like projections shown in Fig. 11b. The perspective formula 22_1 is converted into a digraph by a ring-opening procedure, which follows a similar procedure adopted in the CIP system [11]. Suppose that one residue toward the front edge (C_1 – C_2 – C_3) is considered to be a proligand p_1 and that the other backward residue (C_1 – C_4 – C_3) is considered to be another proligand q_1 . Then, we obtain $22_{1\ell}$ (a Fischer-like projection), as shown in Fig. 11b. The relevant molecules $\overline{22}$, 24 , and $\overline{24}$ are also converted into Fischer-like projections $\overline{22}_{1\ell}$, $24_{1\ell}$, and $\overline{24}_{1\ell}$. Thereby, Fig. 11b is obtained as another expression of the stereoisogram.

4.3.2 *RS*-diastereomeric relationships for specifying *RS*-stereodescriptors

Fischer-like expressions of stereoisograms such as Fig. 11b can be conveniently used to specify *RS*-stereodescriptors. Strictly speaking, however, the conversion of the perspective expression (Fig. 11a) into the Fischer-like projection (Fig. 11b) implies that the group \mathbf{D}_{4h} (and the local point group \mathbf{C}_1) is converted into the group \mathbf{T}_d (and the local point group \mathbf{C}_1). This type of conceptual conversions is always involved in practices of the CIP system, although it is often overlooked by organic chemists.

Because the priority sequence is determined to be $\text{Br} > p_1 > q_1 > \text{H}$, the configuration of $\mathbf{22}_{1\ell}$ is specified to be *S* according to the CIP rule [8, 11]. On a similar line, the corresponding *RS*-diastereomer $\mathbf{24}_1$ is converted into a Fischer-like projection $\mathbf{24}_{1\ell}$, whose *R*-configuration is determined by using the common priority sequence, $\text{Br} > p_1 > q_1 > \text{H}$. Thus, the *S*-stereodescriptor of $\mathbf{22}_1$ and the *R*-stereodescriptor of $\mathbf{24}_1$ are pairwise determined on the basis of their *RS*-diastereomeric relationship.

On the other hand, the *R*-stereodescriptor of $\overline{\mathbf{22}}_1$ and the *S*-stereodescriptor of $\overline{\mathbf{24}}_1$ are pairwise determined on the basis of their *RS*-diastereomeric relationship, where another common priority sequence, $\text{Br} > \overline{p}_1 > \overline{q}_1 > \text{H}$ is employed.

Thus, the determination of the *S*-stereodescriptor of $\mathbf{22}_1$ is different from that of the *R*-stereodescriptor of $\overline{\mathbf{22}}_1$ in the priority sequences to be employed. In general, the *RS*-stereodescriptors of two enantiomers of each pair are by no means determined pairwise. In this context, the foundation of the CIP system should be revised in accord with the present approach. An attempted revision has been reported by Fujita [22].

4.3.3 Correlation diagrams and *RS*-stereodescriptors

The first set of cosets appearing in Eq. 160, i.e., $\left\{ \overset{\times}{\mathbf{C}}_{\overline{1}}^{\times}, \sigma \overset{\times}{\mathbf{C}}_{\overline{1}}^{\times}, \tilde{\sigma}_{15} \overset{\times}{\mathbf{C}}_{\overline{1}}^{\times}, \tilde{\sigma}_{15} \sigma \overset{\times}{\mathbf{C}}_{\overline{1}}^{\times} \right\}$, is collected to give one coset $\overset{\times}{\mathbf{C}}_{s\overline{1}}^{\tilde{\sigma}_{15}}$ appearing in Eq. 159. Then, the coset $\overset{\times}{\mathbf{C}}_{s\overline{1}}^{\tilde{\sigma}_{15}}$ is regarded as corresponding to a stereoisogram for specifying a quadruplet of $\mathbf{22}$, $\overline{\mathbf{22}}$, $\mathbf{24}$, and $\overline{\mathbf{24}}$ (Fig. 11a or b). In parallel ways, the other cosets appearing in Eq. 159 (i.e., $\tilde{\sigma}_{26} \overset{\times}{\mathbf{C}}_{s\overline{1}}^{\tilde{\sigma}_{15}}$, $\tilde{\sigma}_{37} \overset{\times}{\mathbf{C}}_{s\overline{1}}^{\tilde{\sigma}_{15}}$, and $\tilde{\sigma}_{48} \overset{\times}{\mathbf{C}}_{s\overline{1}}^{\tilde{\sigma}_{15}}$) are correlated to respective stereoisograms, where the correspondences concerning respective quadruplets are shown in Eq. 160. These stereoisograms are collected to generate a correlation diagram (Fig. 12), where Stereoisogram #1–#4 correspond respectively to the cosets appearing in Eq. 159, i.e., #1 to $\overset{\times}{\mathbf{C}}_{s\overline{1}}^{\tilde{\sigma}_{15}}$, #2 to $\tilde{\sigma}_{26} \overset{\times}{\mathbf{C}}_{s\overline{1}}^{\tilde{\sigma}_{15}}$, #3 to $\tilde{\sigma}_{37} \overset{\times}{\mathbf{C}}_{s\overline{1}}^{\tilde{\sigma}_{15}}$, and #4 to $\tilde{\sigma}_{48} \overset{\times}{\mathbf{C}}_{s\overline{1}}^{\tilde{\sigma}_{15}}$. Note that each of the cosets in Eq. 159 are divided into four cosets collected in Eq. 160.

Just as Stereoisogram #1 (equivalent to Fig. 11a or b) is used to determine the *RS*-stereodescriptors at the C_1 atoms contained in an *RS*-diastereomeric pair of $\mathbf{22}$ and $\mathbf{24}$ (or of $\overline{\mathbf{22}}$ and $\overline{\mathbf{24}}$), the other stereoisograms are used to determine *RS*-stereodescriptors for respective *RS*-diastereomeric pairs, which are contained in Fig. 12. The resulting *RS*-stereodescriptors are attached to the central atoms of the employed Fischer-like projections, where the priority sequences, $\text{Br} > p_i > q_i > \text{H}$ (or $\text{Br} > \overline{p}_i > \overline{q}_i > \text{H}$), are employed ($i = 1$ to 4) after the symbols p_i ($i = 1$ to 4) denote forward residues started from respective C_1 atoms (C_1 – C_y – 2 – C_3) and the symbols q_i ($i = 1$ to 4) denote backward residues started from respective C_1 atoms (C_1 – C_4 – C_3).

The procedure for constructing the correlation diagram for specifying the C_1 atoms (Fig. 12), i.e., Eqs. 159 and 160 \rightarrow Fig. 11a and b \rightarrow Fig. 12, is applicable to the other *RS*-stereocenters (the C_2 , C_3 , and C_4 -atoms). The counterparts of Eqs. 159 and 160 (generated according to the derivation scheme of Eqs. 114/115 \rightarrow Eqs. 135/136 \rightarrow Eqs. 157/158 \rightarrow Eqs. 159/160) can be obtained by parallel schemes started from Eqs. 116/117 (for the C_2 atom), Eqs. 118/119 (for the C_3 atom), and Eqs. 120/121 (for the C_4 atom). Then, the counterparts of Fig. 11a/b and those of Fig. 12 are also

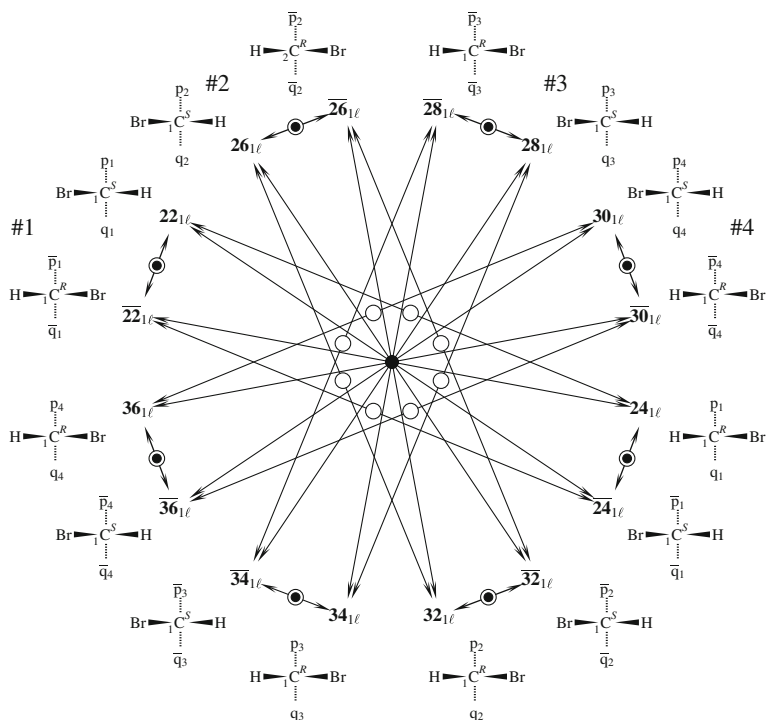
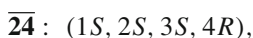
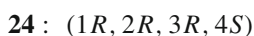
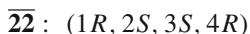
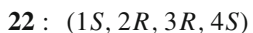


Fig. 12 A correlation diagram of epimeric stereoisomers for characterizing the configurations at the C_1 atoms of stereoisomeric 1-bromo-2-chloro-3,4-difluorocyclobutanes. Each promolecule is represented by a Fischer-like projection, which is derived from the corresponding perspective formula. For example, Stereoisogram #1 corresponds to the two expressions shown in Fig. 11

obtained so as to generate the corresponding correlation diagrams. They are collected to generate a list for summarizing total features of the stereoisomerism, as shown in Fig. 10. The correlation diagram of Fig. 12 is contained as Fig. 10a, where the Fischer-like projections are omitted and only the R - or S -stereodescriptor assigned to each Fischer-like projection is left attached to the respective node. For example, Stereoisogram #1 of Fig. 10a corresponds to Fig. 11b (or Fig. 11a) via Stereoisogram #1 of Fig. 12.

From the data collected in Fig. 10, we are able to assign an RS -stereodescriptor set to each stereoisomer, e.g.,



where we collect, for example, $1S$ of $\mathbf{22}_1$ (Fig. 10a), $2R$ of $\mathbf{22}_2$ (Fig. 10b), $3R$ of $\mathbf{22}_3$ (Fig. 10c), and $4S$ of $\mathbf{22}_4$ (Fig. 10d) in order to assign the set $(1S, 2R, 3R, 4S)$ to

22. The total results of such assignments are summarized in Fig. 8, where an *R*- or *S*-stereodescriptor is attached to each *RS*-stereogenic center to be determined.

4.4 *RS*-stereodescriptors for degenerate cases

Assignments of functions to a stereoskeleton of the $G_{C\sigma}$ -symmetry generate promolecules of various molecular symmetries, which belong to subgroups of $G_{C\sigma}$. For example, one extreme case is a promolecule of C_1 (e.g., **5**) and the other extreme case is a promolecule of D_{4h} (e.g., **7**), when we start from a cyclobutane stereoskeleton of the D_{4h} -symmetry. Between the two extreme cases, there are degenerate cases which belong to intermediate subgroups of D_{4h} (or $G_{C\sigma}$ in general). The term “degenerate” means that a part of stereoisomers (homomers) generated by means of $\widehat{G}_{C\sigma}$ may be reduced into a single molecule.

For example, let us employ the function represented by the following equation:

$$\begin{aligned} f : f(1) = \text{Cl}, f(2) = \text{Cl}, f(3) = \text{Cl}, f(4) = \text{Cl}, \\ f(5) = \text{H}, f(6) = \text{H}, f(7) = \text{H}, f(8) = \text{H}, \end{aligned} \quad (161)$$

which results in the formation of stereoisomeric 1,2,3,4-tetrachlorocyclobutanes. They are depicted in Fig. 13, where each stereoisogram belongs to Type IV so that each quadruplet of *RS*-stereoisomers corresponds to a single molecule. Among them, the molecule **40** (Fig. 13b) is homomeric to **42** (Fig. 13c), **44** (Fig. 13d), and **46** (Fig. 13e). The molecule **48** (Fig. 13f) is homomeric to **52** (Fig. 13h). As a result, there appear four stereoisomeric 1,2,3,4-tetrachlorocyclobutanes, i.e., **38** (Fig. 13a), **40** (Fig. 13b), **48** (Fig. 13f), and **50** (Fig. 13g).

According to a similar procedure for constructing correlation diagrams of stereoisograms of 1-bromo-2-chloro-3,4-difluorocyclobutanes (i.e., Fig. 8 \rightarrow Fig. 12 \rightarrow Fig. 10), the molecules listed in Fig. 13 are examined so as to generate the corresponding correlation diagrams of stereoisograms, as shown in Fig. 14. An *R*- or *S*-stereodescriptors assigned to each *RS*-stereogenic center is attached to the corresponding node contained in the relevant stereoisogram. To show the *s*-configuration of the C_1 atom contained in the molecule **38**, for example, the assignment *1s* is attached to the node denoted by **38**₁, which is involved in Stereoisogram #1 of Fig. 14a. Stereoisogram #1 belongs to Type V, so that the lowercase letter *1s* shows the pseudoasymmetry concerning the C_1 atom of **38**. It should be noted that the *1s* of **38** is paired up with the *1r* of **40**, as found by the *RS*-diastereomeric relationship between **38**₁ and **40**₁ in Stereoisogram #1 of Fig. 14a.

To show the whole configurations of **38**, an *RS*-stereodescriptor set (*1s*, *2s*, *3s*, *4s*) is assigned to **38** by collecting the *1s* of **38**₁ in Stereoisogram #1 of Fig. 14a, the *2s* of **38**₂ in Stereoisogram #1 of Fig. 14b, the *3s* of **38**₃ in Stereoisogram #1 of Fig. 14c, and the *4s* of **38**₄ in Stereoisogram #1 of Fig. 14d. It should be noted, the *2s* of **38** is paired up with the *2r* of **42** (Stereoisogram #1 of Fig. 14b), the *3s* of **38** is paired up with the *3r* of **44** (Stereoisogram #1 of Fig. 14c), and the *4s* of **38** is paired up with the *4r* of **46** (Stereoisogram #1 of Fig. 14d). If we disregard the modes of locant numbering, the references to **40**₁, **42**₂, **44**₃, and **46**₄ are essentially equivalent in the

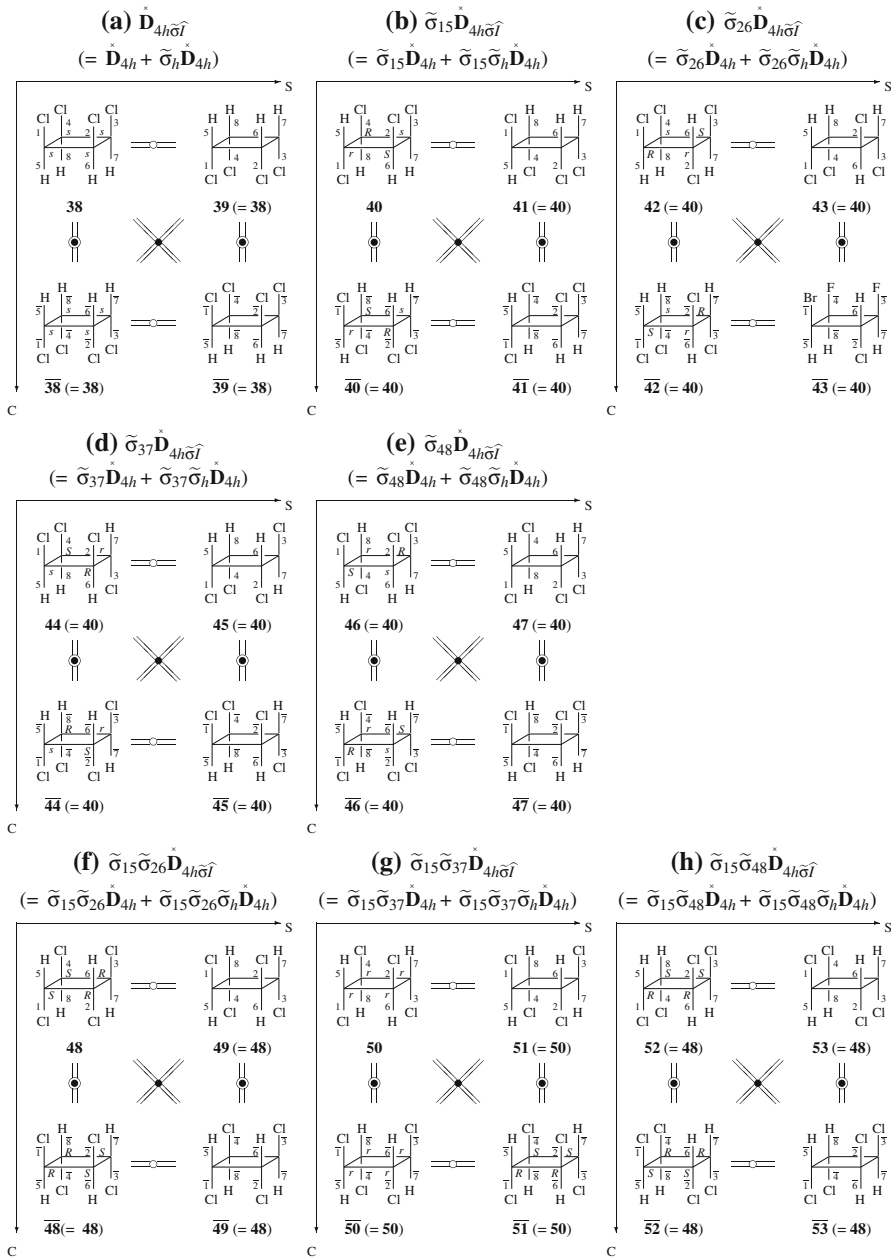


Fig. 13 Main stereoisograms for specifying stereoisomeric 1,2,3,4-tetrachlorocyclobutanes. All of the stereoisograms belong to Type IV

assignment of stereodescriptors. By taking account of the modes of locant numbering, the procedure based on Fig. 14 reveals implications in the CIP system for assigning *RS*-stereodescriptors. Without referring to such correlation diagrams as Fig. 14a–d,

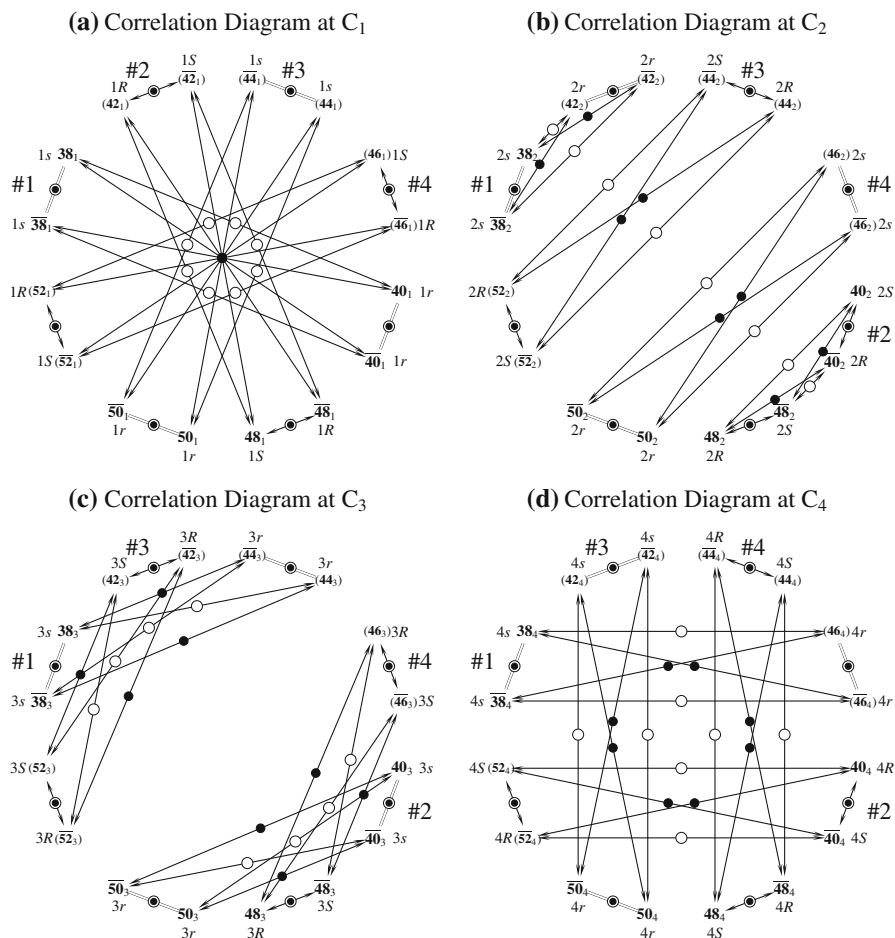
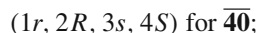
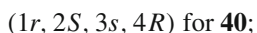


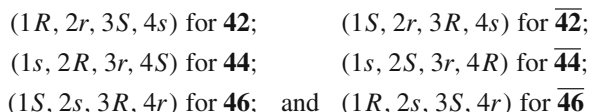
Fig. 14 Correlation diagrams of stereoisograms for characterizing 1,2,3,4-tetrachlorocyclobutanes, which are derived from the skeletons with the following modes of numbering: **a** for C_1 (cf. the skeletons shown in Eq. 115), **b** for C_2 (cf. the skeletons shown in Eq. 117), **c** for C_3 (cf. the skeletons shown in Eq. 119), and **d** for C_4 (cf. the skeletons shown in Eq. 121)

one tends to rely on a simplified procedure which overlooks the four modes of pairing in his processes of specifying *R*- or *S*-configurations.

On the basis of the data collected in Fig. 14, an *RS*-stereodescriptor set is assigned to each molecule. The assignment of each molecule is shown in Fig. 13, where *R* (or *r*) or *S* (or *s*) is attached to each *RS*-stereogenic atom of a cyclobutane skeleton.

Because several modes of locant numbering are available for a single molecule, there emerge several possibilities of *RS*-stereodescriptor sets. For example, **40** is homomeric to **42**, **44**, and **46**. The four molecules (homomers) of different locant numbering (and their enantiomers) provide us with the following possibilities:

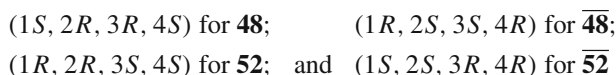




when we refer to the data listed in Fig. 13. Obviously, the *RS*-stereodescriptor sets are converted into others by rotations (or renumbering) of the cyclobutane skeleton. Among them, the *RS*-stereodescriptor set (1*R*, 2*r*, 3*S*, 4*s*) can be tentatively selected on the assumption that a younger locant number has a stereodescriptor selected in the priority sequence $R > r > S > s$.

It should be noted that, even though the *RS*-stereodescriptor set (1*r*, 2*S*, 3*s*, 4*R*) for **40** may not be selected, the 1*r* of **40** is necessary to the pairwise naming of the 1*s* for **38**. This necessity is confirmed by Stereoisogram #1 of the correlation diagram shown in Fig. 14a. As for the tentatively selected *RS*-stereodescriptor set (1*R*, 2*r*, 3*S*, 4*s*) of **42**, the 1*R* is paired with the 1*S* of **48** (Stereoisogram #2 shown in Fig. 14a), the 2*r* is paired with the 2*s* of **38** (Stereoisogram #1 shown in Fig. 14b), the 3*S* is paired with the 3*R* of $\overline{\mathbf{52}}$ (Stereoisogram #3 shown in Fig. 14c), and the 4*s* is paired with the 4*r* of **50** (Stereoisogram #3 shown in Fig. 14d). This means that the *RS*-stereodescriptor set (1*R*, 2*r*, 3*S*, 4*s*) of **42** is not paired with (1*S*, 2*r*, 3*R*, 4*s*) of its mirror-image molecule $\overline{\mathbf{42}}$, which is identical with **42** (=40) itself.

Because the achiral molecule **48** is homomeric to **52**, we find the following possibility of *RS*-stereodescriptor sets:



when we refer to the data listed in Fig. 13. Among them, we are able to select the *RS*-stereodescriptor set (1*R*, 2*R*, 3*S*, 4*S*) if we suppose that a younger locant number has a stereodescriptor selected in the priority sequence $R > r > S > s$.

The remaining stereoisomers are named as follows by referring to the data listed in Fig. 13.

- 38**: (1*s*, 2*s*, 3*s*, 4*s*)-1,2,3,4-tetrachlorocyclobutane
50: (1*r*, 2*r*, 3*r*, 4*r*)-1,2,3,4-tetrachlorocyclobutane

Although these two *RS*-stereodescriptor sets seem to be paired, they have nothing to do with each other, as found by scrutinizing the correlation diagrams listed in Fig. 14.

5 Molecular symmetries of stereoisomers

5.1 Permutations for functions

In the preceding sections, we have presumed that permutations are operated on the set Ω of substitution positions (Eq. 2). In other words, a fixed function f is operated to a set of substitution positions (the modes of locant numbering) which are permuted. Another approach should be developed to examine molecular symmetries, where the

effects of epimerizations are disregarded tentatively. In this approach, a fixed mode of locant numbering (for substitution positions) is regarded as corresponding to permuted functions.

For the sake of convenience, an epimerization operation $\tilde{\sigma}_i$ is renamed as $\tilde{\sigma}_{ij}$, which denotes the permutation between positions Ω_i and Ω_j involved in the set Ω (Eq. 2). The set of epimerization operations generates a set of stereoskeletons governed by $\widehat{\mathbf{G}}_{G\sigma}$. A tentatively fixed function represented by the following equation,

$$f = \{f(1), f(2), \dots, f(i), \dots, f(j), \dots, f(n)\}, \quad (162)$$

is applied to the set of stereoskeletons so as to generate a set of molecules belonging to $\mathbf{G}_{C\sigma}$ or its conjugate subgroup $\tilde{\sigma}_{ij}\mathbf{G}_{C\sigma}\tilde{\sigma}_{ij}^{-1}$. The set of molecules is rearranged to give a set of quadruplets, which is controlled by the coset representation $\widehat{\mathbf{G}}_{G\sigma} (\widehat{\mathbf{G}}_{C\sigma\tilde{\sigma}}^\times)$. For example, the function represented by Eq. 161 produces the molecules listed in Fig. 13.

Each stereoisomer generated by the function f (Eq. 162) can be alternatively generated by applying the following function:

$$\tilde{\sigma}_{ij}f = \{f(1), f(2), \dots, f^i(j), \dots, f^j(i), \dots, f(n)\} \quad (163)$$

to a stereoskeleton with a fixed locant number. There is the pairwise appearance of $\tilde{\sigma}_{ij}f$ and $\tilde{\sigma}\tilde{\sigma}_{ij}f$ so that the corresponding molecules are regarded as separate entities. Note that the pair of $\tilde{\sigma}_{ij}f$ and $\tilde{\sigma}\tilde{\sigma}_{ij}f$ corresponds to a quadruplet of RS -stereoisomers contained in a main correlation diagram (cf. Fig. 6), where the numbering due to $\tilde{\sigma}_{ij}f$ is in a clockwise-anti-clockwise relationship (in other words in an RS -diastereomeric relationship) to the numbering due to $\tilde{\sigma}\tilde{\sigma}_{ij}f$. As a result, the holantimer of $\tilde{\sigma}\tilde{\sigma}_{ij}f$ is shown to be $\widehat{T}\tilde{\sigma}\tilde{\sigma}_{ij}f (= \sigma\tilde{\sigma}_{ij}f)$, which is enantiomeric to $\tilde{\sigma}_{ij}f$.

For example, the function f (Eq. 161) is converted into $\tilde{\sigma}_{15}f$ as follows:

$$\begin{aligned} \tilde{\sigma}_{15}f : f(1) = \text{H}, f(2) = \text{Cl}, f(3) = \text{Cl}, f(4) = \text{Cl}, \\ f(5) = \text{Cl}, f(6) = \text{H}, f(7) = \text{H}, f(8) = \text{H}, \end{aligned} \quad (164)$$

which is applied to a stereoskeleton **1** with a fixed set of locant numbers. Thereby, we obtain the molecule **40'** listed in Fig. 15. As found easily, the molecule **40'** (Fig. 15) is allowed to be equalized to the molecule **40** (Fig. 13). As a counterpart corresponding to **41** (Fig. 13), the function $\tilde{\sigma}\tilde{\sigma}_{15}f (= \tilde{\sigma}_{26}\tilde{\sigma}_{37}\tilde{\sigma}_{48}f)$ generates a counterpart molecule. Although the framework of stereoisograms (S-axes and C-axes) and the relationships of three kinds are left in Fig. 15 for the sake of convenience, their original meanings are not maintained during the transformation from Fig. 13 to 15.

On a similar line, $\tilde{\sigma}_{26}f$ etc. produce the molecule **42'** etc. (Fig. 15), which are allowed to be equalized to the molecule **42** etc. (Fig. 13). Then, the set of molecules listed in Fig. 15 is considered to be governed by $\mathbf{D}_{4h\tilde{\sigma}\widehat{T}}$.

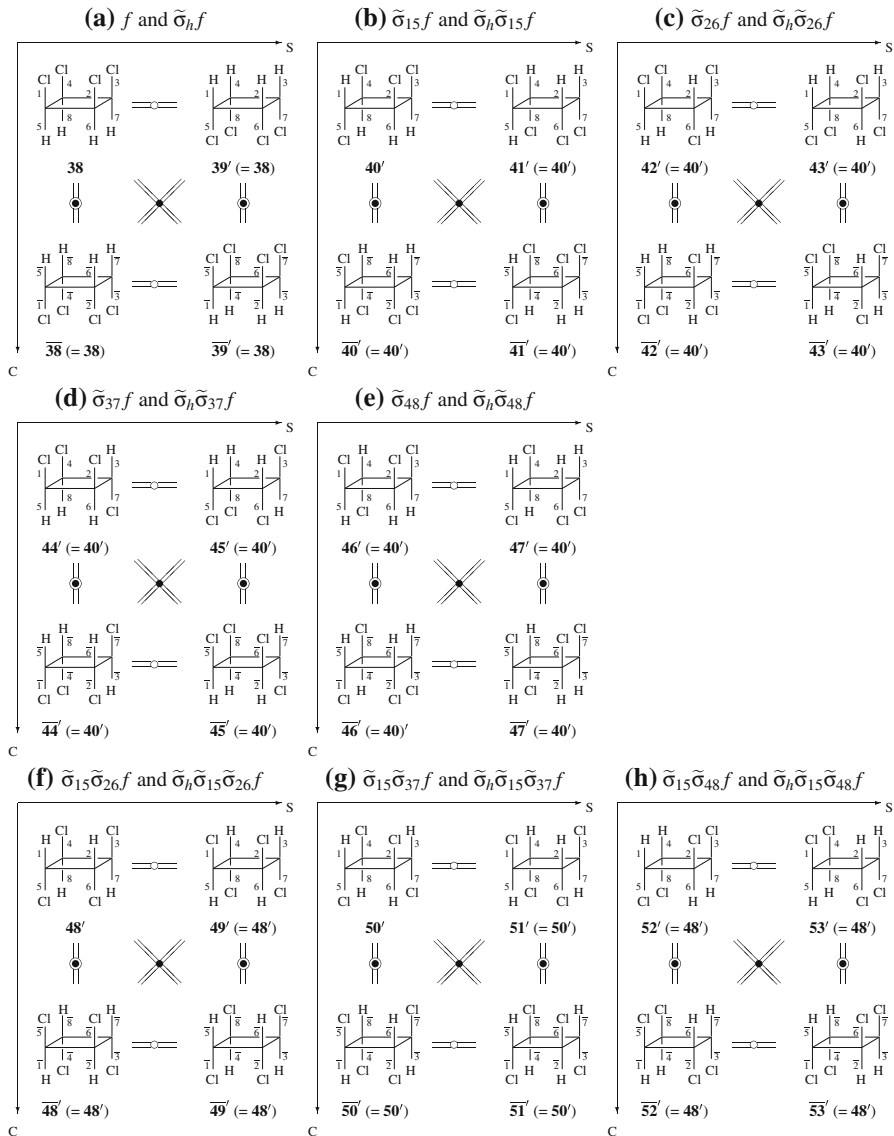


Fig. 15 Stereoisomeric 1,2,3,4-tetrachlorocyclobutanes, where permutations of functions are taken into consideration. Each molecule denoted by a compound number with a prime (e.g., $40'$) corresponds to the counterpart which is denoted by a compound number without a prime (e.g., 40) in Fig. 13

It should be emphasized that the set of molecules listed in Fig. 13 is allowed to be equalized to the other set of molecules listed in Fig. 15. The former set (Fig. 13) is controlled by the coset representation $\widehat{\mathbf{D}}_{4h}(/D_{4h}\tilde{\sigma})$. On the other hand, the latter set (Fig. 15) provides us with an alternative approach, which deals explicitly with molecular symmetries. The next task is to determine how the latter set (Fig. 15) is controlled.

5.2 Molecular-symmetry representations

In the preceding treatments for investigating stereoisomerism, a stereoisomeric group $\widehat{\mathbf{G}}_{C\sigma}$ defined by Eq. 79 has been regarded as a multiple epimerization group $\widetilde{\mathbf{H}}$ (Eq. 77) which is accompanied with a molecular-symmetry group $\mathbf{G}_{C\sigma}$. Note that this standpoint presumes such lists of stereoisomers as shown in Fig. 13. The emphasis on the multiple epimerization group $\widetilde{\mathbf{H}}$ is based on an implicit methodology that the molecular-symmetry group $\mathbf{G}_{C\sigma}$ is tentatively disregarded or is considered to be \mathbf{C}_s (or to be \mathbf{C}_1 in place of \mathbf{G}_C). As a result, the methodology is effective even under extreme cases in which the molecular-symmetry group $\mathbf{G}_{C\sigma}$ (or \mathbf{G}_C) is reduced into \mathbf{C}_s (or \mathbf{C}_1 , i.e., no symmetry) during derivations of stereoisomers by employing functions. In other words, the processes of epimerizations (totally stereoisomerization) can be discussed independent of the molecular-symmetry group $\mathbf{G}_{C\sigma}$.

The stereoisomeric group $\widehat{\mathbf{G}}_{C\sigma}$ can be alternatively regarded as the molecular-symmetry group $\mathbf{G}_{C\sigma}$ accompanied by the multiple epimerization group $\widetilde{\mathbf{H}}$ (Eq. 77). This means that the molecular-symmetry group $\mathbf{G}_{C\sigma}$ can be examined independent of the processes of epimerizations (totally stereoisomerization). Note that this standpoint presumes that alternative lists such as Fig. 15 are used in place of counterpart lists such as Fig. 13. This section is devoted to develop such an alternative methodology according to the standpoint of emphasizing the molecular-symmetry group $\mathbf{G}_{C\sigma}$.

Suppose that the stereoisomeric group $\widehat{\mathbf{G}}_{C\sigma}$ (Eq. 79) is represented by a coset decomposition by the multiple epimerization group $\widetilde{\mathbf{H}}$ (Eq. 77). Obviously, the transversal is composed of the elements of the molecular-symmetry group $\mathbf{G}_{C\sigma}$ (Eq. 3). When the group \mathbf{G}_C is composed of proper rotations represented by

$$\mathbf{G}_C = \{g_1, g_2, \dots, g_{|\mathbf{G}_C|}\}, \quad (165)$$

we obtain the molecular-symmetry group:

$$\mathbf{G}_{C\sigma} = \{g_1, g_2, \dots, g_{|\mathbf{G}_C|}; \sigma g_1, \sigma g_2, \dots, \sigma g_{|\mathbf{G}_C|}\}, \quad (166)$$

where g_1 is an identity element (I). Thereby, the stereoisomeric group $\widehat{\mathbf{G}}_{C\sigma}$ (Eq. 79) is represented as a coset decomposition by $\{I\} \times \widetilde{\mathbf{H}}$, i.e.,

$$\widehat{\mathbf{G}}_{C\sigma} = \{g_1 \times \widetilde{\mathbf{H}} + \dots + g_{|\mathbf{G}_C|} \times \widetilde{\mathbf{H}}\} + \{\sigma g_1 \times \widetilde{\mathbf{H}} + \dots + \sigma g_{|\mathbf{G}_C|} \times \widetilde{\mathbf{H}}\} \quad (167)$$

$$= g_1 \widetilde{\mathbf{H}}^\times + \dots + g_{|\mathbf{G}_C|} \widetilde{\mathbf{H}}^\times + \sigma g_1 \widetilde{\mathbf{H}}^\times + \dots + \sigma g_{|\mathbf{G}_C|} \widetilde{\mathbf{H}}^\times, \quad (168)$$

where $\widetilde{\mathbf{H}}^\times$ is equalized to $\{I\} \times \widetilde{\mathbf{H}}$. Equation 89 implies the relationships between g_i and $\widetilde{\sigma} g_i$ and between σg_i and $\widehat{\sigma} \widetilde{\sigma} g_i (= \widehat{I} g_i)$ as follows:

$$g_i, \widetilde{\sigma} g_i \in g_i \widetilde{\mathbf{H}}^\times; \quad \sigma g_i, \widehat{I} g_i \in \sigma g_i \widetilde{\mathbf{H}}^\times \quad (169)$$

Hence, Eq. 168 is correlated to Eq. 96 by employing an appropriate half of $\tilde{\mathbf{H}}$ to give the following set of cosets:

$$\begin{aligned} \widehat{\mathbf{G}}_{C\sigma} = & \left\{ g_1 \times \tilde{\mathbf{H}}' + \cdots + g_{|\mathbf{G}_{C|}} \times \tilde{\mathbf{H}}' \right\} + \left\{ \sigma g_1 \times \tilde{\mathbf{H}}' + \cdots + \sigma g_{|\mathbf{G}_{C|}} \times \tilde{\mathbf{H}}' \right\} \\ & + \left\{ \tilde{\sigma} g_1 \times \tilde{\mathbf{H}}' + \cdots + \tilde{\sigma} g_{|\mathbf{G}_{C|}} \times \tilde{\mathbf{H}}' \right\} + \left\{ \hat{T} g_1 \times \tilde{\mathbf{H}}' + \cdots + \hat{T} g_{|\mathbf{G}_{C|}} \times \tilde{\mathbf{H}}' \right\}, \quad (170) \end{aligned}$$

where $\tilde{\mathbf{H}}'$ represents the part $\sum_{\omega \leq n/2} \tilde{\sigma}_{[\omega]}$ appearing in Eq. 96. The representatives of the respective cosets appearing in Eq. 170 are the elements of the *RS*-stereoisomeric group $\mathbf{G}_{C\sigma\tilde{\sigma}\hat{T}}$:

$$\begin{aligned} \mathbf{G}_{C\sigma\tilde{\sigma}\hat{T}} = & \{ g_1, g_2, \dots, g_{|\mathbf{G}_{C|}}; \sigma g_1, \sigma g_2, \dots, \sigma g_{|\mathbf{G}_{C|}}; \\ & \tilde{\sigma} g_1, \tilde{\sigma} g_2, \dots, \tilde{\sigma} g_{|\mathbf{G}_{C|}}; \hat{T} g_1, \hat{T} g_2, \dots, \hat{T} g_{|\mathbf{G}_{C|}} \}, \quad (171) \end{aligned}$$

Because the set $\tilde{\mathbf{H}}'$ is not always a group, we should use Eq. 168 which is regarded as a coset decomposition by $\tilde{\mathbf{H}}^\times$. Thereby, we are able to construct the coset representation $\widehat{\mathbf{G}}_{C\sigma}(\tilde{\mathbf{H}}^\times)$.

Definition 14 (*Molecular-Symmetry Representations*) The coset representation denoted by $\widehat{\mathbf{G}}_{C\sigma}(\tilde{\mathbf{H}}^\times)$ controls the molecular symmetry of a pair of enantiomers which is transformed by means of $\tilde{\mathbf{H}}^\times$. The coset representation is called a *molecular-symmetry representation* of the stereoisomeric group $\widehat{\mathbf{G}}_{C\sigma}$.

Let us consider a coset decomposition of $\mathbf{G}_{C\sigma}$:

$$\mathbf{G}_{C\sigma} = g_1 \mathbf{C}_1 + \cdots + g_{|\mathbf{G}_{C|}} \mathbf{C}_1 + \sigma g_1 \mathbf{C}_1 + \cdots + \sigma g_{|\mathbf{G}_{C|}} \mathbf{C}_1, \quad (172)$$

where we put $g_1 = I$ and $\mathbf{C}_1 = \{I\}$. Thereby, we obtain a coset representation $\mathbf{G}_{C\sigma}(\mathbf{C}_1)$. By comparing Eq. 172 with Eq. 168, the molecular-symmetry representation $\widehat{\mathbf{G}}_{C\sigma}(\tilde{\mathbf{H}}^\times)$ (Definition 14) is concluded to be isomorphic to the coset representation $\mathbf{G}_{C\sigma}(\mathbf{C}_1)$. This fact is represented formally:

$$\widehat{\mathbf{G}}_{C\sigma}(\tilde{\mathbf{H}}^\times) \downarrow \mathbf{G}_{C\sigma} = \mathbf{G}_{C\sigma}(\mathbf{C}_1). \quad (173)$$

Hence, Fujita's USCI approach [13, 23] can be applied to discussions on $\widehat{\mathbf{G}}_{C\sigma}(\tilde{\mathbf{H}}^\times)$, just as the approach is applicable to $\mathbf{G}_{C\sigma}(\mathbf{C}_1)$. For example, the set of molecules listed in Fig. 15 can be discussed by using $\mathbf{D}_{4h}(\mathbf{C}_1)$ and then the results are extended to those expected by $\widehat{\mathbf{D}}_{4h}(\tilde{\mathbf{H}}^\times)$.

5.3 Subductions of molecular-symmetry representations

Any one molecule is selected as a starting molecule from the set of molecules such as those listed in Fig. 15. Then, each of the permutation of $\mathbf{G}_{C\sigma}$ is operated to the

selected molecule to generate a set of $|\mathbf{G}_{C\sigma}|$ homomeric molecules, which is governed by the coset representation $\mathbf{G}_{C\sigma}/(\mathbf{C}_1)$ (equivalent to $\widehat{\mathbf{G}}_{C\sigma}/(\widehat{\mathbf{H}}^\times)$). Among the set of $|\mathbf{G}_{C\sigma}|$ homomeric molecules, a subset of molecules identical to the starting molecule is detected to give the corresponding stabilizer $\mathbf{K}_{C\sigma}$ (or equivalently $\widehat{\mathbf{K}}_{C\sigma}$), which is regarded as the symmetry of the set.

By following Fujita's USCI approach [13], the subduction of the molecular-symmetry representation $\widehat{\mathbf{G}}_{C\sigma}/(\widehat{\mathbf{H}}^\times)$ by its subgroup $\widehat{\mathbf{K}}_{C\sigma}$ is calculated as follows:

$$\widehat{\mathbf{G}}_{C\sigma}/(\widehat{\mathbf{H}}^\times) \downarrow \widehat{\mathbf{K}}_{C\sigma} = \frac{|\widehat{\mathbf{G}}_{C\sigma}|}{|\widehat{\mathbf{K}}_{C\sigma}|} \widehat{\mathbf{K}}_{C\sigma}/(\widehat{\mathbf{H}}^\times). \quad (174)$$

Moreover, a further subduction of Eq. 173 by $\mathbf{K}_{C\sigma}$ generates the following equation:

$$\widehat{\mathbf{G}}_{C\sigma}/(\widehat{\mathbf{H}}^\times) \downarrow \mathbf{K}_{C\sigma} = \frac{|\mathbf{G}_{C\sigma}|}{|\mathbf{K}_{C\sigma}|} \mathbf{K}_{C\sigma}/(\mathbf{C}_1). \quad (175)$$

This result is comparable to the subduction of $\mathbf{G}_{C\sigma}/(\mathbf{C}_1)$ by its subgroup $\mathbf{K}_{C\sigma}$:

$$\mathbf{G}_{C\sigma}/(\mathbf{C}_1) \downarrow \mathbf{K}_{C\sigma} = \frac{|\mathbf{G}_{C\sigma}|}{|\mathbf{K}_{C\sigma}|} \mathbf{K}_{C\sigma}/(\mathbf{C}_1), \quad (176)$$

which has once been noted by Fujita (Eq. 7.3 of [13]). The nature of direct-product groups indicates that the factor group $\widehat{\mathbf{G}}_{C\sigma}/\widehat{\mathbf{H}}^\times$ is isomorphic to $\mathbf{G}_{C\sigma}$ as well as that the factor group $\widehat{\mathbf{K}}_{C\sigma}/\widehat{\mathbf{H}}^\times$ is isomorphic to $\mathbf{K}_{C\sigma}$. Thereby, the coefficient $|\widehat{\mathbf{G}}_{C\sigma}|/|\widehat{\mathbf{K}}_{C\sigma}|$ ($= |\mathbf{G}_{C\sigma}|/|\mathbf{K}_{C\sigma}|$) of the right-hand side of Eq. 174 indicates that the presence of $|\widehat{\mathbf{G}}_{C\sigma}|/|\widehat{\mathbf{K}}_{C\sigma}|$ ($= |\mathbf{G}_{C\sigma}|/|\mathbf{K}_{C\sigma}|$) sets of identical molecules where such sets are homomeric and such molecules of each set are stabilized under the action $\widehat{\mathbf{K}}_{C\sigma}$ -symmetry (or $\mathbf{K}_{C\sigma}$ -symmetry).

For example, the molecules collected in Fig. 15 are discussed by means of the following subductions:

$$\widehat{\mathbf{D}}_{4h}/(\widehat{\mathbf{H}}^\times) \downarrow \widehat{\mathbf{C}}_{4v} = 2\widehat{\mathbf{C}}_{4v}/(\widehat{\mathbf{H}}^\times) \text{ or } \widehat{\mathbf{D}}_{4h}/(\widehat{\mathbf{H}}^\times) \downarrow \mathbf{C}_{4v} = 2\mathbf{C}_{4v}/(\mathbf{C}_1) \quad (177)$$

$$\widehat{\mathbf{D}}_{4h}/(\widehat{\mathbf{H}}^\times) \downarrow \widehat{\mathbf{D}}_{2d} = 2\widehat{\mathbf{D}}_{2d}/(\widehat{\mathbf{H}}^\times) \text{ or } \widehat{\mathbf{D}}_{4h}/(\widehat{\mathbf{H}}^\times) \downarrow \mathbf{D}_{2d} = 2\mathbf{D}_{2d}/(\mathbf{C}_1) \quad (178)$$

$$\widehat{\mathbf{D}}_{4h}/(\widehat{\mathbf{H}}^\times) \downarrow \widehat{\mathbf{C}}_{2h} = 4\widehat{\mathbf{C}}_{2h}/(\widehat{\mathbf{H}}^\times) \text{ or } \widehat{\mathbf{D}}_{4h}/(\widehat{\mathbf{H}}^\times) \downarrow \mathbf{C}_{2h} = 4\mathbf{C}_{2h}/(\mathbf{C}_1) \quad (179)$$

$$\widehat{\mathbf{D}}_{4h}/(\widehat{\mathbf{H}}^\times) \downarrow \widehat{\mathbf{C}}_s = 8\widehat{\mathbf{C}}_s/(\widehat{\mathbf{H}}^\times) \text{ or } \widehat{\mathbf{D}}_{4h}/(\widehat{\mathbf{H}}^\times) \downarrow \mathbf{C}_s = 8\mathbf{C}_s/(\mathbf{C}_1) \quad (180)$$

Among these subductions, Eq. 177 means that **38** (for the function f) is selected as an initial molecule to be examined, which is transformed into its homomers by means of the elements of \mathbf{D}_{4h} . The elements of \mathbf{C}_{4v} fix (stabilize) **38**, which is a representative of four identical molecules. The coefficient 2 of the right-hand side of Eq. 177 corresponds to the two sets of identical molecules of \mathbf{C}_{4v} -symmetry, where one set of identical molecules (**38** for the function f) is accompanied by the counterpart set of identical molecules (**39** for the function $\tilde{\sigma}f$ ($= \sigma_{15}\sigma_{26}\sigma_{37}\sigma_{48}f$)). The two sets are

transitive to be regarded as a single *RS*-diastereomeric pair under $\widehat{\mathbf{D}}_{4h}$ (in the form of $\widehat{\mathbf{D}}_{4h}(\widehat{\mathbf{H}}^{\times})$) but they are differentiated from each other under $\widehat{\mathbf{C}}_{4v}$ (in the form of $\widehat{\mathbf{C}}_{4v}(\widehat{\mathbf{H}}^{\times})$). In this case, finally, they are homomeric to each other so as to be recognized as a single molecular entity. As a result, Eq. 177 is linked to the following coset decomposition:

$$\mathbf{D}_{4h} = \underbrace{\mathbf{C}_{4v}}_{\mathbf{38}} + \underbrace{\mathbf{C}_{2(1)}\mathbf{C}_{4v}}_{\mathbf{39'} (= \mathbf{38})}, \quad (181)$$

where the first coset corresponds to **38** and the second coset corresponds to its homomer **39'** (= **38**). Note that the element $\mathbf{C}_{2(1)}$ is a rotation by 180° around the two-fold axis through the \mathbf{C}_1 and \mathbf{C}_3 atoms.

The coefficient 2 of the right-hand side of Eq. 178 indicates the presence of two homomeric sets of identical molecules of \mathbf{D}_{2d} -symmetry (for the function $\tilde{\sigma}_{15}\tilde{\sigma}_{37}f$ and the corresponding cooperative epimerization $\tilde{\sigma}\tilde{\sigma}_{15}\tilde{\sigma}_{37}f$), which coincide with each other to give **50'** under the action of \mathbf{D}_{4h} . As a result, Eq. 178 is linked to the following coset decomposition:

$$\mathbf{D}_{4h} = \underbrace{\mathbf{D}_{2d}}_{\mathbf{50'}} + \underbrace{\mathbf{C}_{2(1)}\mathbf{D}_{2d}}_{\mathbf{51'}}, \quad (182)$$

where the first coset corresponds to **50'** and the second coset corresponds to its homomer **51'**.

The coefficient 4 of the right-hand side of Eq. 179 indicates the presence of four homomeric sets of identical molecules of \mathbf{C}_{2h} -symmetry, among which two homomeric sets of **48'** (for the function $\tilde{\sigma}_{15}\tilde{\sigma}_{26}f$) and **52'** (for the function $\tilde{\sigma}_{15}\tilde{\sigma}_{48}f$) are depicted in Fig. 15. The epimerizations $\tilde{\sigma}_{15}\tilde{\sigma}_{26}$ and $\tilde{\sigma}_{15}\tilde{\sigma}_{48}$ are paired with the epimerizations $\tilde{\sigma}\tilde{\sigma}_{15}\tilde{\sigma}_{26}$ and $\tilde{\sigma}\tilde{\sigma}_{15}\tilde{\sigma}_{48}$, which are correlated to their homomers **49'** and **53'**. As a result, Eq. 179 is linked to the following coset decomposition:

$$\mathbf{D}_{4h} = \underbrace{\mathbf{C}_{2h}}_{\mathbf{48'}} + \underbrace{\mathbf{C}_{2(1)}\mathbf{C}_{2h}}_{\mathbf{49'}} + \underbrace{\mathbf{C}_{2(2)}\mathbf{C}_{2h}}_{\mathbf{52'}} + \underbrace{\mathbf{C}_{2(3)}\mathbf{C}_{2h}}_{\mathbf{53'}}. \quad (183)$$

The total four homomeric sets corresponding to the cosets shown in Eq. 183 coincide with one another to give a single molecular entity under the action of \mathbf{D}_{4h} in this case.

The coefficient 8 of the right-hand side of Eq. 180 indicates that there appear eight homomeric sets of \mathbf{C}_s -symmetry, among which four sets of homomers, i.e., **40'** (for the function $\tilde{\sigma}_{15}f$), **42'** (for the function $\tilde{\sigma}_{26}f$), **44'** (for the function $\tilde{\sigma}_{37}f$), and **46'** (for the function $\tilde{\sigma}_{48}f$), are depicted in Fig. 15. The remaining four sets of homomers are generated by their complementary epimerizations i.e., **41'** (for the function $\tilde{\sigma}\tilde{\sigma}_{15}f$), **43'** (for the function $\tilde{\sigma}\tilde{\sigma}_{26}f$), **45'** (for the function $\tilde{\sigma}\tilde{\sigma}_{37}f$), and **47'** (for the function $\tilde{\sigma}\tilde{\sigma}_{48}f$), which are not depicted. As a result, Eq. 180 is linked to the following coset decomposition:

$$\begin{aligned}
 \mathbf{D}_{4h} = & \underbrace{\mathbf{C}_s}_{40'} + \underbrace{\mathbf{C}_4^3 \mathbf{C}_s}_{42'} + \underbrace{\mathbf{C}_{2(3)} \mathbf{C}_s}_{44'} + \underbrace{\mathbf{C}_4 \mathbf{C}_s}_{46'} \\
 & + \underbrace{\mathbf{C}_{2(1)} \mathbf{C}_s}_{41'} + \underbrace{\mathbf{C}'_{2(1)} \mathbf{C}_s}_{43'} + \underbrace{\mathbf{C}_{2(2)} \mathbf{C}_s}_{45'} + \underbrace{\mathbf{C}'_{2(1)} \mathbf{C}_s}_{47'}. \quad (184)
 \end{aligned}$$

The total eight sets homomeric sets which correspond to the eight cosets appearing in Eq. 184 coincide with each other under the action of \mathbf{D}_{4h} so as to give a single molecular entity.

5.4 Numbers of stereoisomers

By scrutinizing the structures of 1,2,3,4-tetrachlorocyclobutanes listed in Fig. 13, we are able to categorize them into four sets of homomers, i.e., $\{38', 39'\}$, $\{40', 41', 42', 43', 44', 45', 46', 47'\}$, $\{48', 49', 52', 53'\}$, and $\{50', 51'\}$, where each set corresponds to a single molecular entity. The four molecular entities have been interpreted by means of the subductions represented by Eqs. 177–180 or by means of the coset decompositions represented by Eqs. 181, 182, 183, and 184.

The value 4 for the number of stereoisomeric 1,2,3,4-tetrachlorocyclobutanes is algebraically obtained by the data shown in Table 1. To apply the Cauchy-Frobenius Lemma [13, Chapter 13] to the present case, we count fixed structures by applying each element of \mathbf{D}_{4h} to the respective molecules shown in Fig. 13. Each fixed structure is checked by the symbol \checkmark in Table 1 and the numbers of checks are obtained by row and row. The resulting values are shown in the rightmost column of Table 1. As a result, the total number of fixed structures is calculated to be 64. Because $|\mathbf{D}_{4h}|$ is 16, the number of stereoisomers (as enantiomeric pairs) is calculated to be $64/16=4$ by means of Eq. 13.1 of [13]. In this case, all of the stereoisomers are achiral (i.e., self-enantiomeric pairs).

Each column of Table 1 shows the molecular symmetry of each structure. For example, the eight elements checked by \checkmark in the $38'$ -column are collected so as to give the point group \mathbf{C}_{4v} . Thereby we are able to conclude that $38'$ belongs to \mathbf{C}_{4v} .

It should be noted, however, that the case of 1,2,3,4-tetrachlorocyclobutanes depends on a fortunate situation where the sets of homomers generated by $\widehat{\mathbf{D}}_{4h}$ can be equalized to the sets of homomers to be generated by the molecular-symmetry group \mathbf{D}_{4h} . Such a fortunate situation is not always fulfilled. For example, examine the case of 1-bromo-2-chloro-3,4-difluorocyclobutanes (Fig. 8). General solutions for such unfortunate situations are open to future investigations.

6 *RS*-stereogenic and *RS*-astereogenic centers

6.1 Exclusion of *RS*-astereogenic centers

Suppose that several carbon atoms (possible *RS*-stereogenic centers) in a stereoskeleton turn out to be *RS*-astereogenic centers according to their substitution modes. After such *RS*-astereogenic centers are excluded from our consideration, let us take

Table 1 Numbers of fixed structures for homomers of 1,2,3,4-tetrachlorocyclobutanes

	38'	40'	42'	44'	46'	48'	50'	52'	No. of fix.
<i>f</i>	✓	$\tilde{\sigma}_{15,f}$	$\tilde{\sigma}_{26,f}$	$\tilde{\sigma}_{37,f}$	$\tilde{\sigma}_{48,f}$	$\tilde{\sigma}_{15}\tilde{\sigma}_{26,f}$	$\tilde{\sigma}_{15}\tilde{\sigma}_{37,f}$	$\tilde{\sigma}_{15}\tilde{\sigma}_{48,f}$	8 × 2
$\bar{\sigma} f$	✓	$\bar{\sigma}\tilde{\sigma}_{15,f}$	$\bar{\sigma}\tilde{\sigma}_{26,f}$	$\bar{\sigma}\tilde{\sigma}_{37,f}$	$\bar{\sigma}\tilde{\sigma}_{48,f}$	$\bar{\sigma}\tilde{\sigma}_{15}\tilde{\sigma}_{26,f}$	$\bar{\sigma}\tilde{\sigma}_{15}\tilde{\sigma}_{37,f}$	$\bar{\sigma}\tilde{\sigma}_{15}\tilde{\sigma}_{48,f}$	1 × 2
<i>I</i>	✓	✓	✓	✓	✓	✓	✓	✓	2 × 2
<i>C</i> ₄	✓								1 × 2
<i>C</i> ₂ (3)	✓						✓		2 × 2
<i>C</i> ₄ ²	✓								1 × 2
<i>C</i> ₂ (1)									0
<i>C</i> ' ₂ (1)							✓		2 × 2
<i>C</i> ₂ (2)									0
<i>C</i> ' ₂ (2)						✓	✓		2 × 2
σ_h									0
<i>S</i> ₄							✓		1 × 2
<i>i</i>							✓		2 × 2
<i>S</i> ₄ ³								✓	1 × 2
$\sigma_v(1)$	✓	✓		✓			✓		4 × 2
$\sigma_d(1)$	✓					✓			2 × 2
$\sigma_v(2)$	✓						✓		4 × 2
$\sigma_d(2)$	✓							✓	2 × 2
Total									64

account of the remaining mRS -stereogenic centers only. Thereby, the upper limit of the summation Eq. 16 is changed from n to m (where $m < n$) without losing generality to give:

$$\tilde{\sigma}' = \tilde{\sigma}_1 \tilde{\sigma}_2 \dots \tilde{\sigma}_i \dots \tilde{\sigma}_m = \prod_{i=1}^m \tilde{\sigma}_i, \quad (185)$$

because the epimerizations ($\tilde{\sigma}_i$) are commutable. Even by this change, we are able to rely on the axiom of organic stereoisomerism (Definition 3):

$$\sigma' = \tilde{\sigma}' \hat{I} = \hat{I} \tilde{\sigma}'. \quad (186)$$

which is parallel to Eq. 17. Then, the multiple epimerization group (Eq. 77) is limited to be

$$\tilde{\mathbf{H}}' = \prod_{i=1}^m \mathbf{H}_{\tilde{\sigma}_i} = \mathbf{H}_{\tilde{\sigma}_1} \times \mathbf{H}_{\tilde{\sigma}_2} \times \dots \times \mathbf{H}_{\tilde{\sigma}_m}. \quad (187)$$

It follows that the range $\omega \leq n/2$ of Eq. 96 is changed into $\omega \leq m/2$ so as to give the counterpart equation as follows:

$$\begin{aligned} \widehat{\mathbf{G}}'_{C\sigma} &= \tilde{\mathbf{H}}' \times \mathbf{G}_{C\sigma} \\ &= \sum_{\omega \leq m/2} \tilde{\sigma}_{[\omega]} \times \mathbf{G}_{C\sigma \tilde{\sigma} \hat{I}} = \sum_{\omega \leq m/2} \tilde{\sigma}_{[\omega]} \overset{\times}{\mathbf{G}}_{C\sigma \tilde{\sigma} \hat{I}} \end{aligned} \quad (188)$$

On the basis of Eq. 188, the corresponding coset representation $\widehat{\mathbf{G}}'_{C\sigma} (/ \overset{\times}{\mathbf{G}}_{C\sigma \tilde{\sigma} \hat{I}})$ can be constructed in a similar way to the stereoisomeric representation $\widehat{\mathbf{G}}_{C\sigma} (/ \overset{\times}{\mathbf{G}}_{C\sigma \tilde{\sigma} \hat{I}})$ (Definition 13). We are able to these coset representations in a parallel fashion because the modulo $\overset{\times}{\mathbf{G}}_{C\sigma \tilde{\sigma} \hat{I}}$ is common.

As an example, let us examine 1,2-dichlorocyclobutanes, which have been once discussed in a previous paper [19]. In this case, Eq. 188 is written as follows:

$$\widehat{\mathbf{D}}'_{4h} = \overset{\times}{\mathbf{D}}_{4h \tilde{\sigma} \hat{I}} + \tilde{\sigma}_{15} \overset{\times}{\mathbf{D}}_{4h \tilde{\sigma} \hat{I}}. \quad (189)$$

The nature of the direct product $\widehat{\mathbf{D}}'_{4h}$ indicates that $\tilde{\sigma}_{15} \times \widehat{\mathbf{D}}_{4h\tilde{\sigma}\hat{I}} \tilde{\sigma}_{15}^{-1} = \tilde{\sigma}_{15} \times \widehat{\mathbf{D}}_{4h\tilde{\sigma}\hat{I}} \tilde{\sigma}_{15} = \times \widehat{\mathbf{D}}_{4h\tilde{\sigma}\hat{I}}$. This equation has been noted in the previous paper [19] (Eq. 9), although the previous interpretation was insufficient, where the direct-product nature was not been explicitly disclosed. Hence, Eq. 9 of [19] should be interpreted to mean Eq. 189.

As another example, let us examine stereoisomeric 1-bromo-2,3-dichlorocyclobutanes, which have been once discussed in [19]. In this case, Eq. 188 is written as follows:

$$\widehat{\mathbf{D}}''_{4h} = \times \widehat{\mathbf{D}}_{4h\tilde{\sigma}\hat{I}} + \tilde{\sigma}_{15} \times \widehat{\mathbf{D}}_{4h\tilde{\sigma}\hat{I}} + \tilde{\sigma}_{26} \times \widehat{\mathbf{D}}_{4h\tilde{\sigma}\hat{I}} + \tilde{\sigma}_{37} \times \widehat{\mathbf{D}}_{4h\tilde{\sigma}\hat{I}} \quad (190)$$

$$= \times \widehat{\mathbf{D}}_{4h\tilde{\sigma}\hat{I}} + \tilde{\sigma}_{15} \times \widehat{\mathbf{D}}_{4h\tilde{\sigma}\hat{I}} + \tilde{\sigma}_{26} \times \widehat{\mathbf{D}}_{4h\tilde{\sigma}\hat{I}} + \tilde{\sigma}_{15}\tilde{\sigma}_{26} \times \widehat{\mathbf{D}}_{4h\tilde{\sigma}\hat{I}}, \quad (191)$$

where $\tilde{\sigma}_{37} \times \widehat{\mathbf{D}}_{4h\tilde{\sigma}\hat{I}}$ can be replaced by $\tilde{\sigma}_{15}\tilde{\sigma}_{26} \times \widehat{\mathbf{D}}_{4h\tilde{\sigma}\hat{I}}$ because $\tilde{\sigma}_{37}$ and $\tilde{\sigma}_{15}\tilde{\sigma}_{26}$ are complementary to each other (i.e., $\tilde{\sigma}' = \tilde{\sigma}_{15}\tilde{\sigma}_{26}\tilde{\sigma}_{37}$ due to Eq. 185). Note that $\tilde{\sigma}_{15} \times \widehat{\mathbf{D}}_{4h\tilde{\sigma}\hat{I}}$ etc. are stabilized by the $\tilde{\sigma}_{15} \times \widehat{\mathbf{D}}_{4h\tilde{\sigma}\hat{I}} \tilde{\sigma}_{15}$ etc., which are identical with $\times \widehat{\mathbf{D}}_{4h\tilde{\sigma}\hat{I}}$ because of the direct-product nature. This equation has been noted in the previous paper [19] (Eq. 14), whose interpretation was insufficient because the direct-product nature was not been explicitly disclosed. Hence, Eq. 14 of [19] should be interpreted to mean Eq. 191.

6.2 Local symmetry groups after exclusion of *RS*-astereogenic centers

Even if *RS*-astereogenic centers are excluded from our consideration, most of the abovementioned features of stereoisomerism are left to be effective. For example, a local symmetry group $\mathbf{G}_{C\tilde{\sigma}\tilde{\sigma}\hat{I}}^{\tilde{\sigma}_i}$ (Eq. 39 or Eq. 42) can be defined at a remaining *RS*-stereogenic center according to Definition 6.

To exemplify this feature, let us examine 1,2,3-trichlorocyclobutanes, which have been once discussed in [19]. By applying Eq. 42 to this case, the local symmetry group at the C_2 atom is obtained as follows:

$$\widehat{\mathbf{D}}_{4h\tilde{\sigma}_h\hat{I}}^{\tilde{\sigma}_{26}} = \mathbf{H}_{\tilde{\sigma}_{26}} \times \widehat{\mathbf{D}}_{4h\tilde{\sigma}_h\hat{I}} = \times \widehat{\mathbf{D}}_{4h\tilde{\sigma}_h\hat{I}} + \tilde{\sigma}_{26} \times \widehat{\mathbf{D}}_{4h\tilde{\sigma}_h\hat{I}}. \quad (192)$$

This equation has been noted in the previous paper [19] (Eq. 15), although the direct-product nature was not been explicitly disclosed in the previous interpretation. Strictly speaking, Eq. 15 of [19] should be interpreted to mean Eq. 192.

It should be emphasized that Eq. 192 for three *RS*-stereogenic centers is identical with Eq. 68 for four *RS*-stereogenic centers. In principle, the local symmetry group defined by Definition 6 (Eq. 39) is effective even after the exclusion of *RS*-astereogenic centers. This principle is simple but provides us with a deeper insight into stereoisomerism. Thus, we can safely say that previous methodologies have implicitly employed this principle in investigating stereoisomerism. In particular, the independent assignments of *RS*-stereodescriptors at multiple *RS*-stereogenic centers by means of the CIP system turn out to have heavily relied on this principle.

7 Conclusion

The theory of stereoisomerism has been developed on the basis of stereoisomeric groups, which have been derived as an extension of *RS*-stereoisomeric groups after integrating stereoisograms [16] into correlation diagrams as a concept of higher level [19]. The substitution positions of a stereoskeleton belonging to $\mathbf{G}_{C\sigma\tilde{\sigma}\hat{I}}$, are permuted by a set of epimerizations ($\tilde{\sigma}_i$) at the *RS*-stereogenic centers of the stereoskeleton. The product of epimerizations $\tilde{\sigma}$ ($= \prod_{i=1}^n \tilde{\sigma}_i$) and the mirror-image transformation σ of the skeleton characterize the total feature of isomerization, which is based on the axiom of organic stereoisomerism: $\sigma = \tilde{\sigma}\hat{I} = \hat{I}\tilde{\sigma}$, where the operation \hat{I} is correlated to holantimeric relationships contained in stereoisograms. Thereby, essential features common to all *RS*-stereoisomeric groups are characterized by a stereoisogram group: $\mathbf{H}_{\tilde{\sigma}}$ ($= \{I, \sigma, \tilde{\sigma}, \hat{I}\}$). After the definition of an epimerization group $\mathbf{H}_{\tilde{\sigma}_i}$ ($= \{I, \tilde{\sigma}_i\}$), a local symmetry group $\mathbf{G}_{C\sigma\tilde{\sigma}\hat{I}}^{\tilde{\sigma}_i}$ at an *RS*-stereogenic center is defined by the direct product $\mathbf{H}_{\tilde{\sigma}_i} \times \mathbf{G}_{C\sigma\tilde{\sigma}\hat{I}}$, from which an epimeric stereoisogram group and an epimeric *RS*-stereoisomeric group is extracted to characterize stereoisograms (an epimeric stereoisogram and a holantimeric stereoisogram) at the *RS*-stereogenic center. To formulate the multiple appearance of *RS*-stereogenic centers, a multiple epimerization group is defined as $\tilde{\mathbf{H}} = \prod_{i=1}^n \mathbf{H}_{\tilde{\sigma}_i}$, which is further used to construct a stereoisomeric group $\hat{\mathbf{G}}_{C\sigma} = \tilde{\mathbf{H}} \times \mathbf{G}_{C\sigma}$. The stereoisomeric group $\hat{\mathbf{G}}_{C\sigma}$ is rearranged to give a coset decomposition by $\hat{\mathbf{G}}_{C\sigma\tilde{\sigma}\hat{I}}^{\times}$, which is generated by modifying the *RS*-stereoisomeric group. The corresponding coset representation $\hat{\mathbf{G}}_{C\sigma} / (\hat{\mathbf{G}}_{C\sigma\tilde{\sigma}\hat{I}}^{\times})$ is called a stereoisomeric representation, which is employed to discuss correlation diagrams of stereoisograms. To discuss molecular symmetries, a molecular-symmetry representation $\hat{\mathbf{G}}_{C\sigma} / (\tilde{\mathbf{H}}^{\times})$ is defined by starting from a coset decomposition $\hat{\mathbf{G}}_{C\sigma}$ by $\tilde{\mathbf{H}}^{\times}$, which is generated by modifying the multiple epimerization group $\tilde{\mathbf{H}}$.

References

1. J.H. van't Hoff, Arch. Néerl. Sci. Exactes Nat. **9**, 445–454 (1874)
2. J.A. Le Bel, Bull. Soc. Chim. Fr. **22**(2), 337–347 (1874)
3. E. Fischer, Ber. Dtsch. Chem. Ges. **24**, 1836–1845 (1891)
4. E. Fischer, Ber. Dtsch. Chem. Ges. **24**, 2683–2687 (1891)
5. IUPAC Organic Chemistry Division, Pure Appl. Chem. **68**, 2193–2222 (1996)
6. R.S. Cahn, C.K. Ingold, V. Prelog, Angew. Chem. Int. Ed. Eng. **5**, 385–415 (1966)
7. V. Prelog, G. Helmchen, Helv. Chim. Acta **55**, 2581–2598 (1972)
8. V. Prelog, G. Helmchen, Angew. Chem. Int. Ed. Eng. **21**, 567–583 (1982)
9. K. Mislow, J. Siegel, J. Am. Chem. Soc. **106**, 3319–3328 (1984)
10. G. Helmchen, in *A General Aspects. 1. Nomenclature and Vocabulary of Organic Stereochemistry*, ed. by G. Helmchen, R.W. Hoffmann, J. Mulzer, E. Schaumann Stereoselective Synthesis. Methods of Organic Chemistry (Houben-Weyl) Workbench Edition E21, vol. 1, 4th edn. (Georg Thieme, Stuttgart, New York, 1996), pp. 1–74
11. IUPAC Chemical Nomenclature and Structure Representation Division, Provisional Recommendations. Nomenclature of Organic Chemistry, http://www.iupac.org/reports/provisional/abstract04/favre_310305.html (2004)
12. S. Fujita, J. Am. Chem. Soc. **112**, 3390–3397 (1990)
13. S. Fujita, *Symmetry and Combinatorial Enumeration in Chemistry* (Springer-Verlag, Berlin-Heidelberg, 1991)

14. S. Fujita, *Theor. Chim. Acta* **76**, 247–268 (1989)
15. S. Fujita, *J. Math. Chem.* **5**, 99–120 (1990)
16. S. Fujita, *J. Org. Chem.* **69**, 3158–3165 (2004)
17. S. Fujita, *J. Math. Chem.* **35**, 265–287 (2004)
18. S. Fujita, *Match Commun. Math. Comput. Chem.* **54**, 39–52 (2005)
19. S. Fujita, *J. Math. Chem.* (2009) <http://dx.doi.org/10.1007/s10910-009-9539-z>
20. S. Fujita, *Tetrahedron* **47**, 31–46 (1991)
21. S. Fujita, *Tetrahedron* **65**, 1581–1592 (2009)
22. S. Fujita, *J. Comput. Aided Chem.* **10**, 16–29 (2009)
23. S. Fujita, *Diagrammatical Approach to Molecular Symmetry and Enumeration of Stereoisomers* (University of Kragujevac, Faculty of Science, Kragujevac, 2007)